II-C3

COLD REGIONS SCIENCE AND ENGINEERING
Part II: Physical Science
Section C: Physics and Mechanics of Ice

THE MECHANICAL PROPERTIES OF SEA ICE

by

W. Weeks and A. Assur

SEPTEMBER 1967

U.S. ARMY MATERIEL COMMAND
COLD REGIONS RESEARCH & ENGINEERING LABORATORY
HANOVER, NEW HAMPSHIRE

COLD REGIONS SCIENCE AND ENGINEERING
Part II: Physical Science
Section C: Physics and Mechanics of Ice

THE MECHANICAL PROPERTIES OF SEA ICE

by

W. Weeks and A. Assur

SEPTEMBER 1967

U.S. ARMY MATERIEL COMMAND
COLD REGIONS RESEARCH & ENGINEERING LABORATORY
HANOVER, NEW HAMPSHIRE

DA Project 1VO25001A130

PREFACE

This monograph is the first of a series of reviews that will discuss the current status of the field of sea ice physics. Its authors are respectively research glaciologist, Snow and Ice Branch (Weeks) and Chief Scientist (Assur) with USA CRREL. They would like to thank G. E. Frankenstein and D. E. Nevel for their advice and critical comments on a number of aspects of this paper. They also wish to thank Dr. V. L. Tsurikov for providing them with copies of his 1947 papers and L. W. Gold for his encouragement and patience.

The support of the U. S. Coast Guard in the preparation of this manuscript is gratefully acknowledged.

USA CRREL is an Army Materiel Command laboratory.

CONTENTS

ILLUSTRATIONS

CONTENTS (Cont'd)

CONTENTS (Cont'd)

TABLES

LIST OF SYMBOLS

A_a	relative amount of air eq 2.1.
A_b	relative amount of brine eq 2.1.
A_i	relative amount of pure ice eq 2.1.
A_s	relative amount of an individual solid salt eq 2.1.
C	constant eq 2.10.
D	flexural rigidity eq 1.6, 5.18; molecular diffusion coefficient of salt in water eq 3.50.
E	elastic or Young's modulus; elastic spring constant as determined using a Maxwell model.
$\bar{E}$	average value of the elastic modulus considering the complete thickness of the ice sheet.
E_b	elastic modulus as determined by in-situ body wave measurements; elastic modulus of the bottom fiber eq 5.25.
E_f	elastic modulus determined by flexural wave measurements.
E_0	elastic modulus of fresh ice.
E(z)	elastic modulus varying as a function of z.
$E(\mathfrak{Z})$	elastic modulus varying as a function of $\mathfrak{Z}$.
E_1	elastic spring constant in a Maxwell unit determined using a Maxwell and a Voigt unit connected in series.
E_2	elastic spring constant in a Voigt unit determined using a Maxwell and a Voigt unit connected in series.
F	average area of brine pockets in a plane parallel to the solid-liquid interface.
G	shear modulus.
I	moment of inertia about the neutral axis.
$\mathfrak{I}$	moment of inertia of the reduced cross-section calculated using the non-dimensional $\mathfrak{Z}$ scale.
K	stress concentration factor in the ring-tensile test.
L	latent heat of fusion of ice.
M	bending moment.
$\mathfrak{M}_0, \mathfrak{M}_1, \mathfrak{M}_2$	the zeroth, first and second moments calculated using the reduced cross-section eq 5.14.
P	applied force eq 1.2; a parameter related to the geometry of the microstructure eq 3.47; load at failure eq 4.1.
S_b	section modulus of the bottom fiber ($S_b = I/z_b$, see eq 1.1 and 5.21).
$\mathfrak{S}_b$	section modulus for bottom fiber expressed relative to the non-dimensional $\mathfrak{Z}$ scale eq 5.24.

LIST OF SYMBOLS (Cont'd)

S_i	salinity of sea ice.
$\bar{S}_t$	section modulus for top fiber expressed relative to the non-dimensional $\bar{Z}$ scale eq 5.27.
V_a	air porosity eq 4.7 - 4.8.
V_p	velocity of the longitudinal plate wave.
V_s	velocity of the shear wave.
$X_{1 \ldots n}$	parameters affecting the strength of sea ice eq 4.10 - 4.11.
a	radius of a circular load resting on an infinite sheet.
a_b	proportionality constant eq 2.2.
a_i	length associated with where the force is applied eq 1.7.
a_0	plate spacing, the distance between the centers of successive brine layers measured parallel to the c-crystallographic axis.
a_s	proportionality constant eq 2.3.
b_i	length associated with how the force is distributed eq 1.7.
b_0	center to center spacing of brine pockets as measured in the B direction (see Figure 17).
c	$c = \nu_0^{-k}$ eq 3.26; length of a crack eq 3.45; coefficient accounting for turbulent transfer of solute in excess of molecular diffusion eq 3.50.
c_i	length associated with the boundary conditions eq 1.7.
$2c_0$	original grain length.
d	crystal diameter; a length characteristic of the size of the microstructure eq 3.47.
d_0	minimum width of a parallel brine layer before it splits to produce individual brine pockets.
e	overall coefficient of surface heat transfer.
g	length of brine cylinders as measured parallel to the direction of growth.
g_0	spacing of brine cylinders measured parallel to the growth direction.
h	ice thickness.
h_b	ice thickness excluding the strengthless skeleton layer.
h_{sk}	thickness of the strengthless skeleton layer at the bottom of the ice sheet.

LIST OF SYMBOLS (Cont'd)

k	foundation modulus eq 1.14; a constant eq 2.10; stress concentration factor associated with the presence of brine pockets in sea ice.
ℓ	action radius eq 1.5; average length of the test specimen eq 4.1.
n_2	number of holes per cm^2 in a cut perpendicular to the axis of the cylindrical voids or the number of holes in a given length of line.
n_3	number of spherical voids.
r	radius of either the spherical voids or the cylindrical cavities.
$2r_a$	width of brine pockets measured in the c-direction (see Figure 17).
$2r_b$	length of brine pockets measured in the B-direction (see Figure 17).
r_i	inner radius of sample eq 4.1.
r_o	outer radius of sample eq 4.1.
t	time.
v	growth velocity.
w	deflection.
x_i	coordinates of the system.
z	vertical distance from the upper surface of the ice sheet to any location in the sheet.
$\tilde{z}$	transformed dimensionless distance see eq 5.2.
z_b	distance from the neutral axis to the bottom fiber.
z_e	distance from the neutral axis to the extreme fiber of the ice sheet.
z_n	distance from the top of the ice sheet to the neutral axis.
$\tilde{z}_n$	the non-dimensional distance to the neutral axis measured from the bridging layer at the bottom of the ice sheet.
Δz	characteristic length associated with the distance a platelet grows before salt diffusion from neighboring platelets "meets" between platelets.
θ	temperature.
θ_a	air temperature.
θ_b	temperature at the bridging layer at the top of the skeleton layer.
θ_i	ice temperature.

LIST OF SYMBOLS (Cont'd)

θ_0	a characteristic temperature eq 4.15; ice surface temperature at the ice-air interface eq 5.5.
θ_w	water temperature.
$\Delta\theta$	difference between the ambient air temperature θ_a eq 3.51 or the temperature of the upper surface of the ice sheet θ_0 eq 5.3 and the freezing temperature of water.
ψ	plane porosity.
a	theoretical stress concentration factor.
a_0	$a_0 = a_0 F^{-1/2}$.
β	reduced stress concentration factor as observed experimentally.
β_0	relative spacing of brine pockets ($\beta_0 = b_0/a_0$).
γ	relative spacing of brine cylinders ($\gamma = g/g_0$).
γ'	total energy required per unit increase in the area of a crack.
δ	complicated function of c and c_0 eq 3.46.
ϵ	strain; elliptic ratio of the brine pockets ($\epsilon = r_b/r_a$).
$\dot{\epsilon}$	strain rate ($\dot{\epsilon} = d\epsilon/dt$).
η	viscosity; a function of Poisson's ratio see eq 3.46; stress concentration index eq 4.2.
η_1, η_2	viscous dash pot constants in a Maxwell and a Voigt unit respectively determined using a Maxwell and a Voigt unit connected in series.
$\eta(t)$	time dependent viscosity term.
κ	proportion of the stress exerted on the weak crystal eq 3.46; thermal conductivity eq 3.51.
μ	Poisson's ratio.
μ_f	limiting value of Poisson's ratio at very low temperatures.
μ_0	Poisson's ratio extrapolated to 0°C.
ν	total or volume porosity.
ν_a	air porosity.
ν_b	brine volume related to the density of a hypothetical air free sea ice.
ν_b'	brine volume related to the actual density of sea ice.
ν_l	line porosity.
ν_0	volume of brine necessary to cause the ice to have zero strength or elasticity.

LIST OF SYMBOLS (Cont'd)

v_p	plane porosity.
ρ	density of sea ice; a parameter related to brine pocket geometry $\rho = 2r_b F^{-1/2}$ (eq 3.24 to eq 3.28 only).
ρ_a	density of air.
ρ_b	density of brine.
ρ_i	density of pure ice.
ρ_s	density of individual solid salts.
σ	stress.
$\dot{\sigma}$	stress rate $d\sigma/dt$.
σ_b	stress in the bottom fiber.
σ_f	failure strength, also flexural strength.
$\overline{\sigma}_f$	average value of the failure strength considering the complete thickness of the ice sheet.
σ_i	failure strength of pure ice.
σ_0	basic strength of sea ice.
σ_t	stress in the top fiber.
σ_R	a parameter related to the failure strength, $\sigma_R = \sigma_f/\dot{\sigma}^b$ eq 4.11.
τ	relaxation time as determined for a simple Maxwell model.
τ_1	relaxation time ($\tau_1 = \eta_1/E_1$).
τ_2	retardation time ($\tau_2 = \eta_2/E_2$).
ϕ	angle between the axis of the cylindrical test specimen and the ice sheet surface.

EDITOR'S FOREWORD

"Cold Regions Science and Engineering" consists of a series of monographs written by specialists to summarize existing knowledge and provide selected references on the Cold Regions, defined here as those areas of the earth where operational difficulties due to subfreezing temperatures may occur.

Sections of the work are being published as they become ready, not necessarily in numerical order but fitting into this plan, which may be amended as the work proceeds:

I. Environment
- A. General
  - 1. Geology and physiography
  - 2. Permafrost
  - 3. Climatology
    - a. General and Northern Hemisphere 1
    - b. Northern Hemisphere 2
    - c. Southern Hemisphere
    - d. Radioactive fallout in the Northern Hemisphere
  - 4. Vegetation
    - a. Patterns of vegetation
    - b. Regional descriptions
    - c. Utilization of vegetation
- B. Regional
  - 1. The Antarctic Ice Sheet
  - 2. The Greenland Ice Sheet

II. Physical Science
- A. Geophysics
  - 1. Heat exchange at the earth's surface
  - 2. Exploration geophysics
- B. Physics and mechanics of snow as a material
- C. Physics and mechanics of ice
  - 1. Snow and ice on the earth's surface
  - 2. Ice as a material
  - 3. The mechanical properties of sea ice
- D. Physics and mechanics of frozen ground

EDITOR'S FOREWORD (Cont'd)

III. Engineering

A. Snow engineering

1. Engineering properties of snow
2. Construction
   a. Building methods
   b. Site material - investigation and exploitation
   c. Foundations and subsurface structures
   d. Utilities
   e. Snow roads and runways
3. Technology
   a. Explosions and snow
   b. Snow removal and ice control
   c. Blowing snow
   d. Avalanches
4. Oversnow transportation

B. Ice engineering

1. River-ice engineering
2. Drilling and excavation
3. Roads and runways on ice

C. Frozen ground engineering

1. Site exploration and excavation
2. Buildings, utilities and dams
3. Roads, railroads and airfields
4. Foundations
5. Sanitary engineering
   a. General and water supply
   b. Sewerage and waste disposal
6. Artificial ground-freezing for construction

D. General

1. Cold weather construction
2. Materials at low temperatures

EDITOR'S FOREWORD (Cont'd)

IV. Remote Sensing

A. Systems

B. Techniques of image analysis

C. Application to Cold Regions

F. J. SANGER

THE MECHANICAL PROPERTIES OF SEA ICE

by

W. F. Weeks and A. Assur

1. INTRODUCTION

Although sea ice covers up to 12% of the surface of the oceans, it is commonly considered somewhat of a scientific oddity. It is still rare, excluding glaciological circles, to find a person who has even seen sea ice. Therefore, it is not very surprising that careful, detailed observations such as those of Malmgren[97]* concerning the physical characteristics of this material have been few. The most notable exceptions to this are studies of the mechanical properties of sea ice. The need for reliable estimates of the strength of sea ice was clear to Russian investigators in the 1890's.[80,95] The motivation for this interest was ice-breaker design and later over-ice transport related to the effective operation of the Northern Sea Route. Finnish and Japanese investigators became interested in the late 1940's because of pack ice problems in the Baltic and Okhotsk Seas. The Canadians and Americans became involved in the mid-fifties as the result of problems associated with ship and air resupply in the Arctic. Because of linguistic barriers and the fact that the publication of research results has been both sporadic and scattered through a wide array of different types of technical journals, the study of the properties of sea ice has proceeded in a relatively independent manner in these different countries. It is hoped that this review will provide the reader with an estimate of the state of thinking of each of the main groups investigating sea ice and an overall appraisal of the field as a whole.

In the last 10 years, because of the pronounced increase in activities in the Arctic and Antarctic there has been a steady demand for the solution of increasingly difficult problems that depend upon a knowledge of the mechanical properties of sea ice: the design of a barge that will withstand the forces exerted by heavy arctic pack ice, the design of a new generation of ice breakers, the design of off-shore drilling platforms that will not be destroyed by rapidly moving ice floes, the prediction of the effects of the long term loading of an ice sheet, the calculation of the forces exerted on piers as an ice sheet is raised by the tide. Other problems are traffic over sea ice, unloading on the edge of an ice sheet, and the use of ice runways for logistical operations.

Fortunately, most of these problems have certain features in common. For example, consider the problem of calculating the failure of an ice sheet under either bending or buckling

$$\sigma = -\frac{Mz_e}{I} \tag{1.1}$$

where σ is the tensile stress exerted on the extreme ice fiber, M is the bending moment, I is the moment of inertia about the neutral axis and z_e is the distance from the neutral axis to the extreme fiber of the ice. In Cartesian coordinates

*Superscript numbers refer to cited literature (p. 67 to 80).

$$M = -P\left[\frac{\partial^2 \omega}{\partial\left(\frac{x_1}{\ell}\right)^2} + \mu \frac{\partial^2 \omega}{\partial\left(\frac{x_2}{\ell}\right)^2}\right] \tag{1.2}$$

and in polar coordinates with symmetry

$$M = -P\left[\frac{\partial^2 \omega}{\partial\left(\frac{x_1}{\ell}\right)^2} + \frac{\mu}{\left(\frac{x_1}{\ell}\right)} \frac{\partial \omega}{\partial\left(\frac{x_1}{\ell}\right)}\right] \tag{1.3}$$

where the deflection w is given by

$$w = \frac{P\omega}{k\ell^2}. \tag{1.4}$$

Here x_i are the coordinates of the system (i = 1, 2), μ is Poisson's ratio, k is the foundation modulus (in this case the density of sea water), and P is the applied force. The action radius ℓ is given by

$$\ell = \sqrt[4]{\frac{D}{k}} \tag{1.5}$$

where D is the flexural rigidity

$$D = \int_0^h \frac{E(z) \cdot (z - z_n)^2}{1 - \mu^2}\, dz \tag{1.6}$$

z is the vertical distance from the top, z_n is the distance from the top to the neutral axis, and E(z) is the elastic or Young's modulus which varies throughout the ice thickness. A method for calculating these values is given at the end of this paper. The value of ω is determined by

$$\omega = f\left(\frac{a_i}{\ell}, \frac{b_i}{\ell}, \frac{c_i}{\ell}, \mu, \frac{x_i}{\ell}\right) \tag{1.7}$$

where a_i, b_i and c_i are lengths associated with where the force is applied, the distribution of the force, and the boundary conditions respectively. Therefore at failure

$$P = \frac{\sigma_f I}{z_e f(\omega, \mu)} \tag{1.8}$$

where σ_f is the failure strength of the ice.

For the case of a homogeneous, isotropic ice sheet, the neutral axis is in the center of the sheet and

$$z_e = z_n = \frac{h}{2}. \tag{1.9}$$

Also in this case

$$I = \frac{h^3}{12} \tag{1.10}$$

and

$$D = \frac{Eh^3}{12(1 - \mu^2)} . \tag{1.11}$$

The force required for failure is, therefore,

$$P = \frac{\sigma_f h^2}{6 f(\omega, \mu)} \tag{1.12}$$

which in the case of a circular load with radius a acting on an infinite sheet gives[195]

$$P = \frac{\sigma_f h^2}{3} \cdot \frac{\pi \left(\frac{a}{\ell}\right)}{(1 + \mu)\, kei'\left(\frac{a}{\ell}\right)} \tag{1.13}$$

where kei' indicates a Kelvin function.

Therefore, the material parameters or their viscous analogs that are needed for the practical solution of this type of problem are E, μ and σ_f. In addition, in the case of ice acting on a vertical or slightly sloping surface the crushing strength also becomes relevant. Most of the remainder of this paper will be devoted to appraising our knowledge of these parameters. For a more general review of the properties of sea ice see Pounder,[128,130] Peschanskii,[119] Savel'ev,[142] Weeks,[191] or Zubov.[198]

2. PHYSICAL BASIS FOR INTERPRETING SEA ICE STRENGTH

Phase Relations

It is obvious that the mechanical properties of sea ice should be related to the amount of void (brine + air) in the ice at the moment of testing. Therefore, the first prerequisite for a detailed analysis of sea ice data is an adequate phase diagram. This diagram specifies the relative volumes of ice, brine and solid salts that coexist in sea ice at equilibrium at a given temperature. The use of such a diagram assumes, of course, that the ratios of the ions in the system that is frozen are the same as in standard sea water. Figure 1 shows the phase diagram that is currently in general use (Assur,[17] Anderson[2,5]). It gives the amount of brine, ice, and solid salt in the system at any given temperature and indicates the temperatures of crystallization of the solid salts $CaCO_3 \cdot 6H_2O$, $Na_2SO_4 \cdot 10H_2O$, $NaCl \cdot 2H_2O$, etc. This diagram is based on the experimental results of others.[132,104,105] Now it has been known for some time that there were small but significant differences between the results of these investigators at temperatures below -35C. These differences are really not too surprising considering the difficulties in concentrating at these low temperatures a volume of brine sufficient to analyze. These discrepancies were not, however, considered important

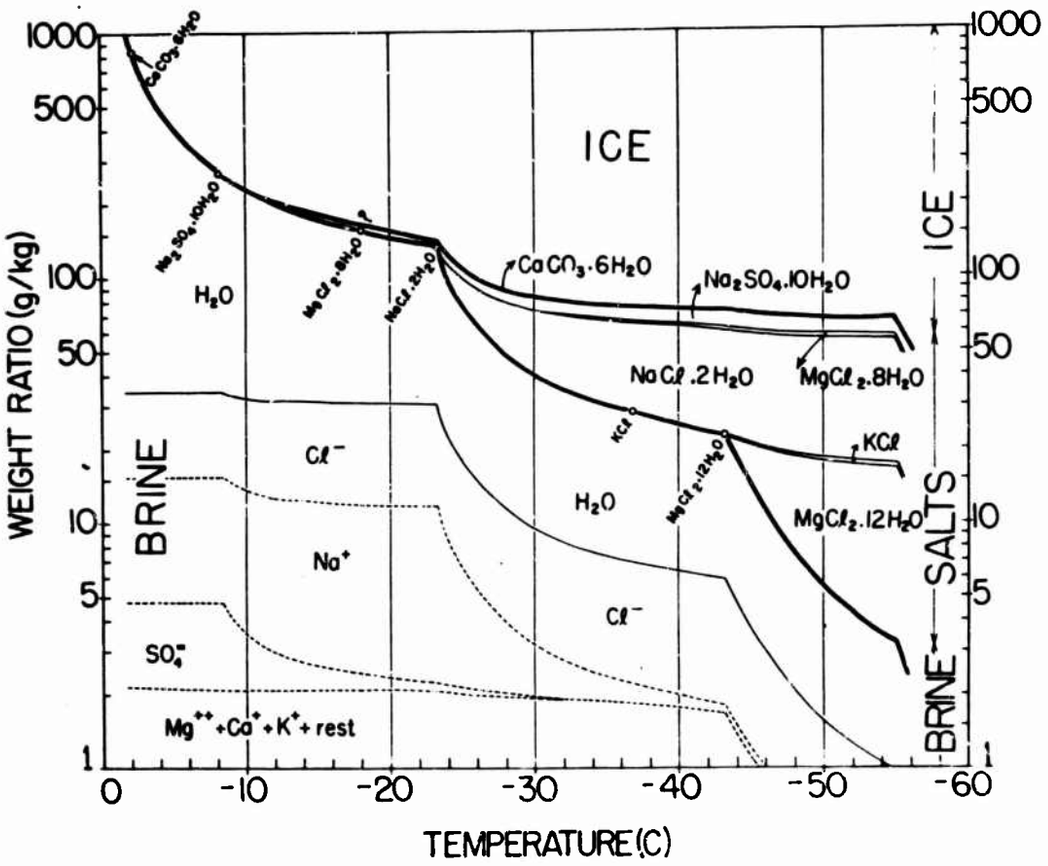

Figure 1. Phase relations for "standard" sea ice. Circles on the brine-salt line indicate temperatures at which the different solid salts precipitate (Assur).[17]

because the temperature of natural sea ice is rarely below -30C. It was also known that the salts precipitating from sea ice brine had never been positively identified by direct (optical or X-ray) methods but instead had been deduced from changes in the brine composition and the general stability ranges of different salts in the individual pure salt-water systems. In addition, certain irregularities in the precipitation of $CaCO_3 \cdot 6H_2O$ could either be explained by metastability or as suggested by Tsurikov[178] by the adsorption of the calcium ion on ice. The possibility of errors being present in the current phase diagram became apparent when the results of the Russian chemist Gitterman finally became available in Savel'ev's book.[142] Savel'ev's analysis of Gitterman's results suggests that $CaSO_4$ precipitates in significant quantities. Note that the possibility of this solid salt occurring is not suggested at all in Figure 1. Gitterman's work also indicates that some of the early-formed salts partially rereact with the brine at lower temperatures and that the last of the brine solidifies at -36C. This last claim, however, appears doubtful inasmuch as Fujino[52] recently (1966) observed a noticeable change in the slope of a plot of the dielectric constant of sea ice vs temperature at roughly -52C. This temperature is close to -54C where Ringer[132] suggested that the last of the brine had solidified. Although there is obviously a considerable amount of checking that needs to be done on the sea ice phase relations, we are optimistic in that we feel that the current diagram will prove to be reasonably accurate at

temperatures above the $NaCl \cdot 2H_2O$ precipitation temperature. This optimism is supported by the recent results of Richardson and Keller[131] who measured the liquid brine content directly by means of a nuclear magnetic resonance spectrometer.

It would also be very important to establish if "selective brine drainage" causes any significant variation in the ratios of the ions in sea ice. The current literature[141, 26, 28] on this subject is discrepant. If there are significant changes in the salt ratios then the precipitation temperatures of some of the salts will change and the applicability of the standard sea ice phase diagram to this "altered" ice may become questionable.

It should be mentioned that there have been two direct methods described for determining the amount of brine in sea ice. Unfortunately, neither the rather involved thermal procedure of Savel'ev[139] nor the nuclear magnetic resonance method of Richardson and Keller[131] can readily be adapted to field use.

Volume of Air

The other component of the void volume is the volume of air in the sample. It is relatively simple to determine the volume of air in a specimen of sea ice, even under field conditions.[10,14,149,83] Therefore, the dependence of sea ice properties on the air volume in the ice was discussed quite early in the Russian literature. Japanese investigators[159,168] have also been able to show some excellent correlations between physical properties and density (void volume). In some of these cases it is quite certain that the initial brine in the sample had drained out and was replaced by air during the trip back to the cold room facilities and the subsequent storage at relatively high temperatures for long periods of time. Canadian and American investigators have, on the other hand, preferred to use the brine volume computed from Assur's tables[17] and have largely ignored the volume of air in the ice. It is, of course, desirable that both the volume of brine and of air be determined independently. Fortunately, the volume of air is also quite easy to determine for natural sea ice. The specific volume of a sea ice sample is

$$\frac{1}{\rho} = \frac{A_i}{\rho_i} + \frac{A_b}{\rho_b} + \sum \frac{A_s}{\rho_s} + \frac{A_a}{\rho_a} \tag{2.1}$$

where ρ is the density and $\underline{A}$ the relative amount of the material specified by the subscripts (b-brine, s-individual salts, i-pure ice, a-air) and ρ is the density of sea ice. Because the amounts of brine and solid salts are proportional to the ice salinity S_i (weight of salt per unit weight of solution)

$$A_b = a_b S_i \tag{2.2}$$

$$A_s = a_s S_i \tag{2.3}$$

where the proportionality constants can be computed from Assur (Table III).[17] A_i can be represented as

$$A_i = 1 - S_i (a_b + a_s). \tag{2.4}$$

Therefore,

$$\frac{1}{\rho} = \frac{1 - S_i(a_b + a_s)}{\rho_i} + \frac{a_b S_i}{\rho_b} + S_i \sum \frac{a_s}{\rho_s} + \frac{A_a}{\rho_a} . \tag{2.5}$$

Dividing by the specific volume of the sample we find that the brine porosity v_b' is

$$v_b' = \frac{\rho a_b S_i}{\rho_b} \tag{2.6}$$

and the air porosity, v_a

$$v_a = \frac{\rho A_a}{\rho_a} . \tag{2.7}$$

Therefore, the total porosity v is

$$v = v_a + v_b' = 1 - \rho\left[\frac{1}{\rho_i} + S_i\left(\sum \frac{a_s}{\rho_s} - \frac{a_b + a_s}{\rho_i}\right)\right]. \tag{2.8}$$

In (2.8), ρ and S_i are measured and $1/\rho_i = f_1(\theta)$ and

$$\sum \frac{a_s}{\rho_s} - \frac{a_b + a_s}{\rho_i} = f_2(\theta) \tag{2.9}$$

can be calculated as functions of temperature (θ) alone from Bader[23] and Assur (Table III)[17] respectively. v_a can also be determined separately by means of a simple experiment.[83] One must make a careful distinction between v_b' in (2.6), which is related to the actual density ρ of the sea ice including air and the relative brine volume v_b as introduced by Assur[17] which is related to the density of a theoretical air-free sea ice. The value of v_b can be calculated from the phase composition and, with rare exception, is the value used throughout this paper. In the future it would be desirable to measure air porosity separately and then calculate the total porosity. One should not attempt to calculate the air porosity from (2.8), by using v_b from tables rather than v_b' for which tables are not readily available as yet.

Structural Considerations

Macrostructure

Once the relative volumes of the major components of sea ice are established, it becomes necessary to understand the structural considerations that control the distribution of the brine, air and solid salts in the ice. To do this, it is important to understand how sea ice forms. In sea water, as in fresh water, the first crystals to form are minute spheres of pure ice. Growth rapidly changes these spheres into thin circular disks in

Figure 2. Photomicrograph of initial disks and stars during the freezing of sea water (1956, Thule, Greenland).

the general growth sequence spheres →disks→hexagonal dendritic stars. The plane of these disks or stars (Fig. 2) is the (0001) or basal plane which is the plane of maximum reticular atomic density in an ice crystal.[113] The arms of the stars form parallel to the a-axis directions $\langle 11\bar{2}0 \rangle$ in the ice crystal which is the shortest lattice vector in the (0001) plane. These star-like crystals grow rapidly across the surface of calm sea water until they overlap and freeze together forming a continuous thin ice skim. Because of the tabular nature of both the initial ice discoids and stars, they float with their basal planes in the plane of the water surface. Ideally this would produce an ice skim with a completely c-axis vertical orientation. However, since water conditions are rarely if ever completely calm, a number of discoids or stars are usually caught in an intermediate position, i.e., with their c-axis inclined at some angle to the vertical. The resulting ice skim shows a fabric diagram similar to that shown in Figure 3: a slight concentration of crystals with their c-axis vertical and a few crystals with almost every other orientation. The formation of surface needles, a common phenomenon in lake water, appears to be fairly rare in sea water.

When there is significant turbulence during freezing, the effective thermal supercooling is reduced, more crystals form per unit volume of sea water, and abrasive action between crystals is increased. When the resulting slush congeals, the ice cover that results is usually several centimeters thick, fine-grained, equigranular in texture, with a random c-axis orientation. A

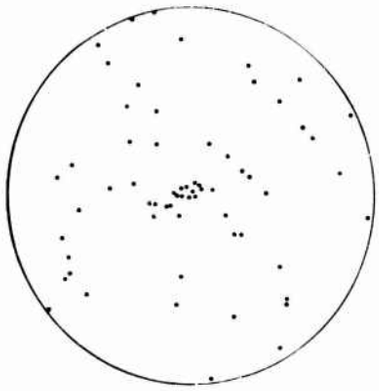

Figure 3. Schmidt net plot (upper hemisphere) of c-axis orientations in an initial ice skim (sea water, 31.6‰, Thule, Greenland, 1956).

series of excellent vertical and horizontal photomicrographs of such ice is shown by Tabata and Ono (Fig. 10 and 11 - 1 to 6).[157] This slush ice should, if possible, be distinguished from infiltrated snow ice. The latter commonly forms in subarctic regions with abundant snow fall when the weight of the overlying snow depresses the surface of the ice sheet below the water level. Percolation of sea water through cracks changes the snow to a brine saturated slush which subsequently freezes forming infiltrated snow ice.[186] There currently is not sufficient information available on the properties of slush and infiltrated snow ice to know whether or not these two ice types can safely be grouped together when physical properties are being considered. At some locations in the Antarctic such a considerable portion of the ice sheet is composed of infiltrated snow ice, that it is necessary to take this fact into account in bearing capacity calculations.[172]

Once a continuous skim of ice has formed across the sea surface, growth rate is determined by the temperature gradient in the sheet and its effective conductivity. When a skim has formed, the ice crystals lose a degree of growth freedom: only if the grain boundaries are exactly perpendicular to the freezing interface can crystal growth proceed without one grain interfering with the growth of another. Any tendency for anisotropic growth will produce geometric selection with the crystals in the favored orientation eliminating the crystals in the other orientations by cutting them off from the melt (Fig. 4).[116,184] Since free-floating ice crystals formed both from fresh and sea water show pronounced anisotropic growth, it is quite reasonable to expect that geometric selection will occur. A typical rubbing of the bottom surface of a 2.5-cm ice skim in which the process of geometric selection is obviously occurring is shown in Figure 5. The blank plane-sided polygonal areas are where c-axis vertical crystals occur. These crystals grow appreciably slower than the surrounding c-axis horizontal crystals. They therefore form depressed (~2 to 5 mm) areas on the bottom surface of the ice skim and do not show in the rubbings. Once the c-axis vertical crystals are eliminated, rubbings from the lower levels in the ice sheet are similar to Figure 6 which shows that all the crystals present have their c-axes roughly horizontal. Note that this process does not require the nucleation of new crystals with a c-axis horizontal orientation. The favored orientation forms by the survival of those grains with this orientation that are present in the initial ice skim. Bennington,[25] on the other hand, has noted rapid orientation changes in the upper layers of sea ice sheets that are difficult to explain by a process of geometric selection. Regardless of the details of the mechanisms involved, it is clear that at a short distance below the upper ice surface, sea ice is mainly composed of ice crystals with their c-axes essentially horizontal. The zone in which this orientation change occurs has been called the transition zone.[16]

Below the transition zone, sea ice has all the characteristics associated with the so-called columnar zone in metal ingots;[183] i.e., a strong crystal elongation parallel to the direction of heat flow, a pronounced crystal orientation (Fig. 7), and an increase in crystal size over crystals closer to the cold

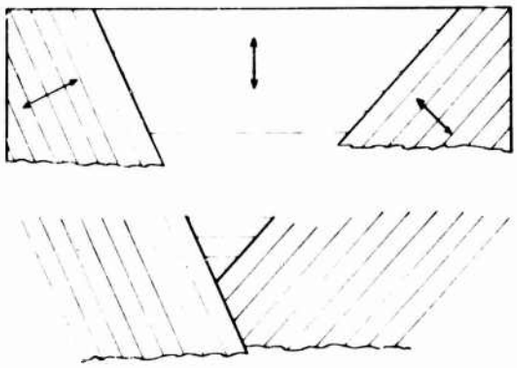

Figure 4. Schematic diagram showing the process of geometric selection, the arrows indicate the direction of the c-axis (Perey and Pounder).[116]

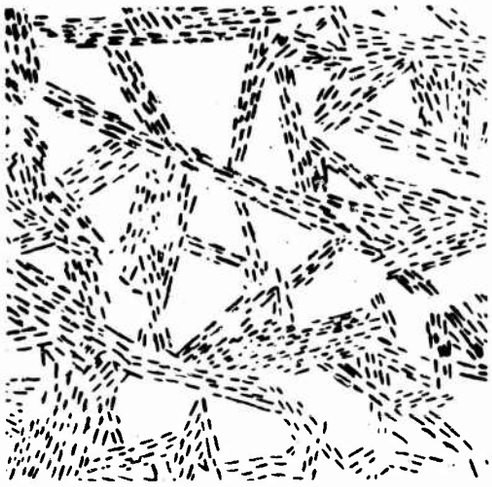

Figure 5. Rubbing of the bottom of a 2.5 cm thick ice skim that is undergoing geometric selection (Hopedale, Labrador, 1955).

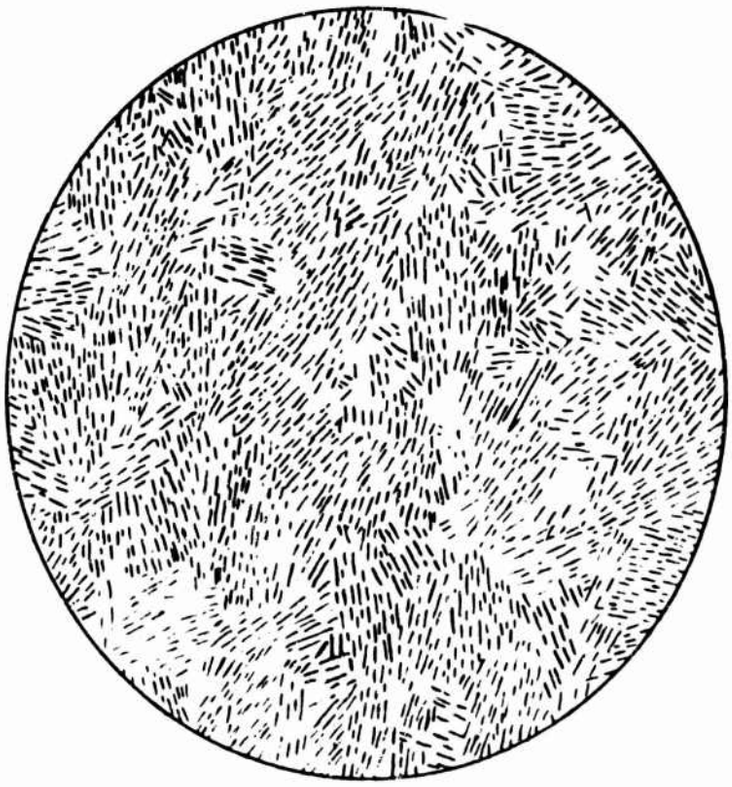

Figure 6. Rubbing of the bottom of a 14.8 cm thick sheet of sea ice; all c-axes are essentially horizontal (Hopedale, Labrador, 1955).

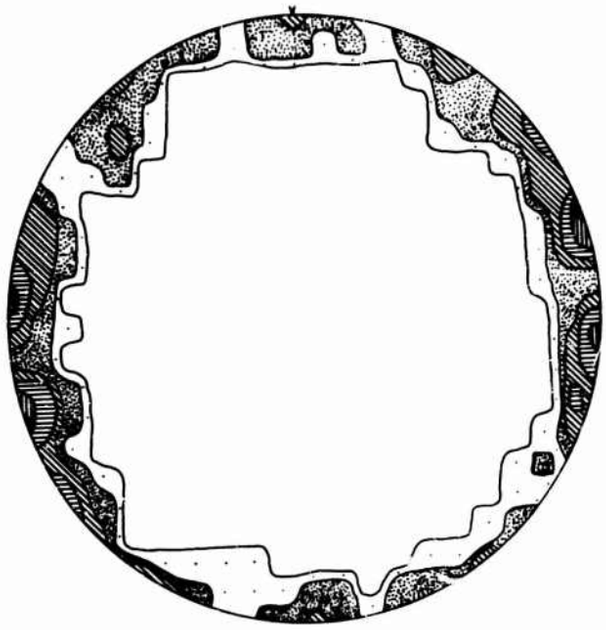

Figure 7. Contoured Schmidt net plot of c-axis orientations at a depth of 10 cm below the upper sea ice surface (Thule, Greenland, 1957). Contours represent 1, 2, 4, 6, 10 and 13 percent per 1 percent of the area; 200 grains.

source. Because the transition layer is thin and occurs at or near the ice-air interface, it commonly sublimes away or recrystallizes into the snow cover as the ice sheet grows. Therefore, the complete thickness of a one winter sheet of sea ice can, to a good approximation, be considered as being in the columnar zone.

The most noticeable change in the upper part of the columnar zone is the marked increase in grain size with depth in the ice sheet. Figure 8 shows a plot of mean crystal diameter $\bar{d}$ vs depth from a 125 cm thick ice sheet at Thule, Greenland. The measurements were stopped at 60 cm because of the large number of crystals that were not completely contained on a given thin section; pronounced linear grain coarsening is evident. It is reasonable to assume that the crystals still present at the bottom of a thick ice sheet not only have their c-axes horizontal but also have one of their a-axes close to vertical.

There are very few observations regarding the grain size at the bottom of thick sea ice sheets. This lack of data is, of course, explained by the difficulty in obtaining large oriented samples. The need to obtain additional information on this subject is quite critical in view of Peyton's[122,123] recent distinction of "bottom ice" as a separate ice type in the columnar zone. This ice is characterized by a c-axis horizontal orientation and an extremely large grain size. Peyton[123] reports examining a 3 x 3 meter block of 1.6 m thick sea ice and finding that the bottom meter exhibited a constant c-axis orientation over the entire 9 m^2 cross section. It also should be noted that in the old sea ice incorporated into the Ice Island Arlis II, Smith[154] observed

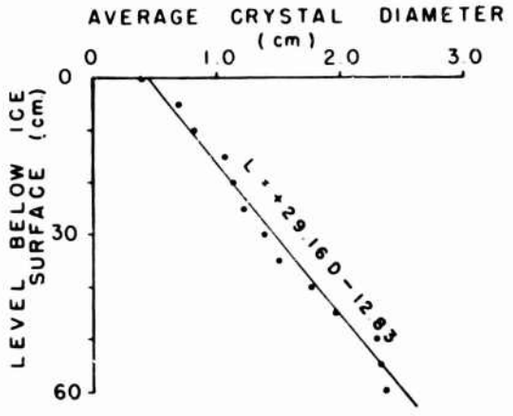

Figure 8. Mean grain diameter $\bar{d}$ vs the level below the upper ice surface (Thule, Greenland, 1957).

areas as large as 10 m on a side with almost perfect c-axis alignment. Whether or not these large areas are actually single crystals or are composed of a number of crystals with roughly similar orientation is not known.

The general relation between the maximum crystal length $\underline{L}$ and the maximum crystal width $\underline{W}$, as measured in horizontal thin sections has been studied by Weeks and Hamilton[188] in sea ice collected at Point Barrow. Their results indicate that the ratio L/W is approximately constant with a value of 2. This indicates that the rates of sidewise and edgewise growth of the individual crystals do not differ nearly as much as might be expected from studies of growth anisotropy in ice.[63,58] Highly sutured grain boundaries and complex crystal intergrowths are common[145] and appear to be associated with the fact that sea ice grows with a cellular to dendritic solid-liquid interface.

There are several petrographic features of the columnar zone which are best observed in vertical thin sections. In contrast to the parameters discussed above, which are either constant or change gradually in the vertical (z) direction, these features commonly appear as sharp bands which extend for large lateral distances. Small scale horizontal banding in sea ice has been noted in widely separated regions.[152,167,85,25] For example, Shumskii observed a total of 58 secondary layers in a 291-cm section of old pack ice giving an average layer thickness of 5 cm. In many cases these layers are produced by changes in the amount of impurities (brine + air) trapped in the ice. In most cases this layering is not accompanied by the nucleation of new crystals. Similar air bubble layering in lake ice is well known.

The other type of horizontal layer is that produced by the summer melt cycle in multiyear pack. Inasmuch as there are no observations relating this type of layering to strength problems, it will not be treated here. For detailed discussions of this layering see Cherepanov[39] and Schwarzacher.[145]

It is important that any determinations of the physical properties of sea ice accurately specify the type of ice tested. The indiscriminant mixing of varied ice types will undoubtedly make a significant contribution to increasing an already large natural variability.

Microstructure

As is obvious from examining a rubbing of the bottom surface of a sea ice sheet (Fig. 6), sea ice crystals possess a pronounced microstructure. The details of the formation of this substructure are poorly understood but the general nature of the phenomena is clear. When sea water freezes the rejection of solute by the solid causes a solute concentration maximum in the liquid next to the advancing solid-liquid interface. This solute profile, via the phase relations, specifies an equilibrium freezing temperature profile in the liquid. If certain temperature profiles occur in the liquid, a zone of constitutionally

supercooled liquid is produced ahead of the interface. As a result of the formation of this supercooled zone, a planar interface ceases to be stable and a cellular or dendritic interface forms. For a detailed description of this process refer to references 134, 170, 171, 59, 100. When attempts are made to apply the formal diffusion limited constitutional supercooling theory to the natural freezing of sea and lake water, severe discrepancies are noted.[191] These are undoubtedly the result of the fact the main transfer mechanism controlling the distribution of solute in the liquid ahead of the advancing interface is, in these cases, convection instead of diffusion. Regardless of this difficulty, it clearly appears that the existence of a non-planar interface during the solidification of sea water is the result of some form of constitutional supercooling.

Once a non-planar interface forms, its exact geometry is specified by the details of the growth conditions. James[72] has discussed the morphological changes during the transition to a fully developed cellular or dendritic interface. Although there are no detailed observations of sea ice interfaces during natural growth, an examination of the resulting substructure suggests that typical morphologies are similar to the elongated cell shown in Figure 9 (Tiller)[171] or the array of parabolic platelets diagrammed by Weeks.[191] It is easy to visualize how brine becomes trapped in the intercellular grooves producing the characteristic sea ice substructure shown in Figures 10 and 11. Growth accidents also may cause slight orientation differences between neighboring plates producing small angle grain boundaries. Since each sub-grain represents an ice platelet that grew into the underlying sea water, the pronounced (0001) elongation of the plates is produced by a slower crystal growth perpendicular to the basal plane than parallel to it. Certain geometric aspects of these plates have been studied by Weeks and Hamilton.[188] As shown in Figure 10, single crystals of sea ice are easily delineated under crossed polaroids because they behave as common extinction units. Each single crystal is composed of a "packet" of plates and each plate is separated by an array of brine pockets.

The distance between adjacent brine layers in the same crystal measured parallel to the c-axis has been termed the plate spacing a_o. This distance changes systematically with position in an ice sheet. That such changes in a_o should be expected could be anticipated from the metallurgical literature[46] and has been demonstrated for sea ice,[164, 188] and for NaCl ice.[189] Figure 12 shows the vertical variations in the mean plate spacing $\bar{a}_o$ for a sheet of NaCl ice. The main factor controlling this variation is the general decrease in growth velocity as the ice sheet thickens. Assur and Weeks[20, 21] have attempted to fit the existing NaCl ice data using a relation of the general form

$$a_0 \, v^k = C \qquad (2.10)$$

where v is the growth velocity, k is a constant with a value of 1/2 and C is another constant. The resulting fit is adequate (Fig. 13) giving $C = 3.64 \times 10^{-4}$ when a_0 and v are in cm and cm/sec respectively. Unpublished results of Lofgren and Weeks show that the power k appears to be a function of v, changing from $k \sim 1$ at high v to $k \sim 0$ at low v. The use of $k = 1/2$ does, however, appear to be a convenient first approximation over a wide range of growth velocities. More detailed experimental observations are needed on this subject.

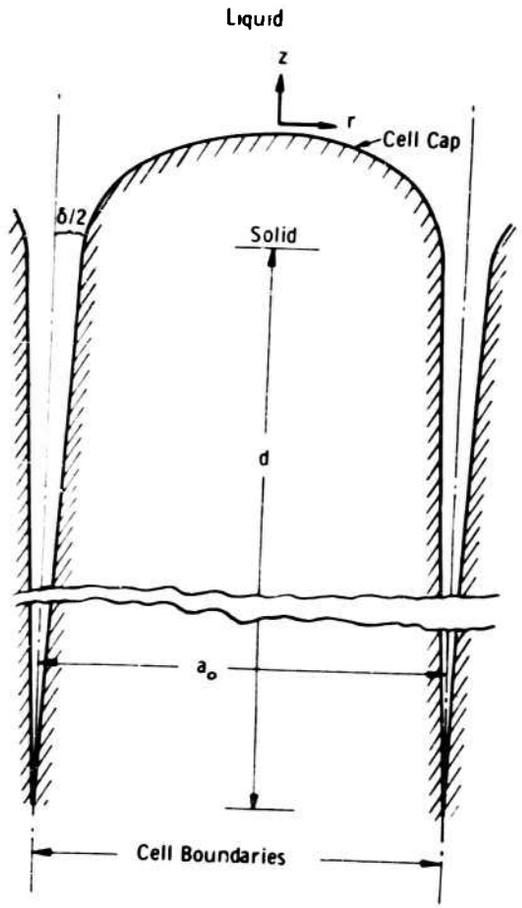

Figure 9. Schematic representation of a cut through a 2-dimensional cell illustrating the relative dimensions of the cell groove, δ, to the cell or plate spacing a_0 (Tiller).[171]

Figure 10. Photomicrograph of a thin section of sea ice, Point Barrow, Alaska, 1960; photograph taken using crossed polaroids; grid is 1 cm on a side.

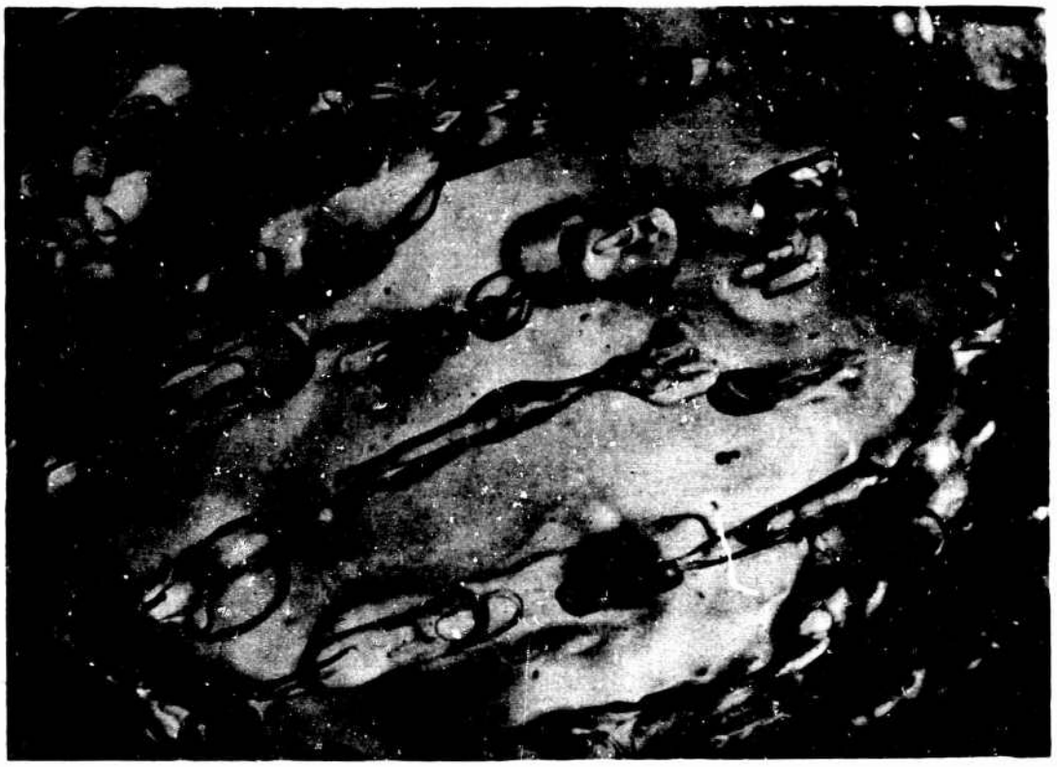

Figure 11. Photomicrograph of a thin section of sea ice illustrating brine pocket shapes.

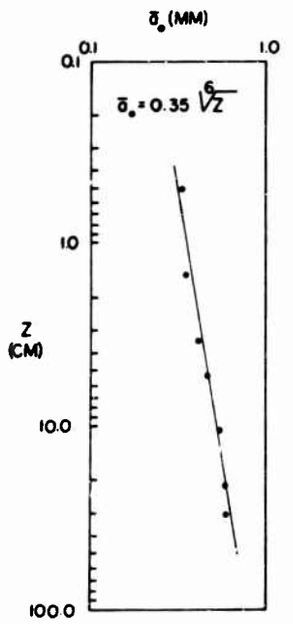

Figure 12. Increase in $\bar{a}_0$, the average plate spacing, as a function of the distance below the surface of the ice sheet, z (Weeks and Assur).[189]

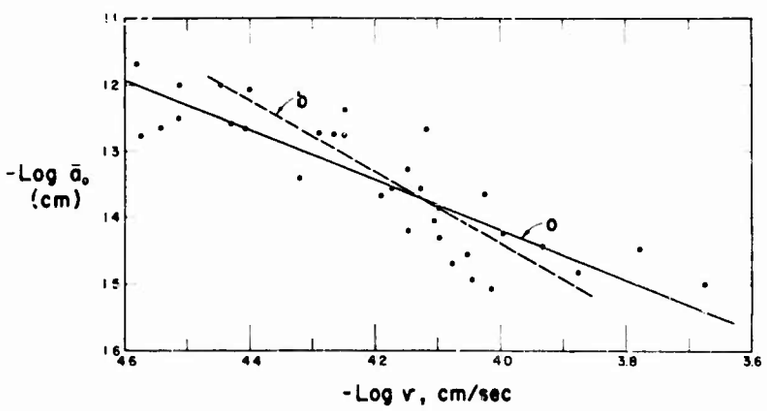

Figure 13. Logarithmic plot of average plate spacing $\bar{a}_0$ vs growth velocity v (Assur and Weeks).[21] Here (a) is the least-squares fit, log $\bar{a}_0$ = -2.9105 - 0.3729 log v and (b) is a least-squares fit assuming a slope k of -1/2, which gives C = 3.64×10^{-4} (eq 2.10).

It should be noted that currently the only aspect of the sea ice substructure that has definitely been related to the growth velocity when a given increment of ice forms is the plate spacing. We feel that it is very reasonable to suppose that other structural features such as the systematic spacing between brine pockets as measured in a horizontal plane (see Fig. 15) are also some function of $\underline{v}$. As will be shown later, it is very important that such relations, if they exist, be documented and incorporated into a formal sea ice strength theory.

3. THEORETICAL CONSIDERATIONS

Strength Models

Even the most casual examination of a sea ice specimen that has fractured reveals that the fracture surface is controlled by the substructure. Figure 14[4] is a rubbing of a horizontal section of a sea ice beam that failed in tension. Similar rubbings have been published by Tabata.[162] The parallel lines are, of course, the edges of individual ice plates. Note how the break only transects the platelets in a few unfavorably located grains. In addition the large variations in measured strength values for sea ice made the development of formal models highly desirable in that they would suggest compact forms for correlating and extrapolating strength results.

The treatment of the mechanical properties of sea ice on the basis of structural models was pioneered by Tsurikov.[174] In a subsequent paper[175] he modified some of his initial calculations. Although he initially considered porosity only in terms of air content, he later[176] introduced brine volume on the basis of Malmgren's 1927 calculations.[97] In his structural models he assumed either uniformly distributed spherical or uninterrupted cylindrical inclusions as voids. Tsurikov's imaginative approach also introduced the effect of the orientation of stresses. His concepts were way ahead of their time. There are, unfortunately, many errors in principle or oversights in Tsurikov's work but his essential ideas can be condensed and presented in the following way.

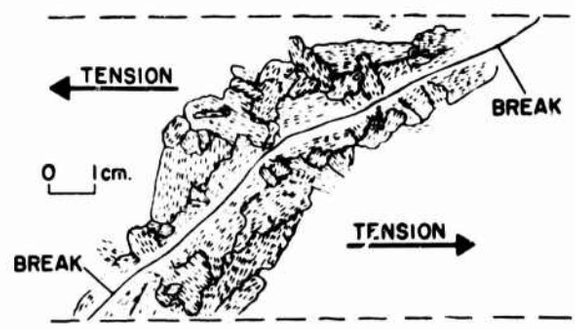

Figure 14. Rubbing of a broken segment of sea ice (Anderson and Weeks).[4]

If there are n_3 spherical voids with radius r uniformly distributed in 1 cm^3 of sea ice, then the volume porosity is

$$v = \frac{4}{3} \pi n_3 r^3. \tag{3.1}$$

It is essential to assume that failure occurs in a preferred plane which has the maximum plane porosity v_p. The number of holes in that plane is therefore $n_3^{2/3}$ and

$$v_p = \pi n_3^{2/3} r^2. \tag{3.2}$$

The relative strength of sea ice then becomes

$$\frac{\sigma_f}{\sigma_0} = 1 - \pi n_3^{2/3} r^2 \tag{3.3}$$

where σ_f is the failure strength and σ_0 is the basic strength of sea ice (see p. 18). Because r can be expressed in terms of v from eq 3.1

$$\frac{\sigma_f}{\sigma_0} = 1 - \left(\frac{v}{v_0}\right)^{2/3} \tag{3.4}$$

with

$$v_0 = \frac{4}{3\sqrt{\pi}} \tag{3.5}$$

where v_0 is the brine volume for which the ice has zero strength.

In Tsurikov's subsequent paper,[175] he deviated from this approach by assuming that the solidity of a line cut through sea ice is

$$1 - v_\ell = \sqrt{1 - v} \tag{3.6}$$

where v_ℓ is the line porosity (our notation and definition). This is in error. With a random distribution of voids, the line porosity equals the plane porosity equals the volume porosity. In a systematic array the corresponding porosity values depend upon the arrangement. Due to the error in his basic assumptions, his resulting equations should not be used. For bending Tsurikov reduced the width and square of the height which is in error.

For cylindrical voids the number of holes (n_2) in a cut perpendicular to the cylinders expressed per cm^2 becomes important. The plane porosity equal to the volume porosity is

$$v_p = v = \pi n_2 r^2. \tag{3.7}$$

Again assuming failure in a preferred plane parallel to the cylinders, the maximum line porosity ν_ℓ becomes important. The number of holes in that line is $\sqrt{n_2}$ and the line porosity is

$$\nu_\ell = 2\sqrt{n_2}\, r. \tag{3.8}$$

The relative strength of sea ice in a plane parallel to the cylinder becomes

$$\frac{\sigma_f}{\sigma_0} = 1 - 2\sqrt{n_2}\, r \tag{3.9}$$

and substituting for r from eq 3.7

$$\frac{\sigma_f}{\sigma_0} = 1 - \left(\frac{\nu}{\nu_0}\right)^{1/2} \tag{3.10}$$

with

$$\nu_0 = \frac{\pi}{4}. \tag{3.11}$$

The corresponding equation in Tsurikov[174] is wrong by oversight but was corrected later.[175] For failure in a plane perpendicular to the cylinders, the strength is simply

$$\frac{\sigma_f}{\sigma_0} = 1 - \nu \tag{3.12}$$

which is always higher than eq 3.10.

Other Russian investigators appear to have paid little attention to Tsurikov's work although it has been referenced in a recent Russian review[70] of American work in sea ice physics. Tsurikov's papers clearly indicate the possibility of developing a structurally based theory of sea ice strength. The next step one must take is a proper consideration of the platelet-like microstructure of sea ice crystals where brine pockets are arranged in systematic parallel arrays.

This step was provided by Assur,[17] Anderson and Weeks,[4] and Anderson[2,5] who fortunately had available a considerable amount of information on the structure of sea ice. They noted that in a relatively cold sample of sea ice (Fig. 15) with a small brine volume, the brine pockets are small and widely spaced. When a potential failure plane between two ice plates is considered, it is found that an appreciable percentage of this plane is ice. Therefore, this sea ice would be expected to have a significant tensile strength. The specimen shown in Figure 16, on the other hand, contained a very large volume of brine while it was located in the ice sheet. This brine was later lost during storage and preparation. A plane can be passed through this sample without encountering more than a few ice-ice bonds.

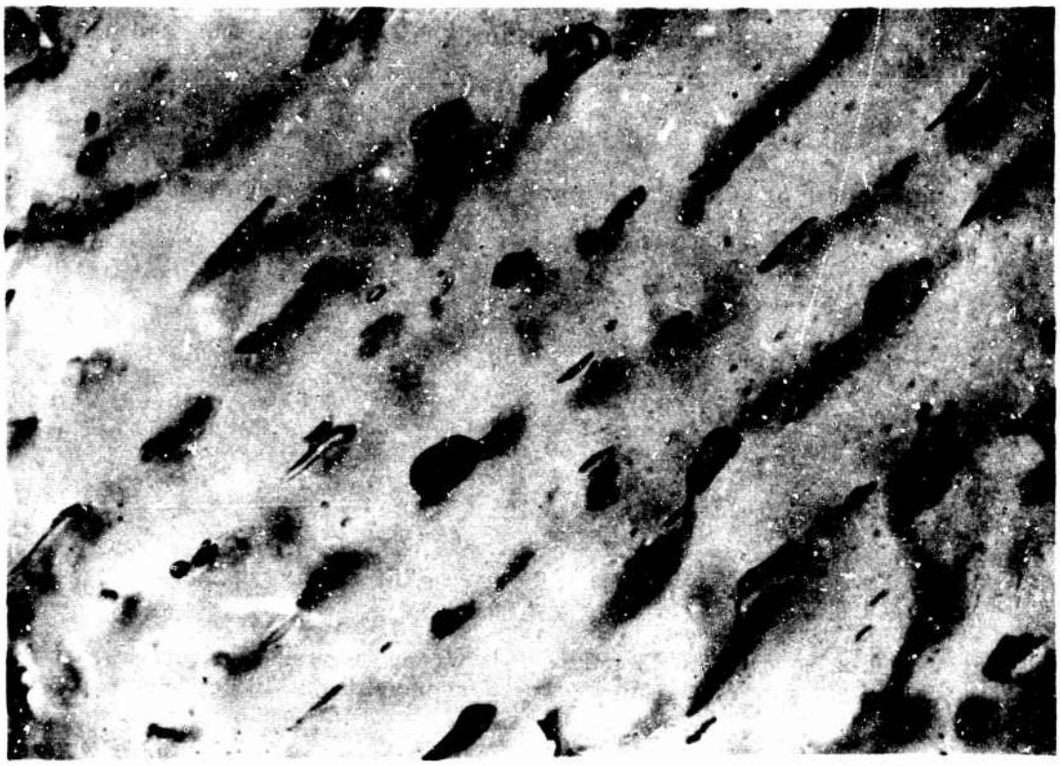

Figure 15. Photomicrograph of sea ice at low temperatures (Thule, Greenland, 1957).

Therefore, this specimen would be expected to have a tensile strength close to zero even though it contains an appreciable amount of ice. This is exactly what is observed in strength tests (see Fig. 22): the failure strength σ_f decreases from a maximum σ_0 at zero brine volume ($v_l = 0$) to a strength of zero at a brine volume v_0. Therefore, it should be possible to express sea ice strength in the general form

$$\frac{\sigma_f}{\sigma_0} = 1 - \psi \tag{3.13}$$

where σ_0 can be considered the basic strength of sea ice (i.e., the strength of an imaginary material that contains no brine, but still possesses the sea ice substructure and fails as a result of the same mechanism that causes failure in natural sea ice) and ψ is the "plane porosity" or relative reduction in area of the failure plane as the result of the presence of brine and air inclusions. The critical value of ψ in the failure plane is

$$\psi = f(v) = f(v_a + v_b) \tag{3.14}$$

where v is the void volume or porosity and v_a and v_b are the volume of air and brine respectively in the ice. We will now for simplicity consider a sea

Figure 16. Photomicrograph of sea ice at a temperature only slightly below the freezing temperature (-3C, Thule, Greenland).

ice specimen in which $\nu_b >> \nu_a$. To express ψ in terms of ν_b, a simplified model of the geometry of the brine pockets must be given. This can be done[17] as shown in Figure 17. Here the relative brine volume is

$$\nu_b = \frac{Fg}{a_0 b_0 g_0} \tag{3.15}$$

where the symbols are defined in Figure 17. Now defining

$$\beta_0 = \frac{b_0}{a_0} \tag{3.16}$$

$$\gamma = \frac{g}{g_0} \tag{3.17}$$

we find that the reduction in cross sectional area as the result of the presence of the brine pockets is

$$\psi = \frac{2 r_b g}{b_0 g_c} = \frac{2 r_b \gamma}{\beta_0 a_0} . \tag{3.18}$$

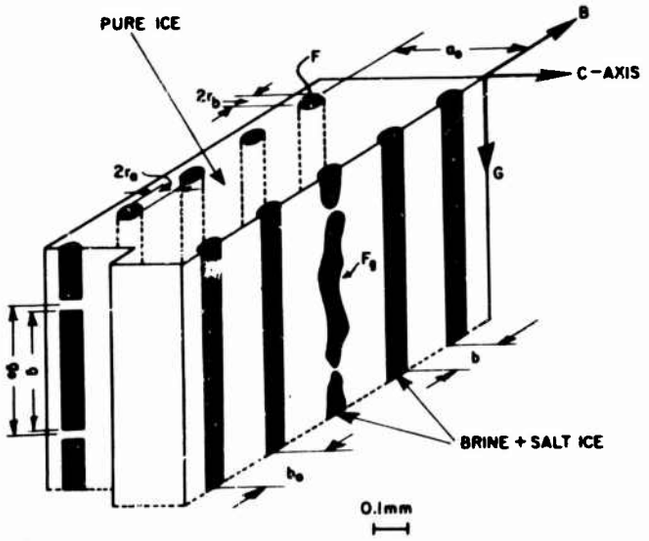

Figure 17. Idealized diagram of the shape of the brine inclusions in sea and NaCl ice (Assur).[17]

The effective strength due to this reduction in cross sectional area becomes

$$\frac{\sigma_f}{\sigma_0} = 1 - \frac{2 r_b \gamma}{\beta_0 a_0}. \tag{3.19}$$

The question now is how the geometric parameters r_b and γ vary with ν_b. Here a number of different assumptions can be made. The simplest case is to assume that geometric similarity is preserved only along the B-axis (see Fig. 17) and that the width as well as the length of the brine pockets remains constant. In this case r_b must change proportionally to ν_b and an equation of the form

$$\frac{\sigma_f}{\sigma_0} = 1 - c\,\nu_b \tag{3.20}$$

results. If, on the other hand, the average length and spacing of the brine cylinders remain constant, then changes in ν_b will be reflected only in the BC cross section. If geometric similarity is preserved in this cross section, then our equation is of the form

$$\frac{\sigma_f}{\sigma_0} = 1 - c\,\nu_b^{1/2}. \tag{3.21}$$

If all brine pockets remain of a similar shape during changes in ν_b, all linear dimensions will change proportionally to $\sqrt[3]{\nu_b}$ (geometric similarity in space). This results in an equation of the form

$$\frac{\sigma_f}{\sigma_0} = 1 - c\,\nu_b^{2/3}. \tag{3.22}$$

These three sets of models can be represented as straight lines in σ_f, v^k coordinates where k is 1, 1/2 and 2/3 respectively. The σ_f axis intercept is σ_0 and

$$c = v_0^{-k} \tag{3.23}$$

where v_0 is the volume of brine necessary to cause the ice to have zero strength. Defining

$$\rho = \frac{2 r_b}{\sqrt{F}} \tag{3.24}$$

and

$$a_0 = \frac{a_0}{\sqrt{F}} \tag{3.25}$$

v_0 for the three classes of models may be written

$$k = 1, \quad v_0 = \frac{1}{\rho a_0} = \frac{F}{2 r_b a_0} \tag{3.26}$$

$$k = \frac{1}{2}, \quad v_0 = \frac{\beta_0}{\rho^2 \gamma} = \frac{b_0 g_0 F}{4 r_b^2 g a_0} \tag{3.27}$$

$$k = \frac{2}{3}, \quad v_0 = \left(\frac{\beta_0}{\rho^3 \gamma a_0}\right)^{1/2} = \frac{F}{a_0}\left(\frac{b_0 g_0}{8 g r_b^3}\right)^{1/2}. \tag{3.28}$$

A large number of specific models can be developed under these three categories[17,4]. The two that have been utilized in discussing specific strength results are the constant width and the elliptical cylinder models.

In the constant width model

$$F = 4 r_a r_b \tag{3.29}$$

and

$$v_0 = \frac{2 r_a}{a_0} = \frac{d_0}{a_0} \tag{3.30}$$

where d_0 is the minimum width of a parallel brine layer before it splits as the result of interfacial tension to produce individual brine pockets It is usually assumed[189,4] that $d_0 \sim$constant because the ice-brine interfacial tension would not be expected to be particularly temperature-sensitive in the temperature interval where sea ice observations are made. A value of d_0 of 7×10^{-3} cm has been measured in natural sea ice[4] by direct petrographic methods and a value of 11×10^{-3} cm in NaCl ice by an indirect calculation.[189] When a brine layer becomes thinner than this value it necks, causing ice-ice bonds to form. When the first of these bonds forms between the growing plates at the bottom of an ice sheet, it establishes the location of the so-called bridging layer. The ice platelets below this location are

not laterally connected and therefore have zero tensile strength. This strengthless layer has been termed the skeleton layer since it can be considered to be the result of "skeletal" growth.

In the elliptical cylinder model let

$$\epsilon = \frac{r_b}{r_a} \tag{3.31}$$

and

$$F = \pi r_b r_a = \frac{\pi r_b^2}{\epsilon} \tag{3.32}$$

and eq 3.21 becomes

$$\frac{\sigma_f}{\sigma_0} = 1 - 2\sqrt{\frac{\epsilon\gamma}{\pi\beta_0}}\sqrt{\nu_b} \tag{3.33}$$

If we wish to consider circular cylinders ($\epsilon = 1$) and neglecting any interruption of brine pockets in the vertical direction ($\gamma = 1$), eq 3.33 becomes

$$\frac{\sigma_f}{\sigma_0} = 1 - \frac{2}{\sqrt{\pi\beta_0}}\sqrt{\nu_b} \tag{3.34}$$

As will be discussed in detail later, recent experimental results[50] have verified the tentative suggestion of Assur[17] that the strength of warm sea ice does not approach zero as a linear function of ν_b^k as suggested by these previous models. Instead, if the test results are plotted on σ_f, $\sqrt{\nu_b}$ coordinates, the resulting curves appear to be convex toward the origin of the coordinate system in the high brine part of the diagram (Fig. 26). It is possible to modify eq 3.33 in such a way that it more properly describes this observed strength variation

$$\frac{\sigma_f}{\sigma_0} = 1 - \sqrt{\frac{\nu_b}{\nu_0}} \tag{3.35}$$

where

$$\sqrt{\nu_0} = \sqrt{\frac{\pi\beta_0}{4\gamma\epsilon}} \tag{3.36}$$

with a value of $\sqrt{\nu_0} \sim 0.5$ if $\sqrt{\nu_0}$ is computed from the linear intercept. We may choose a power $n > 1$ for

$$\frac{\sigma_f}{\sigma_0} = \left[1 - \sqrt{\frac{\nu_b}{\nu_0}}\right]^n \tag{3.37}$$

without losing the advantages of the theoretical models. The simplest possible assumption is n = 2 which gives an expression that can be linearized in the form

$$\sqrt{\sigma_f} = \sqrt{\sigma_0} \left[1 - \frac{\nu_b}{\nu_0}\right] \tag{3.38}$$

where by plotting $\sqrt{\sigma_f}$ vs $\sqrt{\nu_b}$, we obtain $\sqrt{\sigma_0}$ as the intercept and $\sqrt{\sigma_0/\nu_0}$ as the slope. From eq 3.37 with n = 2 we obtain

$$\frac{d\sigma_f}{d\sqrt{\nu_b}} = -\frac{2\sigma_0}{\sqrt{\nu_0}} \left[1 - \sqrt{\frac{\nu_b}{\nu_0}}\right] \tag{3.39}$$

which for $\nu_b = \nu_0$ equals zero. Therefore, the proper choice of ν_0 may not be important since the change in σ_f in its vicinity is small. Equation 3.39 expresses a gradual vanishing of σ_f rather than an abrupt decrease. Equation 3.37 with n = 2 can also be written in the form

$$\frac{\sigma_f}{\sigma_0} = 1 - 2\sqrt{\frac{\nu_b}{\nu_0}} + \frac{\nu_b}{\nu_0} \tag{3.40}$$

which is a second order polynomial in $\sqrt{\nu_b}$. Here we have a combination of the two main models discussed above; one is linear in $\sqrt{\nu_b}$, the other in ν_b. From eq 3.40

$$\frac{d(\sigma_f/\sigma_0)}{d\sqrt{\nu_0}} = -\frac{2}{\sqrt{\nu_0}} + \frac{2}{\nu_0}\sqrt{\nu_b} \tag{3.41}$$

where for $\nu_b = 0$ exactly and for small ν_b as an approximation gives

$$\frac{d(\sigma_f/\sigma_0)}{d\sqrt{\nu_0}} = -\frac{2}{\sqrt{\nu_0}} \tag{3.42}$$

with the simplest possible assumption $\nu_0 = 1$, we have

$$\frac{d(\sigma_f/\sigma_0)}{d\sqrt{\nu_0}} = -2 \tag{3.43}$$

which is in very good agreement with observation.[17,187,50]

Stress Concentration and Brittle Fracture

By reading Assur,[17] Anderson and Weeks,[4] Anderson,[2,5] and the discussion in National Academy of Sciences - National Research Council 598, it becomes apparent that there has been considerable diversity of

opinion regarding certain aspects of the problem of stress concentration in sea ice. The main portion of this discussion was involved with Anderson and Weeks[4] presenting eq 3.13 in the form

$$\sigma_f = \frac{\sigma_i}{k} (1 - \psi) \tag{3.44}$$

where σ_i is the strength of pure ice and k is a stress concentration factor caused by the presence of brine pockets in sea ice. For small isolated circular brine pockets, k was assumed to be ~ 3. This implied that the basic strength of sea ice σ_0 was 1/3 the strength of lake ice and that this difference was produced by the presence of brine pockets in sea ice. That this was incorrect was shown experimentally when Weeks[187] and Graystone and Langleben[57] demonstrated that $\sigma_i \sim \sigma_0$ for NaCl ice and sea ice respectively. This does not mean that stress concentrations are not produced by the sea ice microstructure but only as suggested by Assur[17], that similar stress risers also occur in fresh water ice. The factor of ~ 3 observed by Anderson and Weeks[4] was produced by differences in stress concentration associated with differences in testing procedures and not with differences in k associated with the presence or absence of the microstructure. In actuality, the equating of σ_0 with σ_i is a suspect procedure.[53] Inasmuch as the microstructure of the fresh water ice is unspecified, σ_i is undetermined. In addition fresh water ice which by definition contains no brine pockets quite possibly fails by a different mechanism than does sea ice.[54]

Goetze[53] has pointed out that it also is possible to approach the sea ice strength problem as a problem in elastic instability in a brittle material. The well known Griffith crack problem is of this type. In the Griffith crack analysis, it has been shown that two conditions must be satisfied for spontaneous crack growth:

1. A stress concentration must exist that is sufficient to overcome the intrinsic strength of the material and

2. Elastic readjustment as the crack develops must provide a decreasing energy path for the specimen as a whole.

Griffith's criterion for a failure stress is

$$\sigma_f \geq \sqrt{\frac{2E\gamma'}{\pi c}} \tag{3.45}$$

where σ_f is the failure stress, E is Young's modulus, γ' is the total energy required per unit increase in the area of the crack (comprised of the true surface energy and the plastic work done by the stress concentration at the tip of the moving crack), and c is the crack length. Goetze has extended this treatment by considering the failure criterion for a polycrystalline, elastic material which contains a "microstructure" capable of generating a stress concentration. This is done by considering a grain that has for some reason, perhaps orientation differences, an apparent E lower than its surroundings. The result is

$$\sigma_f \geq \sqrt{\frac{8\gamma' G}{\pi(\eta + 1)\left(1 - \frac{\kappa\delta}{\pi}\right)c_0}} \tag{3.46}$$

where G is the shear modulus, $\eta = (3 - \mu)/(1 + \mu)$ where μ is Poisson's ratio, κ is the proportion of the stress σ that is exerted on the weak crystal ($0 \leq \kappa \leq 1$), and δ is a complicated function of c_0 and c where $2c_0$ is the original grain length and $(c - c_0)$ is the length of the crack (prior to cracking $c = c_0$ and $\delta = \pi$). If $(1 - \kappa) > 0$, failure can clearly occur for sufficiently large σ without the presence of a crack prior to failure. This is not true in a homogeneous material. Goetze then shows by a dimensionless argument that elastic instability can occur during plane stress when

$$\sigma \geq \sqrt{\frac{2E\gamma'}{\pi P d}} \tag{3.47}$$

where P has a value close to 1 and when a class of materials is considered in which the microstructure varies only in size, P remains constant. The length d is taken to be a characteristic of the size of the microstructure. Therefore, when dealing with failure stresses

$$\sigma_f^2 \, d = \frac{2E\gamma'}{\pi P} \sim \text{const.} \tag{3.48}$$

Considering ring tensile results on sea ice, we find that $\sigma_f \sim 15$ kg/cm^2 and that $E \sim 5 - 10 \times 10^{10}$ dynes/cm^2, $\gamma' \sim 76$ ergs/cm^2 and, assuming that $P \sim 1$, eq 3.48 implies that the fracture originates in a microstructure with a size of 0.1 to 1.0 mm. This is clearly of the same scale as the brine pockets in sea ice.

To treat sea ice as an instability problem it is necessary to assume that only the brine pockets within a given plane interact elastically. This, of course, is quite reasonable considering the structure of sea ice. We then must obtain the elastic solution for a periodic array of cracks. This apparently is not known. Therefore, Goetze makes a number of approximations to get some idea of the general solution. If b_0 and r_b are defined as shown in Figure 17, his approximate fracture relation is

$$\sigma_f \geq \text{const} \left[\frac{b_0}{2r_b} - 1 \right]. \tag{3.49}$$

He then assumes that $2r_b$ can be identified with $\sqrt{\nu_b}$ where ν_b is the brine volume and shows that a σ_f vs $1/\sqrt{\nu_b}$ plot of Assur's[17] ring tensile data is to a good approximation linear. There are some obvious difficulties with eq 3.49 - note that when $r_b \to 0$, $\sigma_f \to \infty$. Yet it is cold sea ice with its correspondingly low brine volumes that most closely approximates the brittle behavior postulated by an elastic instability analysis. Nevertheless this is an interesting and promising approach, if not for sea ice which is always quite close to its melting temperature, then for other porous materials which show brittle fracture characteristics. Work along these lines should be continued.

Air Bubbles and Salt Reinforcement

It should be noted that additional petrographic observations are needed on the distribution of air pockets in sea ice. If, as seems reasonable, air bubbles are localized along the same substructure as the brine pockets, then we may simply treat ν_a as an additional contribution to ν_b and deal with the

total void volume v where $v = v_a + v_b$. If, on the other hand, the geometrical considerations governing the distribution of the air bubbles are quite different from those controlling the brine distribution, v_a will have to be considered separately.

There has been some discussion in the recent sea ice literature regarding the possible effects of $Na_2 SO_4 \cdot 10H_2 O$ and $NaCl \cdot 2H_2 O$ in increasing the values of σ_f beyond the normal increase that would be associated with the decrease in the size of the brine pockets as the solid salt precipitates. Possible hypotheses for this so-called solid salt reinforcement of the brine pockets have been advanced by Assur[17] and Peyton.[123] Because the experimental verification for this effect is still in doubt, we will not discuss these theories here. It should, however, be noted that both hypotheses depend upon how the solid salts are distributed in the brine pockets during precipitation. The salts may precipitate in a solid mixture with the ice in which case reinforcement is possible. Or the solid salt crystals may remain in the liquid brine in which case no reinforcement is possible. If the solid salts enter into a solid mixture with ice, they will not participate in further brine drainage and a change in the ion ratios with time should be observed. If the solid salts drain together with the brine, the ion ratios should remain constant in sea ice. Sporadic evidence to support either of these views is available.[26,28,142]

Interrelations Between Growth Conditions and Strength

Assur and Weeks[20,21] have discussed how changes in the geometry of the sea ice microstructure as produced by changes in the meteorological conditions during growth can influence the failure strength. To do this one may assume that eq 2.10, the relation between the plate spacing a_0 and the growth velocity (Fig. 13), can be expressed as

$$a_0 \sqrt{v} = 2\sqrt{cD\Delta z} \sim \text{const.} \tag{3.50}$$

Here D is the molecular diffusion coefficient of salt in water, c is a coefficient which accounts for turbulent transfer of solute in excess of molecular diffusion and Δz is a characteristic length associated with the distance a platelet grows before the salt diffusion for neighboring platelets meets between the platelets preventing another platelet from protruding. It should be noted that the fact that details of the justification for eq 3.50 are undoubtedly incorrect is not important in the following discussion as long as some relation of this general form holds. Now the fresh ice growth equation is

$$t = \frac{\rho L h}{\Delta\theta}\left[\frac{1}{e} + \frac{h}{2\kappa}\right] \tag{3.51}$$

where t is the time, h the ice thickness, ρ the density of ice, L the latent heat of fusion of ice, $\Delta\theta$ the difference between the ambient temperature and the freezing temperature of the water, e the overall coefficient of surface heat transfer, and κ the thermal conductivity. This relation may be applied to sea ice if slight adjustments are made in the values of L and κ. Now rearranging and differentiating eq 3.51

$$\frac{dh}{dt} = v = \frac{\Delta\theta}{\rho L\left[\frac{1}{e} + \frac{h}{\kappa}\right]} \tag{3.52}$$

which when combined with eq 3.50 gives

$$a_0 = \sqrt{\frac{4cD\Delta z\rho L}{\Delta\theta}\left[\frac{1}{e} + \frac{h}{\kappa}\right]}. \tag{3.53}$$

For thin ice $1/e >> h/\kappa$ and a_0 is independent of the ice thickness h, while for thick ice $h/\kappa >> 1/e$ giving a_0 varying proportional to $\sqrt{h}$. The empirical power of 1/6 as determined by Weeks and Assur[189] lies between these theoretical limits of zero and 1/2 (Fig. 12).

Because a_0 appears in our model strength equations we may substitute in 3.20 and 3.30 giving

$$\frac{\sigma_f}{\sigma_0} = 1 - \frac{2\nu_b}{d_0}\sqrt{\frac{cD\Delta z\rho L}{\Delta\theta}\left[\frac{1}{e} + \frac{z}{\kappa}\right]} \tag{3.54}$$

which for thin ice gives

$$\frac{\sigma_f}{\sigma_0} = 1 - \text{const}\ \frac{\nu_b}{\sqrt{\Delta\theta}} \tag{3.55}$$

and for thick ice

$$\frac{\sigma_f}{\sigma_0} = 1 - \text{const}\ \nu_b\sqrt{\frac{z}{\Delta\theta}} \tag{3.56}$$

where z is the distance of a given ice layer below the upper ice surface. Equation 3.55 provides a scientific justification for the intuitive conclusions of early Russian observers who felt that the strength of young sea ice was in some way influenced by its growth conditions. Assur and Weeks[20, 21] also consider the effect of a snow cover and ways of incorporating the change in the salinity of the ice sheet with time. Although it is beyond the scope of this review to discuss the sea ice salinity profile and its time dependence, an appraisal of the current knowledge of this subject can be obtained from references 178, 28, 190 and 179.

4. EXPERIMENTAL RESULTS

The quality of experimental studies on the mechanical properties of sea ice is quite varied. The fact that a large number of published papers do not contain sufficient supplementary information to permit an analysis of strength results was noted by Zubov in 1945 and unfortunately is still true. Ideally every measurement of a mechanical property should at least be coupled with a measurement of the salinity S_i and temperature θ_i of the tested sample ($\nu_b = f(S_i\theta_i)$). A measurement of the air temperature θ_a is not adequate. It is very perplexing to attempt to analyze data that are accompanied only by a statement that θ_a = +4C. In addition, the orientation of the sample, the rate of stress application $\dot{\sigma}$, the volume of included air ν_a, details of the exact location of the sample in the ice sheet, the history of the ice sheet and the handling of the sample after it is removed from the sheet should be noted. It is also desirable to have at least a limited petrographic description of the structural aspects of the sample. In this

review we will, in general, only discuss those papers which have provided reasonable supplementary information. Exceptions will only be made in cases such as shear strength where there are almost no data available regardless of quality. We have, however, in the references attempted to give a fairly complete list of the papers that consider any aspect of the mechanical properties of sea ice.

General descriptions of recommended test procedures and equipment that has been used in studying the mechanical properties of sea ice in Russia and in the United States and Canada are given in Kudriavtsev[82] and Peschanskii,[119] and Butkovich[35] respectively. The main types of tests considered are tensile (ring and "dog-bone"), flexural (small beam and in-situ) and shear. Kudriavtsev also discusses an indentation test and a rather involved determination of the shear modulus and the coefficient of viscosity by torsion. These two tests have apparently not been used on sea ice. Although there are some differences, the test procedures suggested are, in general, similar. Particular stress is placed on the importance of determining the salinity and temperature of the sample, and it is recommended that for tests concerned with the elastic behavior of sea ice the rate of stress application $\dot{\sigma}$ should be greater than 0.5 kg/cm^2 - sec. This particular value of $\dot{\sigma}$ is based[35] on the observation by Jellinek[73] that the tensile strength of snow ice cylinders is independent of $\dot{\sigma}$ at $\dot{\sigma} > 0.5$ kg/cm^2 - sec (Fig. 18). Evidence for pure ice also shows this to be a reasonable value.

The importance of testing sea ice immediately after it has been removed from the ice sheet should be stressed. Exceptions to this procedure should only be made when storage facilities with ambient temperatures of -30C or colder are available. If the sample is stored, the coaxial hole should not be drilled until shortly before testing. If these procedures are not followed brine drainage invariably results in the surface layer of the specimen where failure is initiated. If samples are stored for appreciable lengths of time at temperatures warmer than -23C, extensive brine drainage throughout the complete sample results. When this occurs, the correlation between the mechanical properties of the ice and its brine volume disappears and is replaced by a "fictitious" correlation between mechanical properties and sample density as observed, for instance, by Tabata.[159,161]

If a test temperature other than the in-situ temperature is desired, it is necessary to let the specimen sit for approximately 3 hours before the temperature change at the center of the core is 95% complete.[126] Conversely

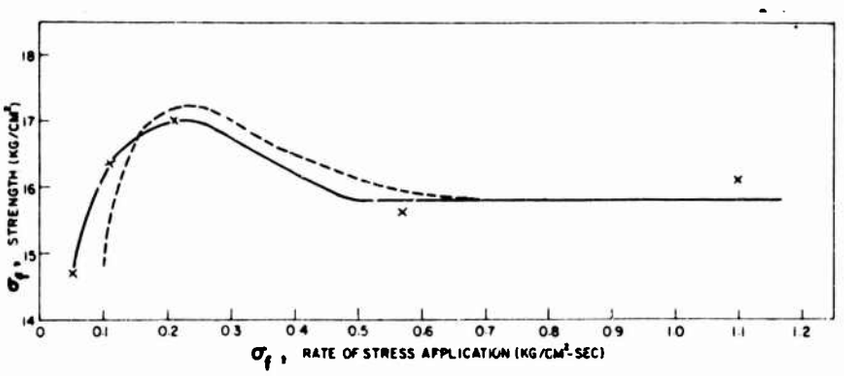

Figure 18. Average tensile strength as a function of rate of stress application $\dot{\sigma}$ for snow ice cylinders; height 2 cm, diam 2 cm (Jellinek.)[73]

if an in-situ test temperature is desired and it is necessary to test at a different temperature, the center temperature of the core can be assumed to be within 5% of the original temperature if the test can be performed within approximately 10 minutes of the time of removal of the specimen. No information is available on the rate of change of the ice surface temperature which is an important factor in strength tests.

Tensile Strength

Ring tensile tests

The ring tensile test has been extensively applied to studies of sea ice. There are several reasons for this: the SIPRE coring auger produces a suitable sample, the test is simple, easy to perform, and shows pronounced changes with temperature, salinity, depth and microstructure. The test was initially designed to study the tensile strength of such brittle materials as concrete and rock. The theory for the test was developed in an article by Ripperger and Davids[133] and further elaborated by Assur.[17] The test specimen consists of a sea ice cylinder with a 3-in. (7.6-cm) diam in which a 1/2-in. (1.27-cm) to 1-in. (2.54-cm) coaxial hole has been drilled. The specimen is then subjected to a compressive force normal to the axis of the cylinder. The sample fails as a result of tensile stresses that develop in a vertical plane with a maximum at the inner hole perpendicular to the direction of the load. The equation for computing the ring tensile strength is

$$\sigma_f = \frac{KP}{\pi r_o \ell} \tag{4.1}$$

where P is the load at failure, ℓ is the average length of the sample, and r_o is the outer radius of the sample. K is a stress concentration factor that is a complicated function of the ratio of the inner and outer radii (r_i/r_o) of the hollow cylinder. The theory for the test predicts K = 1 for a solid cylinder without a hole. For an infinitesimally small hole K = 6 and for r_i/r_o = 1/6, which has commonly been used, K = 7.09. Studies of the effect of variation of the hole size on the resulting strength have been made by Butkovich[37] and Frankenstein.[60] Butkovich found no change in the values of σ_f for glacier ice when the ratio (r_i/r_o) was changed from 1/3 to 1/6. Frankenstein compared sea ice tests performed on specimens with a radial hole diameter of 1/2 in. (1.27 cm) with tests performed on solid sea ice cylinders without a predrilled hole but containing brine pockets. Assuming that the solid cylinder should give the same σ_f value as the predrilled specimen, a new K with a value of 5.2 was computed. Ice temperature and brine volume do not appear to affect this value.

Because of the geometry of the ring tensile test, initial failure is restricted to a very small volume. It is difficult to estimate this volume exactly, but an approximate calculation[53] suggests a region 1.5 mm x 0.3 mm x the length of the cylinder. In short, ring tensile tests force failure upon a volume that has dimensions only slightly larger than the dimensions of the sea ice microstructure.

The theory predicts sharp stress concentrations in this small volume. No doubt, stress relief occurs as a result of plastic deformation which should be a function of temperature. This causes exaggerated values and

additional difficulties in interpretation. Sala[137] has discussed this difficulty but has not contributed sufficient experimental evidence to document his suggestion that the stress concentration index for natural sea ice

$$\eta = \frac{\beta - 1}{\alpha - 1} \tag{4.2}$$

where α is the theoretical stress concentration factor and β the reduced stress concentration factor as observed in experiments, is close to zero.

Butkovich[34] was the first investigator to apply the ring tensile test to the study of sea ice at Hopedale, Labrador. He found that the failure strength σ_f did not appear to be a strong function of either the sample density or its position in the ice sheet. He also showed that σ_f increased with decreasing ice temperature θ_i in the temperature range -2.5 to -19.1C for sea ice specimens with comparable densities and salinities. In a later series of tests at Thule, Greenland, Butkovich[36] further documented the increase in σ_f with a decrease in θ_i. He also showed that σ_f decreased as the brine volume ν_b increased (Fig. 19). Samples obtained by horizontal coring which were oriented so that failure occurred across the microstructure gave consistently higher σ_f values than values obtained from vertical cores with no specific orientation to the microstructure. As Butkovich pointed out, this difference in σ_f is quite reasonable in terms of the structure of the sea ice. He also noted that for identical values of ν_b and θ_i Thule ice gave consistently higher σ_f values than Hopedale ice. A possible explanation was advanced for this difference: that σ_f is in some way influenced by the past thermal history of the sample. A similar hypothesis had also been advanced by Assur[17] who proposed that strength changes might lag appreciably behind changes in θ_i. Attempts to resolve these suggestions by studying the Thule data were inconclusive.

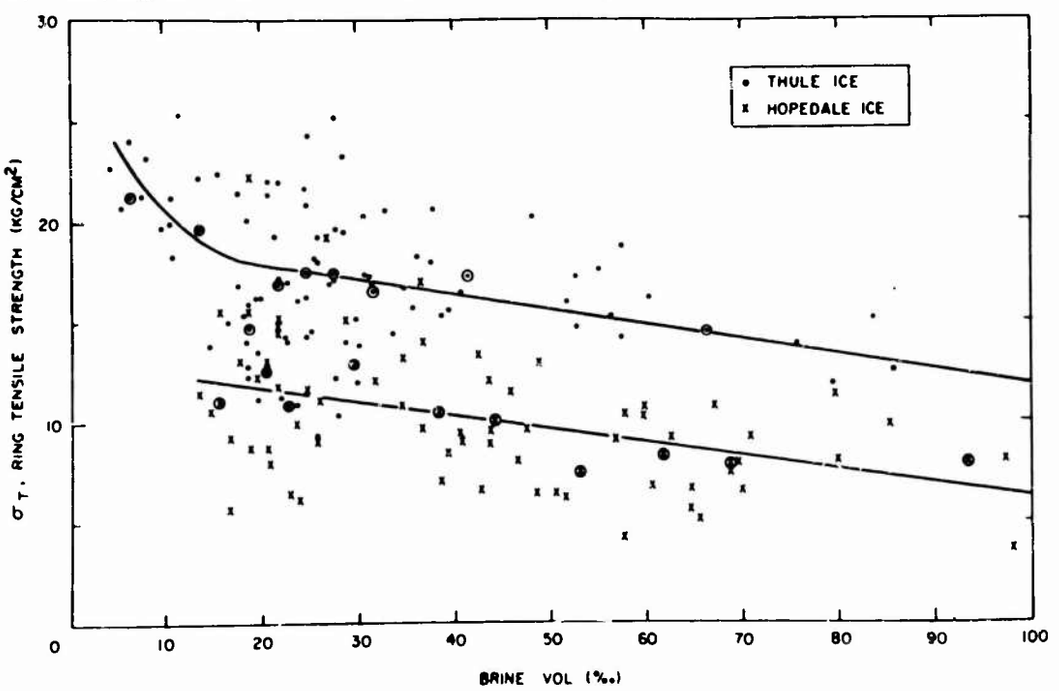

Figure 19. Ring tensile strength of sea ice vs brine volume, vertical cores. Circled points are group averages of 10 or more tests (Butkovich).[36]

Assur[17] reanalyzed some of Butkovich's data in addition to new data, in terms of a σ_f vs $\sqrt{\nu_b}$ plot which was suggested by the development of strength models as discussed earlier. His final graph is shown as Figure 20. From this graph and accompanying theoretical arguments, he advanced a number of hypotheses regarding the strength behavior of sea ice. The more important of these were

1. At high temperatures (above -8.2C), the strength of sea ice significantly decreases with increase in $\sqrt{\nu_b}$ (Fig. 20, line B_f-B_2).

2. At temperatures between -8.2 and -22.9C, the presence of solid $Na_2SO_4 \cdot 10H_2O$ increases the strength of the ice by roughly one third (Fig. 20, line C_f-C).

3. At temperatures below -22.9C, the precipitation of $NaCl \cdot 2H_2O$ causes sea ice to have strength values over twice that of fresh water ice (line D_1-D), provided that identical testing procedures are used. This increase in strength is dependent upon the amount of solid salt that has precipitated. Later tests have shown that these values are excessive.

When this postulated behavior is plotted on a graph that shows the relative strength (the strength of sea ice/the basic strength of sea ice σ_0) vs θ_i, it appears as shown in Figure 21. Assur also postulated other possibilities including a simple curve σ_f versus $\sqrt{\nu_b}$ convex to the center of coordinates. This now appears to be more justified.

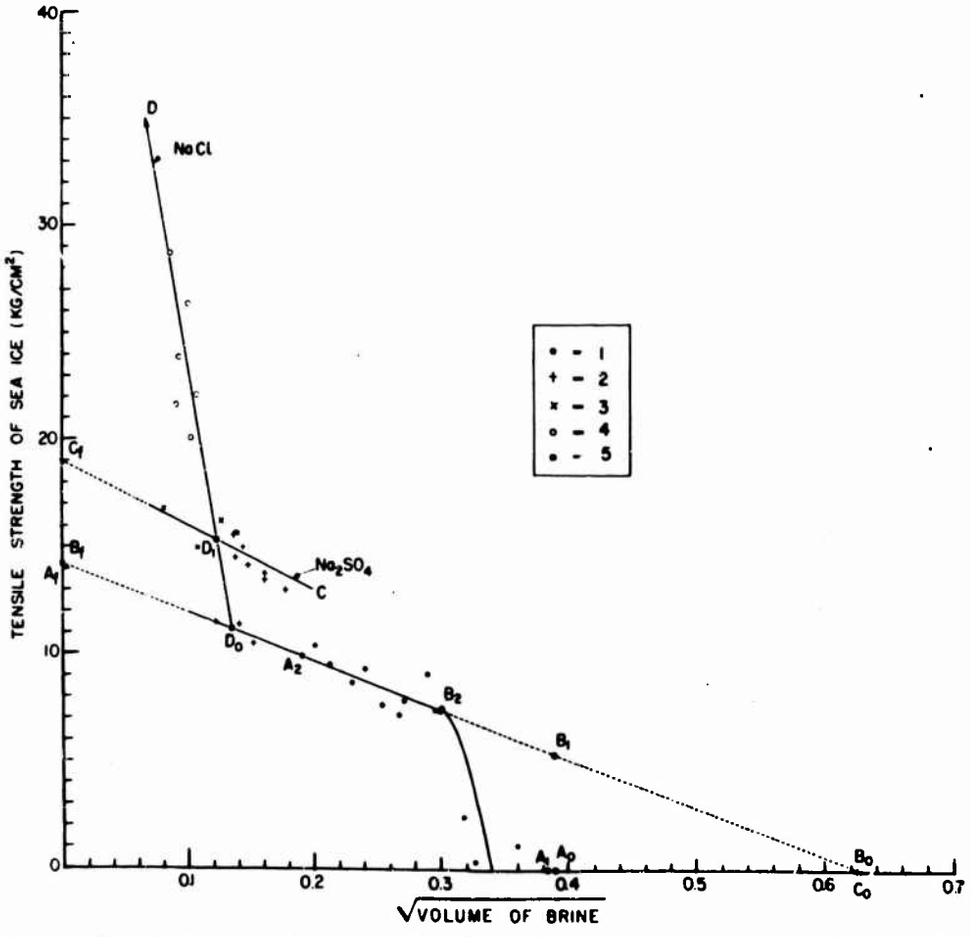

Figure 20. Ring tensile strength of sea ice vs square root of the relative brine volume ν_b. Each point represents on the average nine tests (Assur).[17]

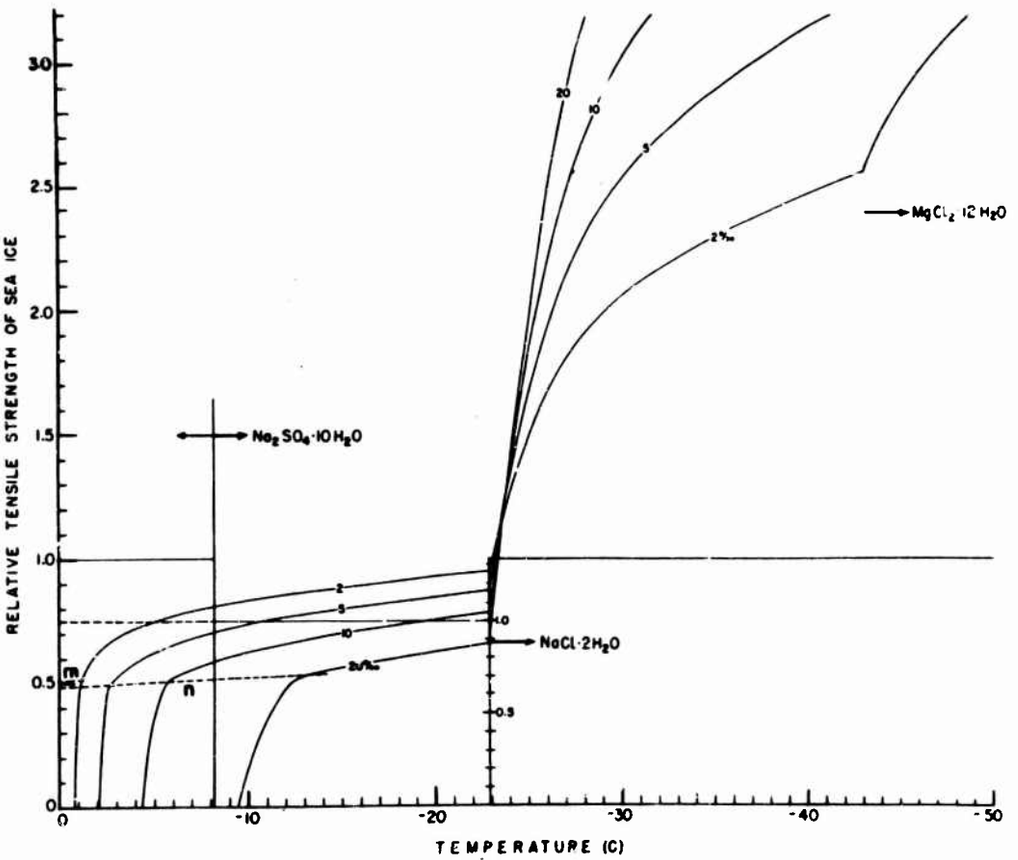

Figure 21. Relative ring tensile strength of sea ice (σ_f/σ_0) as a function of temperature and salinity. The right hand scale indicates a strength increase of 1/3 associated with the precipitation of $Na_2SO_4 \cdot 10H_2O$. Assur[17] recommended this scale be used for perennial ice and for annual ice in the temperature range $-8.2 \geq \theta \geq -22.9$C.

Soon after the publication of this paper, Langleben[85] reported on the ring tensile strength of ice fom Shippegan, New Brunswick, Canada. He considered only ice below the transition zone which in this case was located approximately 23 cm below the upper ice surface because of the formation of an appreciable thickness of infiltrated snow ice. No pronounced correlation between σ_f and either $\sqrt{\nu_b}$ or $\sqrt{\nu}$ was found. He did, however, note an increase in σ_f with increasing depth in the ice sheet z and suggested that this effect was the result of brine between the crystals being more efficient in reducing strength than brine within the crystals (the microstructure). This argument, however, seems improbable because of the extremely small volume "sampled" by the ring tensile test. Even in the small crystals just below the transition layer, the average grain size $\bar{d}$ is four times the size of the largest dimension of the ring tensile test volume. Therefore in most cases the ring tensile test would not "see" the grain boundaries.

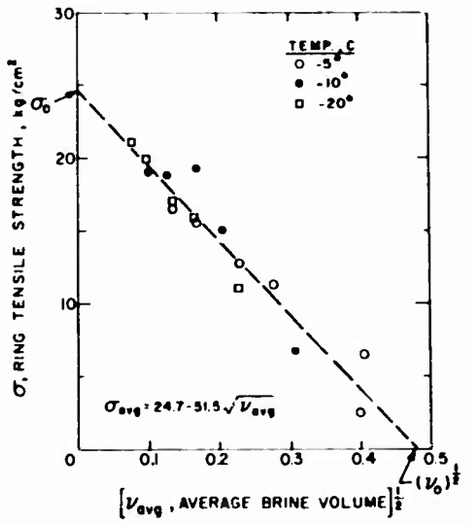

Figure 22. Average ring tensile strength vs square root of the average brine volume, NaCl ice (Weeks).[187]

In an attempt to resolve a number of the questions posed by Assur's paper,[17] Weeks[187] ran an extensive series of tests on ice formed by freezing NaCl solutions. He found a simple linear relation between σ_f and $\sqrt{\nu_b}$ (Fig. 22) at temperatures warmer than -21.2C with a σ_f axis intercept σ_0 = 24.7 kg/cm^2 and a ν_c value of 231‰. The value of σ_0 was slightly lower than the σ_f value determined by similar runs on fresh water ice (29.6 kg/cm^2 at -10C). This suggests that the ratio of stress concentration in salt ice to that in fresh water ice is in the range 1.1 to 1.5 and defeats the previous hypothesis of Anderson and Weeks[4] who assumed that the maximum strength of sea ice was one-third that of fresh ice based on the assumption of stress concentrators in sea ice. Tests on NaCl ice colder than the eutectic temperature indicate that the strength is essentially independent of both the sample temperature and the volume of $NaCl \cdot 2H_2O$ in the sample. When the strength of the ice matrix is corrected to -10C, the strength of the $NaCl \cdot 2H_2O$ ice is 26.5 kg/cm^2 or only slightly more than σ_0. There is, therefore, no indication of a pronounced strengthening effect associated with the precipitation of $NaCl \cdot 2H_2O$. Assur's data were also studied relative to the possible 1/3 increase in strength associated with the precipitation of $Na_2SO_4 \cdot 10H_2O$. This reanalysis suggests either (1) that the effect, if it exists, causes a strength increase of 20% or less, or more likely (2) that there is no strength increase associated with $Na_2SO_4 \cdot 10H_2O$. Peyton[123] has again recently discussed possible $Na_2SO_4 \cdot 10H_2O$ reinforcement on the basis of compression tests. These results will be discussed later.

Several experiments were made to check the suggestion of Butkovich[36] that the change between the σ_f values at Hopedale and Thule was produced by differences in the past thermal history of the sample. It was found that σ_f for samples tested at temperatures higher than the eutectic temperature can be considered as independent of the details of the thermal history immediately before testing (Fig. 23). This assumes, of course, that extensive brine drainage or redistribution has not occurred. On the other hand, the strength of ice tested at temperatures below the eutectic point is strongly dependent upon whether or not the specimen has been subjected to temperatures above the eutectic point. This loss of strength is presumably due to brine drainage or redistribution in the small near surface volume of ice where failure is initiated. It may also result from microcracks introduced by the phase changes. There was no evidence for any significant metastable lag between the time a sample reaches a given temperature and the time the "equilibrium" σ_f value is reached.

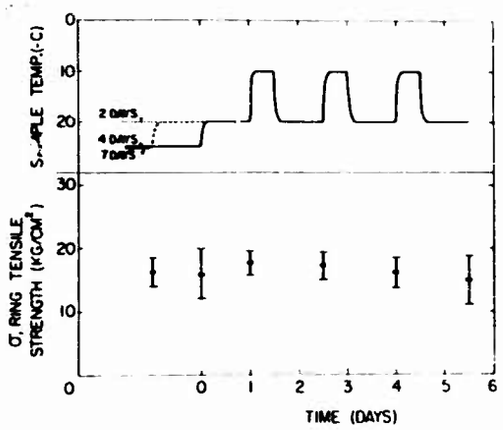

Figure 23. Study of the effect of thermal cycling on the ring tensile strength of NaCl ice; test temperature -20C, cycled to -10C (Weeks).[187]

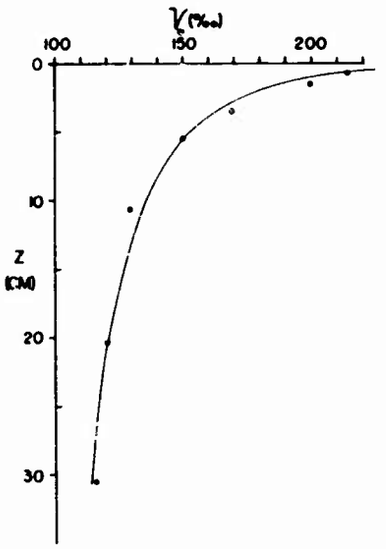

Figure 24. Variation in brine volume ν_0, produced in a constant width model ($d_0 = 7 \times 10^{-3}$ cm) as a result of the variation of $\bar{a}_0$ with z (Weeks and Assur).[189]

In a further analysis of this NaCl ice data, Weeks and Assur[189] pointed out that a systematic increase in the value of the plate spacing a_0 with increasing depth in the ice sheet z should result in a systematic decrease in the value of ν_0. Using the $a_0 = f(z)$ relation observed for this NaCl ice (Fig. 12) and assuming a constant width model with $d_0 = 7 \times 10^{-3}$ cm, the calculated change in ν_0 vs z is shown in Figure 24. They then examined the NaCl ice ring tensile results to see if such a change could be found. Figure 25 shows their results: a systematic decrease in ν_0 as determined from σ_f vs $\sqrt{\nu_b}$ plots as z increases. They then suggest that similar results should occur in natural sea ice. They explain the pronounced increase in σ_f with increasing z[85] as the result of the deterioration in the strength characteristics of the upper part of the ice sheet during the formation of infiltrated snow ice. Further theoretical considerations based on these results are discussed in Assur and Weeks[20] and were outlined earlier in this paper.

Graystone and Langleben[57] reported on results from annual ice in the Canadian Arctic. Their tests were performed immediately after the sample was removed from the ice sheet and the resulting equation was

$$\sigma_f = 29.0 \left[1 - \sqrt{\frac{\nu_b}{0.296}} \right] \qquad (4.3)$$

for samples whose ice temperature was higher than -8.2C. This was additional strong experimental evidence in favor of the previously assumed sea ice models and was also in good agreement with the results of Weeks[187] on NaCl ice. Note that the σ_0 value is almost identical with the ring tensile

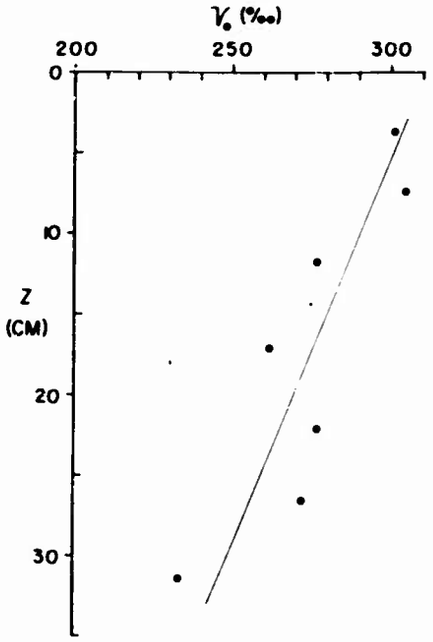

Figure 25. Decrease in the brine volume, ν_0 (‰), with increasing distance below the surface of the ice sheet, z. The ν_0 values were determined from plots of σ_f vs $\sqrt{\nu_b}$ (Weeks and Assur).[189]

strength of pure ice as determined by Weeks. The σ_f values for samples colder than -8.2C and therefore containing $Na_2 SO_4 \cdot 10H_2 O$ fall on this same curve. These authors obtained very poor results when samples stored at temperatures warmer than -20.5C were used. These erratic results are presumably produced by brine drainage. Although brine drainage corrections were made, no significant improvement in the quality of the data was noted.

Results similar to those of Graystone and Langleben were obtained by Dykins[44]

$$\sigma_f = 30.14\left[1 - \sqrt{\frac{\nu_b}{0.585}}\right] \qquad (4.4)$$

on ice cylinders in which no holes had been drilled. Dykins assumed that K = 6 (that brine pockets were acting as infinitesimally small holes) in making these calculations. But using the empirical K of 5.2 determined by Frankenstein[50] we obtain a σ_0 value of 27.2 kg/cm^2 for Dykins' data.

Langleben and Pounder[88] expanded their studies to two year old and polar (multi-year) ice at Isachsen, N.W.T. Because of low air temperatures (-10 to -15C) and low ice salinities (S_i<1‰), $\sqrt{\nu_b}$ was always less than 0.1 (ν_b <10‰). Graystone and Langleben,[57] on the other hand, had ν_b values up to 100‰. Comparing their results with the strength of annual ice with the same brine volume (eq 4.3), they found that biennial ice is 21% stronger than annual ice and 6% stronger than polar ice. These differences are difficult to explain. Assur[17] also found higher strength values for warm perennial ice. Hendrickson and Rowland's[62] data for perennial ice are also slightly higher. A slight but apparently non-significant difference was found between σ_f values from horizontal and vertical cores: σ_f (horizontal) > σ_f (vertical by 4%. It should be noted that the horizontal cores were not systematically placed in the "hard fail" orientation in the manner used by Butkovich[36] who found that horizontal cores gave consistently higher values than vertical cores from annual ice. They observed that the standard deviation of the σ_f values for horizontal cores (7.6 kg/cm^2) was appreciably greater than that of the vertical cores (4.7 kg/cm^2).

The most extensive study of ring tensile results currently available is that of Frankenstein[50] who reports the results of over 1400 individual tests (Fig. 26). Each point in this figure represents roughly nine tests. The least-squares equation for a straight line fit to the data when $\sqrt{\nu_b}$ < 0.400 is

$$\sigma_f = 28.51\left[1 - \sqrt{\frac{\nu_b}{0.234}}\right]. \qquad (4.5)$$

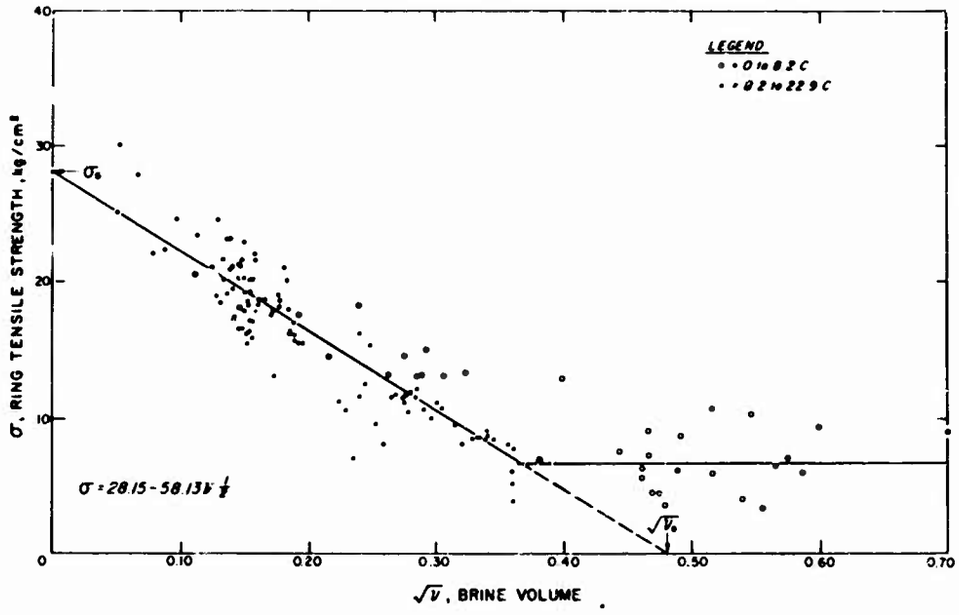

Figure 26. Ring tensile strength vs square root of the brine volume, sea ice (Frankenstein).[50]

Equation 4.5 is in good general agreement with the results of Weeks[187] and Langleben and Pounder.[88] When $\sqrt{\nu_b} > 0.400$, σ_f remains constant at approximately 6.7 kg/cm^2. It is, however, very doubtful that this is the proper relation at high brine volumes inasmuch as the equation 4.1 used to calculate these results assumes a high stress concentration near the hole. Plastic relief undoubtedly takes place at high brine volumes; therefore the true relation in this range will probably lie between the laboratory results of Weeks and the field results of Frankenstein. A possible way of incorporating the σ_f values at $\sqrt{\nu_b} > 0.400$ into a general theory was discussed earlier. Figure 26 does not show an appreciable strength difference in the $Na_2 SO_4 \cdot 10H_2 O$ range.

Although there is no obvious reason to expect Antarctic sea ice to be different, it is interesting to investigate this point. Figure 27[62] shows the arctic-ice curve of Frankenstein, an Antarctic-ice curve of Hendrickson and Rowland which includes results from one-and two-year ice and perennial ice, and a plot of the 1964-65 data from McMurdo Sound and Hallett Station. Although small differences in the slope remain to be explained, the curves are in reasonable agreement indicating a σ_0 value of roughly 29 kg/cm^2. Unfortunately there are not sufficient σ_f values with $\sqrt{\nu_b} > 0.400$ to prove that $\sigma_f \sim 6.7$ kg/cm^2 at high brine volumes. The data, however, give no reason to suspect that such is not the case. Other tests available from the Antarctic are those of Abele and Frankenstein.[1] Their results, however, cover only a very limited range of ν_b values making estimates of σ_0 and ν_0 uncertain.

Smirnov[153] has reported the results of a large number of "roller" tensile tests. This test is performed by compressing 10 x 10 x 20 cm rectangular blocks of sea ice between two cylindrical rollers, and appears to give slightly higher strengths than the ring tensile test. The results clearly show a pronounced variation with changes in the salinities of the samples. It appears

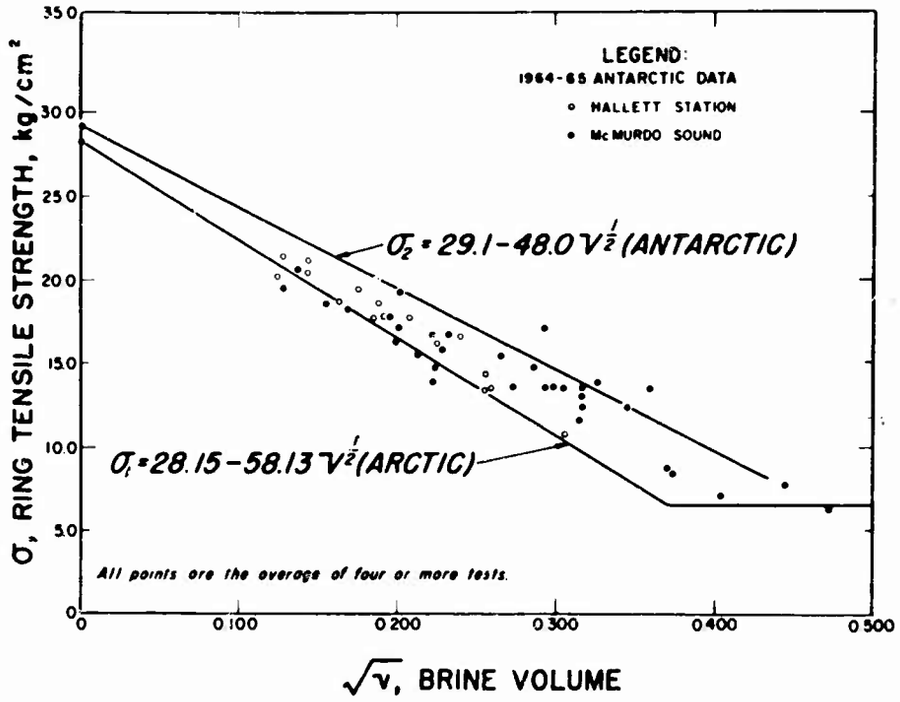

Figure 27. Ring tensile strength of Antarctic sea ice compared with Arctic sea ice, 1964-65 (Hendrickson and Rowland).[62]

quite probable that this test will give a σ_f vs $\sqrt{\nu_b}$ relation similar to that established for ring tensile tests.

Direct tensile tests

Until recently there have been no detailed investigations using the conventional tensile strength test. Fortunately, Dykins[45] has just published a series of direct tensile tests performed on laboratory-grown sea ice. The reduced cross section in his tests had an area of ~ 13 cm² and the extension rate was 1.2 cm/min. The ice showed plate spacing values that increased from 0.35 mm near the top of the ice sheet to 0.45 mm near the bottom. A very pronounced increase in grain size was noted over this same vertical distance, from 8 grains/cm² at the top to 0.3 grains/cm² near the bottom (an increase by a factor of 25 in 41 cm of ice). Because his strength profiles show no pronounced vertical variation, this can be considered as evidence that changes in grain size have no major influence on strength. There was a consistent variation with $\sqrt{\nu_b}$ however (Fig. 28), of the same general trend as shown by the ring tensile tests. Although the data are limited, there does not appear to be any significant change in the strength characteristics associated with the precipitation of solid salts. The orientation of the specimen relative to the direction of growth of the sea ice has a pronounced effect on tensile strength. As should be expected in this test, vertical specimens which are forced to break across the ice plates show strengths similar to horizontal specimens in the "hard fail" orientation but higher strengths (2 to 3 times) than horizontal specimens in the "easy fail" orientation. As a result of these differences, horizontal specimens show an appreciably greater scatter than vertical specimens. Dykins suggests that the results of these direct tension

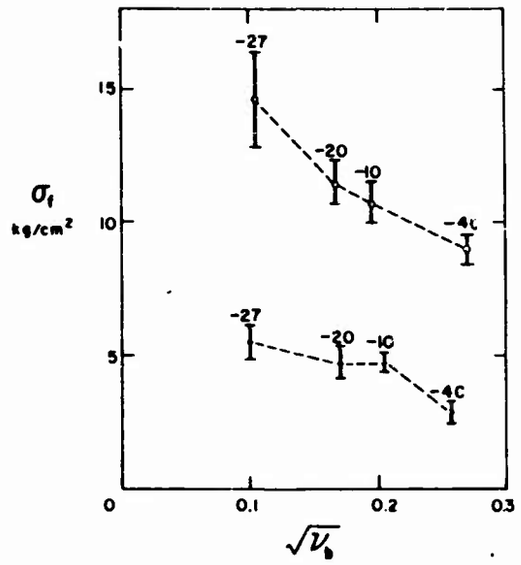

Figure 28. Tensile strength of sea ice vs square root of the brine volume. In the stronger samples, tension is exerted parallel to the growth direction and in the weaker samples, perpendicular. The brackets indicate the 95% confidence limits on the mean (Dykins).[45]

tests can be compared directly with flexural strength results for sea ice. If further tests substantiate this suggestion, this type of testing procedure should prove to be very useful.

The only other direct tension results are those of Peyton.[122,123] Unfortunately these results are currently presented in a form which makes them difficult to use or compare with other published results.

Flexural Strength

Small-beam tests

The small-beam flexural strength test was among the tests first applied to sea ice studies.[80,95] Recently, however, the test appears to have lost "favor" relative to the ring tensile test. The reasons for this are twofold. Ring tensile samples are easier to prepare and also give better correlations with such parameters as brine volume and microstructure than do small sample flexural tests.

Prominent among the earlier studies were the results of Arnol'd-Aliab'ev[11,16] who on the basis of least-squares gave

$$\sigma_f = 4.7 - 0.96\,\theta - 0.31\,\theta^2 \qquad (4.6)$$

where σ_f is in kg/cm^2, as the temperature dependence ($-0.4 \geq \theta \geq -18.5$C) for small beam flexural results. He then interpreted the deviations from this curve in terms of the salinity of the ice S_i (‰) which in turn he empirically related to air porosity V_a (cm^3/kg)

$$V_a = 96. - S_i. \qquad (4.7)$$

Combining his equations we obtain

$$\sigma_f = +18.76 - 0.96\,\theta - 0.31\,\theta^2 - 0.15\,V_a \qquad (4.8)$$

which indicates that σ_f increases as θ and V_a decrease. It is interesting to note that although Arnol'd-Aliab'ev pioneered techniques for the determination of the air content of sea ice, he correctly realized that a considerable percentage of the air porosity is the result of brine drainage prior to testing.

The first set of recent small beam results accompanied by sufficient supplementary information for an analysis was published by Butkovich[34,36] who performed tests on both horizontally-, and vertically-, cut center-loaded simple beams. In the horizontal beams, the direction of loading was normal

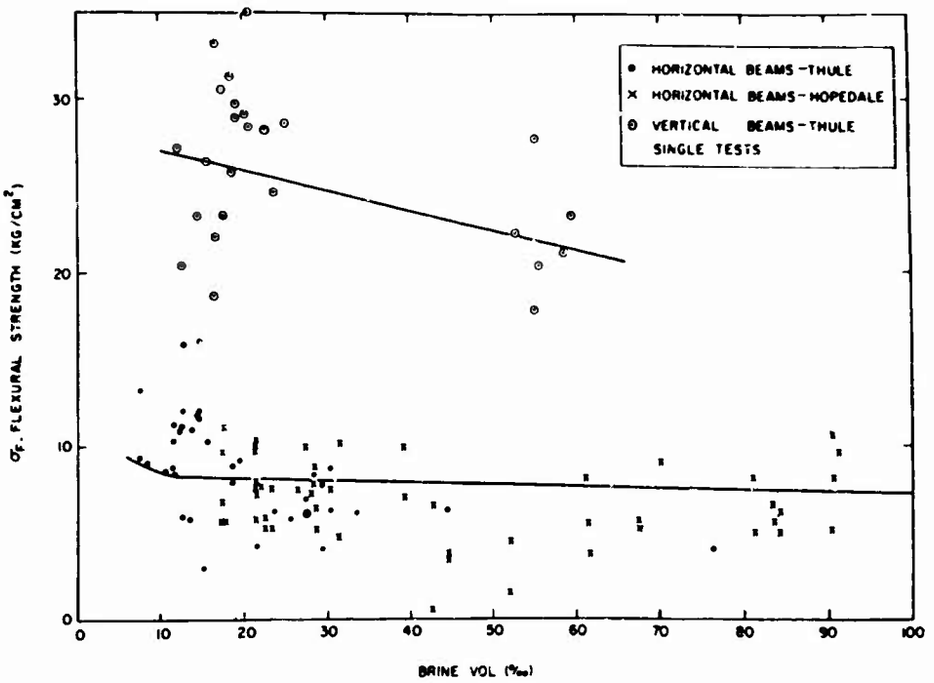

Figure 29. Small beam flexural strength of sea ice vs brine volume (Butkovich).[36]

to the ice sheet while in the vertical beams the long axes of the crystals were parallel to the length of the beam. The test results are shown in Figure 29. There is a large scatter and vertical beams give significantly higher values than horizontal beams. No appreciable difference is indicated between the Hopedale and Thule results. This is interesting inasmuch as a definite difference was indicated by ring tensile tests. Note also that the small beam values are consistently lower than ring tensile results from the same ice (8 kg/cm^2 as compared with 18 kg/cm^2). The pronounced dependence of σ_f on ν_b as shown in ring tensile tests is also absent. Quantitatively similar results have been obtained by Petrov[121] and Smirnov,[153] Tabata,[162] and by Abele and Frankenstein[1] for ice from the Arctic Ocean, the Okhotsk Sea, and from McMurdo Sound in the Antarctic respectively. Qualitatively similar results were also reported by Pounder and Little[125] although no salinity determinations were made on their samples. Russian observers[146, 147, 24] have also made similar measurements in the vicinity of Mirny Station in the Antarctic. Unfortunately the only supplementary data they provide are air temperatures[146,147] and salinities and densities.[24] They do show, however, that during the testing periods the maximum ice strength occurred near the center of the ice sheet.

Butkovich[36] has attempted to explain the observation that ring tensile tests give larger values than small beam and in-situ flexural tests on the following basis. If it is assumed[73] that sea ice contains a distribution of flaws and that each of these flaws can withstand stresses up to a certain size, then it follows that the probability of the "weakest" imperfection occurring in this volume is proportional to the volume size. Therefore tests that force failure on a small volume (ring tensile) should presumably yield

higher strength values. As Goetze[53] has pointed out, this volume effect is very pronounced in coal and glass where the flaw distribution shows a wide scatter. On the other hand, in polycrystalline materials, where the flaws are related to the microstructure, the variation in well-annealed samples is much less. A reanalysis by Goetze of Jellinek's[73] results concerning the effect of the sample volume on the strength of fresh water ice shows that the strength appears to be independent of volume as long as the minimum sample dimension is larger than roughly 2 mm. This implies that in samples with dimensions smaller than 2 mm there is some "interference" with the microstructure that is initiating the failure. It should be recalled that earlier arguments (eq 3.48) suggested that in sea ice the size of this microstructure is in the range 0.1 to 1.0 mm.

Goetze further argues that the difference between the small beam flexural and the ring tensile values is caused by different aspects of the microstructure controlling the fracture mechanism. In small beams the fracture may be related to the dimensions of the crystals as compared to the dimensions of the brine pockets in ring tensile tests. Some justification for this suggestion may be obtained by calculating the constant in eq 3.48 from Butkovich's[37] results on the flexural strength of well-annealed, uniform, isotropic glacier-ice from the Tuto Tunnel. When Goetze does this he obtains an average value for $(\sigma_f \cdot d)$ of 111. Now extending this argument to the typically larger grain diameters encountered in sea ice (1 to 2 cm) he obtains σ_f values of 10.5 and 7.5 kg/cm^2 respectively. These values are in the range of σ_f values as determined by small beam flexural tests. It should be quite simple to verify this suggestion of a grain size related fracture mechanism. All that is required is a series of small beam tests on ices with a constant brine volume and a range of grain sizes. It should be pointed out that Dykins'[45] direct tension results do not appear to support the grain size argument. If the fracture mechanism was related to grain size in Dykins' tests, a pronounced vertical variation should have been observed in the failure strength. This was not the case. Because of the large cross sectional area of his tensile samples ($\sim$13 cm^2), the test volume does not appear to be of a size that would interfere with a grain size related fracture mechanism. Another reason for the reduced strength of larger samples is the presence of large holes and defects such as brine drainage channels[25] and macro-cracks. The probability that such defects would occur in a small sample is quite low.

On the other hand, ring tensile tests may be subjected to an unknown plastic reduction in stress concentration as suspected by Sala.[137] Evidence for this suggestion can be found in the tests of Smirnov[153] who compared a large number of "roller" tensile values with flexural results determined on similar ice. His results are shown in Figure 30. Theoretically the flexural strength should be equal to the tensile; in practice this is rarely observed. Nevertheless it might be expected that the ratio of the two strengths would be constant. Figure 30 shows that this is not the case. For low salinities sea ice is brittle and the tensile and flexural strength is roughly equal. For high salinities sea ice is plastic and the tensile strength is considerably higher than the flexural strength. We suggest that this is caused by the plastic relief of stress concentrations near everpresent small holes in the "roller" tensile samples. Smirnov's data therefore indicate that plastic relief of stress concentrations may be an important factor in certain types of tests.

The small beam flexural test has also been extensively utilized by Tabata[162, 168] to study the relation between failure strength and rate of applied stress. These results will be discussed later. A reliable approach to evaluate the strength of sea ice sheets from small sample tests is not available as yet.

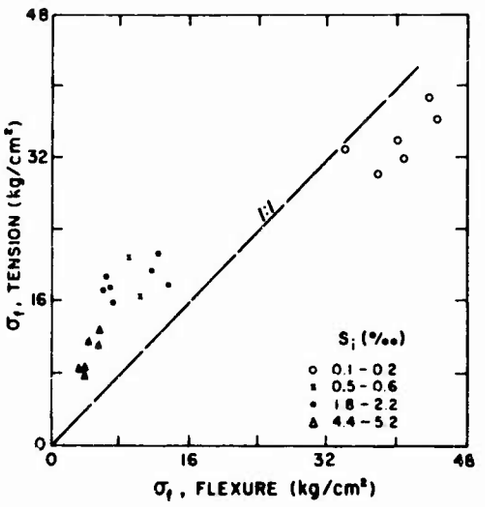

Figure 30. Average values of "roller" tensile strength vs small beam flexural strength as determined on similar sea ice samples under similar conditions (Smirnov).[153]

In-situ cantilevers

The in-situ cantilever or key test was first described by Neronov[106] in conjunction with a series of tests on lake ice. Although cantilever results have commonly been used in estimating σ_f values in bearing capacity problems via relations such as eq 1.12, there is surprisingly little documentation of the results of such tests in the literature. The reasons for this paucity of data are obvious to anyone who has ever performed or tried to analyze the results of cantilever tests. The test is quite time-consuming if the ice is thicker than ~50 cm. Therefore at the end of a testing program one invariably finishes with an insufficient amount of data to "make" a satisfactory technical report. In addition the analysis of cantilever tests is, as is the analysis of any test that considers the ice sheet as a whole, far from unambiguous.

The only extensive study utilizing the results of cantilever tests is that of Weeks and Anderson[185] who performed 208 tests on thin (less than 40-cm) sea ice. They demonstrated the dependence of the flexural strength on the average ice salinity and temperature but did not plot their results against brine volume. This is done in Figure 31. Figure 31 also contains the results of Butkovich[34] and those of Brown[32] (his Figure 11) that have not been subjected to high temperature cycling. The equation obtained from Figure 31 is

$$\sigma_f = 7.5\left[1 - \sqrt{\frac{\nu_b}{0.202}}\right] \qquad (4.9)$$

for $\sqrt{\nu_b} < 0.33$. When $\sqrt{\nu_b} > 0.33$, σ_f is constant with a value of roughly 2.0 kg/cm². Although additional data are badly needed, these results are quite encouraging in that the strength variation appears similar to that found by ring tensile tests although strength values are much lower. Note also that the ν_0 values are quite similar: 202 ‰ as compared with 234 ‰.

In these tests little difference was noted between "pull-ups" and "push-downs." This is in contrast to results on lake ice where the "pull-up" strength is significantly higher than the "push-down" strength.[48, 49] This difference is presumably the result of the presence of extensive thermal surface cracks on lake ice.[55]

It is interesting to note the pronounced effect that a warm temperature cycle had on Brown's[32] cantilever results. This is in striking contrast to the experimental results of Weeks[187] where no change was noted in ring-tensile specimens cycled and tested above the $NaCl \cdot 2H_2O$ precipitation temperature.

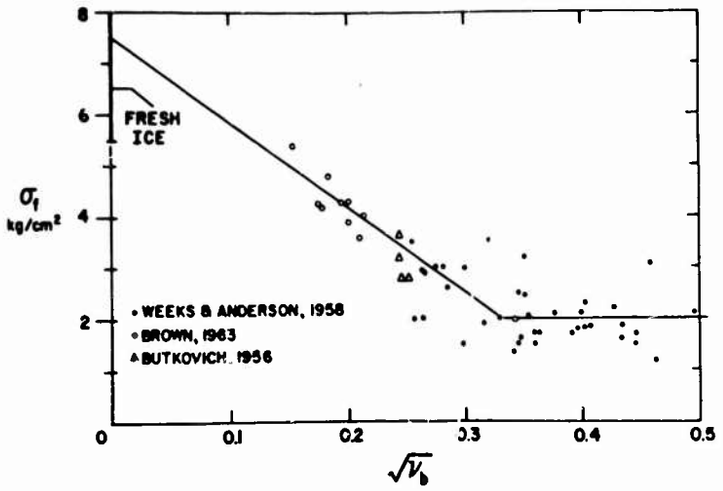

Figure 31. Flexural strength measured by in-situ cantilever beam tests vs square root of the brine volume.

There has been considerable discussion regarding possible stress concentration at the sharp corner at the butt of the beam during cantilever tests. Comparisons of in-situ cantilevers with in-situ simple beams (Frankenstein, personal communication) suggest that stress concentration is of the magnitude of 10% or less. Similar conclusions have been proposed on the basis of limited data by Sala.[137]

Shear Strength

The information available on the shear strength of sea ice is extremely limited. In addition many of the values described as shear strengths are actually the result of mixed mode failures.[34,146] The test results of Butkovich[34] from Hopedale, Labrador, were obtained by encasing the core in three close fitting metal cylinders and shearing out the central third of the core. These results, when plotted against $\sqrt{\nu_b}$, show a large scatter and indicate an average shear strength of $\sim$21 kg/cm^2 for $\sqrt{\nu_b} = 0.19$. There is no obvious correlation between σ_f and $\sqrt{\nu_b}$. The data do suggest a slight increase in σ_f with decreasing test temperature. These shear strengths are considerably higher than the tensile strengths reported by Butkovich on vertical cores. The reason for this is presumably that the shear failures are forced to occur across the columnar grains and therefore must break across the ice platelets.

Serikov[146] has reported the results of 11 shear or punch tests in which failure mode is questionable. His average shear stress is 8.6 kg/cm^2 with a maximum (11.2 kg/cm^2) near the center of the ice sheet. The only supplementary information provided is that the air temperature varied between -0.9 and -4.1C during the tests. Petrov[121] has also reported the results of a large number of shear tests on arctic pack ice. Unfortunately his results have not, at present, been analyzed in terms of either ν_b or ν_a.

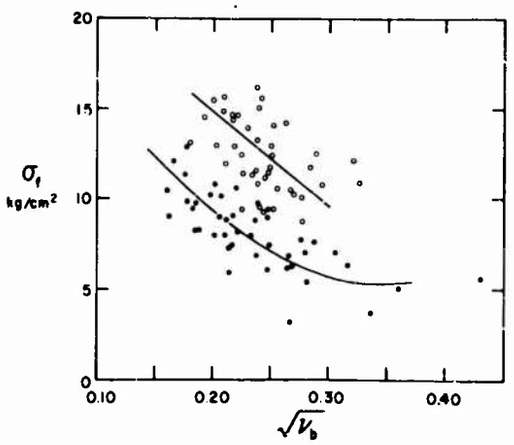

Figure 32. Shear strength (solid circles) and ring-tensile strength (open circles) vs square root of the brine volume (Paige and Lee).[114]

The best set of shear tests available is by Paige and Lee[114] from McMurdo Sound. Their results (Fig. 32), determined on 7.6 cm diam cores, were obtained by using specially designed shearing heads which moved at 20 cm/min during the application of the failure load. Note that their shear strengths are consistently lower than their ring tensile values and that the shear strength decreases as $\sqrt{\nu_b}$ increases in the same general manner as in the ring tensile and in-situ cantilever results.

Compressive Strength

As has been noted by several authors, the values obtained by crushing tests depend to a considerable extent on the conditions of deformation: i.e. the dimensions of the sample and the stress rate $\dot{\sigma}$.[35,181] These variations are, of course, superimposed on the variations caused by differences in the structure and orientation, the specimen temperature, and other factors. Unfortunately there have been consistent differences between the sample geometry used by American and Canadian as compared with Russian investigators. In general the North Americans have used 3 in. (7.6 cm) diam ice cylinders with a 3 to 1 ratio of length to width. In fresh water ice as the length to width ratio decreases, the strength increases due to different failure modes. Limited data bearing on this problem can be found in Butkovich.[35] Kudriavtsev[82] recommends using 10-cm cubes while Serikov[146] has used 4.3-cm cubes.

Butkovich[34, 36] found that the compressive strength of vertical cores of sea ice is considerably greater than that of horizontal cores. This difference is quite reasonable in view of the structure of sea ice. In vertical cores failure is forced to occur across the ice platelets, while in horizontal cores fracture can more readily take advantage of the planes of weakness in the ice crystals. Similar differences were noted by Bruns and Deriugin[198] who also found that the ratio of the vertical to the horizontal compressive strengths decreased and approached unity for deteriorated summer ice. For vertical specimens, Butkovich found median strength values ranging from 78 kg/cm² at -5C to roughly 120 kg/cm² at -16C. Average values on horizontal cores in the same temperature range vary from 21 to 43 kg/cm². Serikov[146] obtained values between 10 and 60 kg/cm² at -5C for 4.3-cm cubes collected at Mirny.

The most complete set of compressive strength observations available is reported by Peyton[123] who ran tests on a large number of samples of different sea-ice petrographic types at various orientations and stress rates. He found a marked dependence of compressive strength on sample orientation as shown in Figure 33. In this figure the upper curve represents compression results while the lower curve represents direct tension tests. The ice used in these tests was bottom ice with a grain size larger than the dimensions of the specimens. Therefore each sample can be considered a "single" crystal.

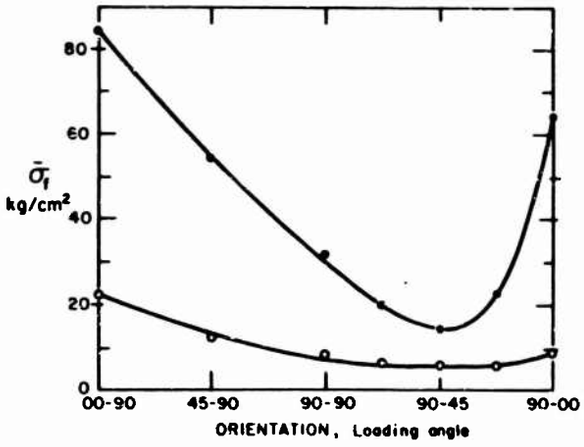

Figure 33. Average failure strength in compression (solid circles) and in direct tension (open circles) vs sample orientation: bottom ice, -10C (Peyton).[123] For orientation notation, see text.

In this ice type c-axis orientations in the ice sheet are always close to horizontal. The loading angle notation is as follows: the first number gives the angle between the axis of the test sample and the vertical, while the second number gives the angle between the sample and the c-axis of the ice crystal. Note that the ratio of the strength obtained from vertical cores to that obtained from horizontal cores is about 3:1, in agreement with the results of Butkovich.[36]

Peyton noted a relation between the compressive strength and the stress rate $\dot{\sigma}$, the brine volume of the ice sample, and the position of the specimen in the ice sheet. These results were obtained by multiple regression techniques, but unfortunately Peyton does not give all the regression constants. Therefore the results are at the present* only of use in a qualitative manner.

Inasmuch as the failure strength σ_f is a function of $\dot{\sigma}$, Peyton has attempted to "remove" this variation as follows. If the regression equation is of the general form

$$\sigma_f = a\,\dot{\sigma}^{b} X_1^{y_1} X_2^{y_2} \cdots X_n^{y_n} \tag{4.10}$$

a new parameter σ_R can be defined as

$$\sigma_R = \frac{\sigma_f}{\dot{\sigma}^{b}} = a X_1^{y_1} X_2^{y_2} \cdots X_n^{y_n}. \tag{4.11}$$

This parameter is, of course, related to the original σ_f value but unfortunately it is currently impossible with the information provided by Peyton to

*A greatly expanded version of Peyton's report[123] is currently (1967) being published by the Arctic Environmental Engineering Laboratory, University of Alaska.

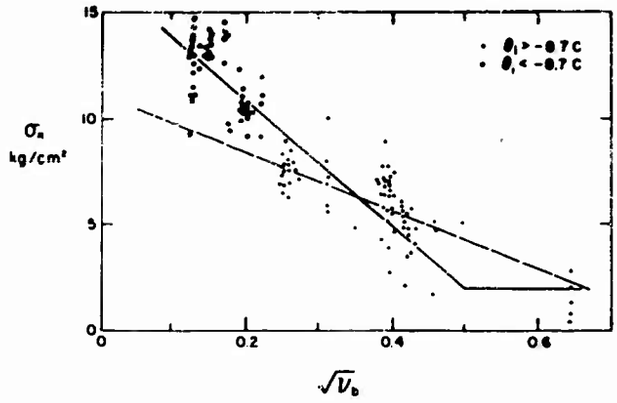

Figure 34. σ_R from compression tests vs square root of the brine volume (Peyton).[123] For the difference between the solid and dashed lines see discussion in text.

interpret σ_R values in terms of actual measured compressive strengths. It would have been more useful to simply correct all strength values to a common value of $\dot{\sigma}$. We can, however, consider σ_R as a strength index. If σ_R is plotted against $\sqrt{\nu_b}$ (Fig. 34) and a least squares straight line is fitted through those data points where the ice was at a higher temperature than -8.7C, the dashed line results. Peyton interprets the fact that ice strengths determined at temperatures below -8.7C lie above this line to indicate that $Na_2 SO_4 \cdot 10 H_2 O$ precipitation is effective in strengthening the ice. This may well be the case. There is, however, another possible interpretation of Figure 34. Remembering that in other types of tests (Fig. 26, 31, 32) σ_f decreases as a linear function of $\sqrt{\nu_b}$ at low brine volumes, and becomes approximately constant at high brine volumes, we may, as a hypothesis, assume that the five data points at $\sqrt{\nu_b} > 0.6$ are associated with this latter type of behavior. If this is the case the data may be approximated by the solid line shown in Figure 34 and it may not prove necessary to invoke $Na_2 SO_4 \cdot 10 H_2 O$ reinforcement. Examination of Peyton's results as a whole suggests that they would be well fitted by a simple curvilinear relation of the general form of eq 3.40. Regardless of the salt reinforcement question, Figure 34 is quite important in that it shows that compressive strengths can also be analyzed using equations 3.35 and 3.40.

Elastic Modulus

Of all the mechanical properties of ice, the elastic or Young's modulus, E, appears to have been the most extensively studied. Experimental results for pure ice were available as early as the 1820's and are summarized in tabular form by Weinberg et al.[193] and Voitkovskii.[181] There is a very considerable scatter in the E values: 3×10^9 to 1×10^{11} dynes/cm^2 for static measurements and 6×10^{10} to 1×10^{11} dynes/cm^2 for dynamic measurements. Dynamic measurements are invariably larger than the static, show a smaller scatter, and are more readily reproducible. The reason for these differences can be explained as follows:[181] in static tests which measure strain after the application of a load, the deformation can be measured only after a finite time interval. Because of the viscoelastic behavior of ice, this interval

is invariably sufficient to permit viscous as well as the desired elastic deformation. Therefore, a static E determination which is specified by the measurement of total deformation does not characterize the resistance of ice to an instantaneous elastic deformation, but also a viscous time dependent deformation after a specific time interval. The greater the stress, the more important the viscous and creep components become: the elastic component is directly proportional to the stress while the creep rate is proportional to the stress to some power (~2 to 4 at high stress levels). Therefore, the value of E calculated on the basis of strain measurements decreases as stress increases. That this holds for fresh ice has been shown by the results of Pinegin[181] on river ice. It is to be expected that these arguments are even more applicable to sea ice.

The value of E determined by dynamic methods is, on the other hand, based on the determination of either the rate of propagation of vibrations in the ice or the natural (resonant) frequencies of different types of vibrations. Here the displacements are extremely small and, for many purposes, anelastic effects can be neglected. The results of dynamic measurements of E are, therefore, reasonably reproducible and are usually preferred over static measurements of E. A review of the different methods of determining E for sea ice is given by Anderson.[3]

Dynamic measurements

In-situ seismic. Two main approaches have been used to obtain dynamic determinations of E for natural sea ice. The first utilizes seismic field techniques to measure the velocity of propagation of P, S, surface and flexural waves in the ice sheet. If the P and S wave velocities and the density are known, all the other elastic constants can be calculated provided that the ice sheet is assumed to be homogeneous and isotropic. These simplifying assumptions are reasonably adequate for lake ice, but are far from correct for sea ice. A general theory for treating elastic wave propagation in a medium consisting of n layers of a transversely isotropic material, which well approximates the real properties of sea ice, has been developed by Anderson.[6,7,8] Unfortunately, published results of the detailed application of these theoretical developments to seismic measurements on sea ice are still not available. Another difficulty in analyzing seismic results lies in relating the results to the "state" of the sea ice. For flexural waves, which are controlled by the "average" properties of the ice sheet, the salinity and temperature profiles can be used to calculate an average brine volume or, preferably, an effective flexural rigidity. Average ice sheet properties may also be used with some confidence during the summer months when the ice sheet is fairly close to being both isothermal and isosaline. However, during the sea ice growth season it is necessary to use the average properties of the cold, higher velocity upper portion of the ice sheet to analyze the velocity variations of P and S waves. These waves do not travel directly along the ice surface but penetrate to a depth which depends on the physical properties of the upper portion of the ice sheet. Unfortunately, the exact "dimensions" of this high velocity channel are somewhat arbitrary.[3,31,32] This introduces an additional degree of uncertainty into the analysis of field results.

A representative sampling of the results of seismic field determinations of the elastic modulus of sea ice is given in Table I. An examination of this table indicates that E varies from 1.7 to 5.7 x 10^{10} dynes/cm^2 when measured from flexural waves (E_f) and 1.7 to 9.1 x 10^{10} dynes/cm^2 when determined

Table I. Representative seismic field determinations of the elastic parameters of sea ice: E_b and E_f, elastic moduli from body wave and air coupled wave measurements, G, shear modulus, μ, Poisson's ratio, and h, ice thickness.

Ice type and location	Season	h (cm)	E_b (10^{10} dy/cm^2)	E_f (10^{10} dy/cm^2)	G (10^{10} dy/cm^2)	μ	Source and reference no.
Fast ice, North c Baltic Sea?	--	80	7.2	--	--	--	78
Fast ice, Barter Island, Alaska	Spring	~180	5.5	--	2.1	.32	112
Fast ice, Hopedale, Labrador	Winter	--	9.1	--	--	--	Pomeroy[1]
Fast ice, Hopedale, Labrador	Spring	--	3.3-4.8	--	--	--	Pomeroy[1]
Pack ice, Arctic Ocean	--	--	5.9	--	--	.29	117
Pack ice, Bering Sea	Spring	~ 90	5.6	--	--	--	51
Pack ice, 1 year, Arctic Ocean, NP-4	Spring	190	6.0	--	2.2	--	80
Pack ice, perennial, Arctic Ocean, NP-4	Spring	~400	6.8	--	2.5	--	80
Fast ice, Thule, Greenland	Fall	15	5.5	--	--	--	5
Fast ice, Thule, Greenland	Fall	52	--	2.5	--	--	5
Fast ice, Thule, Greenland	Winter	112	--	5.7	--	--	5
Fast ice, Thule, Greenland	Winter	122	7.3	--	--	--	5
Fast ice, Thule, Greenland	Spring	127	--	1.7	--	--	5
Fast ice, Thule, Greenland	Spring	152	3.1	--	--	--	5
Fast ice, Cape Schmiot, USSR	Spring	130-210	3.7	--	1.9	.37	94
Fast ice, Hokkaido, Japan	Winter	14-26	2.9	--	1.1	.38	68
Pack ice, Arctic Ocean, Station Alpha	Fall	~313	5.4	--	2.0	.36	66
Pack ice, Arctic Ocean, Station Alpha	Winter	~310	7.8	--	3.0	.29	66
Pack ice, Arctic Ocean, Station Alpha	Summer	~310	7.2	--	2.6	.38	66
Fast ice, Wales, Alaska	Winter	--	4.6	--	1.7	.31	52
Fast ice, Wales, Alaska	Spring	--	3.3	--	1.3	.25	52
Fast ice, Thule, Greenland	Winter	135	7.7	--	2.8	.38	52
Fast ice, Hokkaido, Japan	Winter	21	1.7	--	.6	.37	69
Fast ice, 2 year, Isachsen, N.W.T.	Spring	170	7.2	--	2.9	.25	129

from in-situ body wave velocities (E_b). E_b is invariably larger than E_f when determined on similar ice. This is reasonable inasmuch as E_f is representative of the whole thickness of the ice sheet while the value of E_b is controlled by the properties of the high velocity channel in the usually colder and stronger upper portion of the ice sheet. The values of E show a systematic variation throughout the year from low values for young, warm, high-salinity new ice to high values for cold winter-ice. A decrease occurs again in the spring when the ice temperature rises. This decrease is clearly shown by Listov's results[118] on ice from the Laptev Sea. As the temperature of this ice increased in the spring, the ice thickness decreased from 2 m to 1.4 m and the values of E showed a pronounced decrease (Fig. 35). One of the major contributing factors to this variation in E is the annual variation in V_p, the velocity of the longitudinal-plate wave. The value of V_p has been determined on thick (~3 m) pack ice throughout a complete year by Hunkins[66] and has been found to vary from a low of 2300 m/s in the summer to a high of 3200 m/s in the winter (Fig. 36). Similar but less detailed results on V_p values and flexural wave dispersion curves have been obtained on annual sea ice.[3]

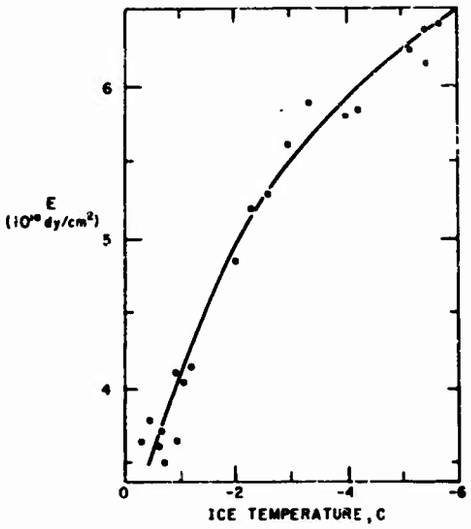

Figure 35. Decrease in elastic modulus E with increasing ice temperature as determined by in-situ seismic measurements; Laptev Sea, spring (data of Listov).[118]

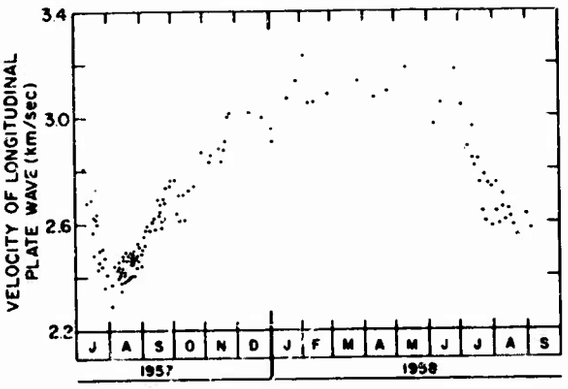

Figure 36. Seasonal variation of longitudinal plate velocity (Hunkins).[66]

These changes in V_p and in E are clearly related to changes in the temperature of the ice.[29,30,66] Figure 37 shows a plot of E vs temperature (mean ice temperature) for annual fast ice with a thickness of 1.3 to 2.1 m from Cape Schmidt, Siberia.[94] The marked increase in E with decreasing temperature is presumably related to the brine volume, but because detailed salinity profiles are not given, the brine volume is difficult to estimate. Fortunately the relation between seismic determinations of E and the brine volume ν_b in the ice at the time of the determination have been studied by Anderson[3] at Thule, Greenland, (Fig. 38) and by Brown and Howick[31] on the Bering Sea. Anderson assumed that the high velocity "channel" extended to the depth where a rapid increase in ν_b was noted in the ν_b profile. Brown[32] (his Fig. 9) has made a similar analysis of field data collected at Wales, Alaska, and Thule, Greenland. In specifying the properties of the high velocity "layer," the brine content of the coldest 20-cm layer was used. Considering these difficulties the results of both Anderson and Brown are in remarkably good agreement indicating a "pure" ice intercept of roughly 9 to 10 x 10^{10} dynes/cm^2 for $\nu_b = 0$ and a rapid decrease in E as ν_b increases. An interesting attempt to develop a theory relating sea ice strength to its elasticity via a perforated plate model has been made by Brown.[32]

Small specimen. The main alternate approach to the determination of the elastic modulus of sea ice utilizes small samples which presumably are reasonably isothermal and isosaline. By using either cold rooms or "heated" rooms at a field site, a much wider range of temperatures and, therefore, brine volumes can be studied than is possible when the ice sheet is treated as a whole. Considerable care must, however, be taken to prevent brine drainage. The natural resonance frequencies or the velocities of propagation of sonic waves through the specimens are determined and the elastic constants are calculated from the results. For the purposes of this particular review, the small-specimen results are more interesting than the field seismic results and will be discussed in more detail.

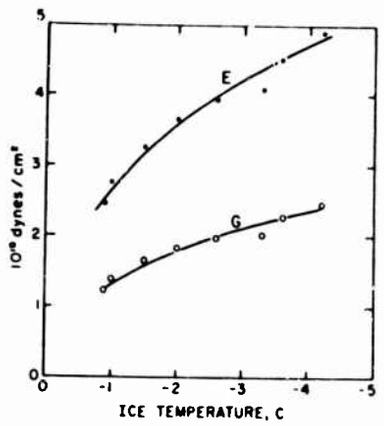

Figure 37. Elastic modulus E and shear modulus G as determined by in-situ seismic measurements vs mean ice temperature, annual fast ice, spring, Cape Schmidt, Siberia (Lin'kov).[94]

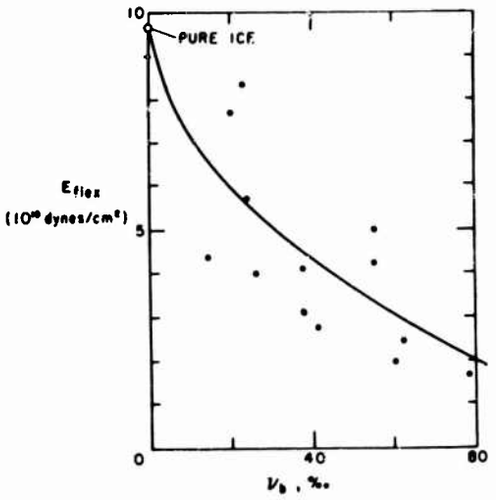

Figure 38. Elastic modulus E, as determined by seismic measurements, vs brine volume ν_b (Anderson).[3]

The first small-specimen results were reported by Tabata,[158, 161, 162] who obtained the natural resonance frequency of sea-ice bars with dimensions of roughly 2 x 3.5 x 35 cm. Even though the initial ice blocks were obtained from young high salinity sea ice, the long storage periods before actual testing permitted extensive brine drainage causing sample salinities to be in the range 0.2 to 3.2 ‰. Therefore, attempts to correlate variations in E with changes in ν_b were unsuccessful. Inasmuch as most of the initial brine had been replaced by air, a plot of E vs $\nu = \nu_b + \nu_a$ was also prepared (Fig. 39) where ν_a was measured directly. This figure suggests a strong linear dependence of E on ν of the general form

$$\frac{E}{E_0} = 1 - \frac{\nu}{\nu_0} \tag{4.12}$$

where E_0 is the sonic modulus of fresh ice[197] and ν_0 is the ν axis intercept ($\nu_0 \sim 180 - 220$ ‰). Infiltrated snow ice appears to have slightly higher values of E for a given value of ν than does normal sea ice. This is to be expected inasmuch as the ordered brine arrays in normal sea ice crystals should cause E to decrease more rapidly with increases in ν_b than would occur with a random array of brine pockets.

When the variation in E with specimen temperature was studied, Tabata found a slight increase with decreasing temperature at temperatures lower than -10C. There was also a pronounced decrease in E at temperatures higher than -10C. Because this decrease has not been observed in fresh ice,[197] it undoubtedly is the result of the rapid increase in the volume of brine in the ice at temperatures near the melting point. There are slight changes in slope in some of the E vs temperature plots at temperatures of roughly -8 and -23C.[161] It is interesting that while these changes are noticeable in most of the infiltrated snow ice samples, they can only be noted in one of the eight

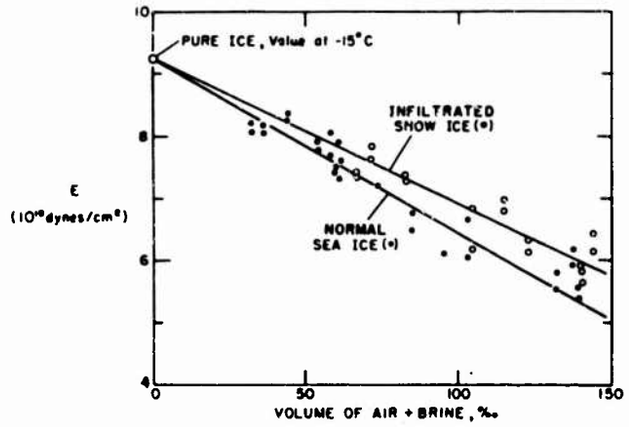

Figure 39. Elastic modulus, E, vs volume of air plus brine, v; young sea ice (Tabata).[159]

sea ice curves. These slope changes are probably the result of both rapid changes in the brine volume and the presence of solid salts. There has not been, at present, any attempt to separate these two effects.

The first published results of small specimen determinations of E on sea ice that had not undergone significant brine drainage were by Pounder and Stalinsky.[127] They measured transit times for pulses of supersonic frequence through sections of sea ice cores from Barrow Strait, west of Cornwallis Island, N. W. T. Although they observed an appreciable scatter in the data, there clearly appeared to be a linear relation between E and ice salinity at a constant temperature. This implies a linear relation between E and v_b.

These studies were continued by Langleben[86] and Langleben and Pounder[87] on sea ice from several locations in the Canadian Arctic and Greenland. Their results (averages from over 300 measurements) for cold arctic sea ice are shown in Figure 40 and indicate a linear relation between E and v_b. The scatter is small. The results of tests on warm polar ice also appear to be linear on a E vs v_b plot but with a lower intercept ($E_0 \sim 8.8 \times 10^{10}$ dy/cm^2) and a smaller slope. However, as pointed out by Langleben and Pounder,[87] not as much confidence should be placed on these values because of brine drainage and rapid changes in the phase diagram for warm sea ice.

Further measurements[129] on 2 year old and multiyear pack ice ($S_i \sim 1$ ‰) at Isachsen, N. W. T., have shown that both give E values roughly 4 to 5% lower than values determined under similar conditons from winter ice with an identical brine volume. An examination of the data also gives the distinct impression that the dependence of E on v_b has decreased. However, as Pounder and Langleben have pointed out this impression may be caused by the limited range of v_b values that were available during this test series. There were no differences noted between the values obtained on the 2 year and on the multiyear ice. This suggests that the decrease in E is in some way associated with effects that occur during the first summer and is apparently not intensified by cycling through further melt periods. It is also interesting to note[88] that an appreciable difference was found between the

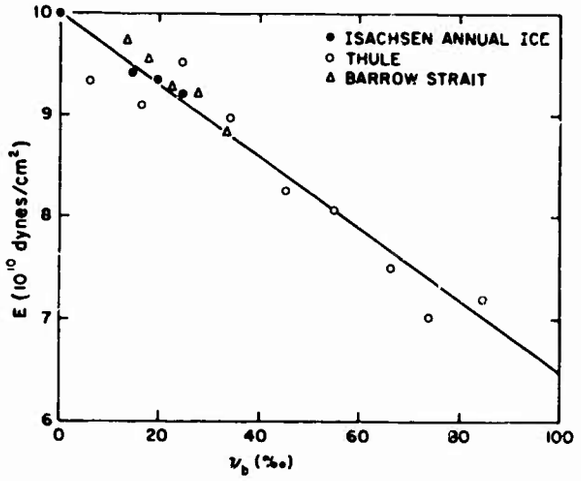

Figure 40. Elastic modulus of cold, arctic sea ice vs brine volume: small specimen tests (Langleben and Pounder).[87]

ring-tensile strengths of these two ice "types." A similar linear relation between E and ν_b has been obtained by Abele and Frankenstein[1] on annual sea ice from the McMurdo Sound region, Antarctica. Serikov[146] has also measured similar small sample values of E (3.9 to 5.0 x 10^{10} dy/cm^2) on 1 year spring ice in the Antarctic as has been reported using standard field seismic methods on similar ice in the Arctic (Table I).

Static measurements

There have been only a very limited number of determinations of E by static methods. Butkovich[34] determined values from the slopes of the straight line portion of stress-strain curves in compression. The values of E ranged from 0.4 to 1.0 x 10^{10} dynes/cm^2 and mean values systematically increased (0.76 to 0.83 x 10^{10} dynes/cm^2) as the specimen temperature decreased (-4 to -18C). His values, however, were affected by deformation in the loading apparatus.

The same experimenter[36] later determined E on simple small beams. Although there is considerable scatter in the results, a linear decrease in E with increasing ν_b is indicated as in the dynamic tests. In contrast to the dynamic results,[129] tests run on vertical beams gave appreciably higher results than tests on horizontal beams. There also appears to be a decrease in E with time after removal of the specimens from the ice sheet. E values determined by similar tests have also been reported by Tabata.[168] The most important aspect of his results deals with the dependence of E on $\dot{\sigma}$ (see p. 56). As was expected E values determined by static methods were consistently lower than those determined by dynamic techniques.

Shear Modulus and Poisson's Ratio

Accurate determinations of the velocity of propagation of shear waves in sea ice are much rarer than determinations on compressional wave velocities. In general it has been found that in ice impulsive shear waves are not generated by standard non-directional explosive sources and that second

arrivals cannot be picked with the accuracy of the first compressional arrival.[112,66] Therefore, either mechanical devices or shaped charges must be used to generate the shear waves. Hunkins[66] also found that it was difficult to obtain good shear wave arrivals at distances of more than 250 m from the wave source.

An examination of the shear modulus (G) values presented in Table I and Figure 37 shows that, on the average G is 38% of the value of E and varies in a similar manner with the "state" of the sea ice. The reason for the similarity in the variation of E and G can be seen by examining eq 4.13.

$$G = \frac{E}{2(1+\mu)}. \tag{4.13}$$

Although Poisson's ratio μ varies slightly, its variation is small compared to the variation in E. Therefore, in general G follows E.

There is, at present, insufficient information on the variation of μ with the state of the sea ice. In most cases (Table I), it appears that μ is high for young saline ice and decreases as the ice becomes colder and the brine volume decreases. Support for this conclusion is found in the data of Lin'kov[94] who calculated μ from the general relation

$$\mu = 1 - 2\left(\frac{V_s}{V_p}\right) \tag{4.14}$$

where V_s and V_p are the velocities of the shear and compressional plate waves respectively. We express these results in the form

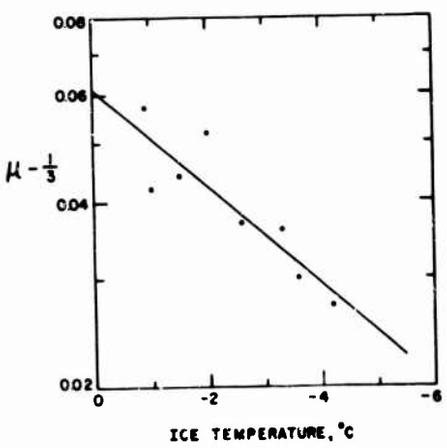

Figure 41. (μ - 1/3) vs mean ice temperature, based on Lin'kov's in-situ seismic determinations, Cape Schmidt, Siberia.[94]

$$\mu = \mu_f + (\mu_0 - \mu_f)\exp\left(-\frac{\theta_i}{\theta_0}\right) \tag{4.15}$$

where μ_0 is Poisson's ratio extrapolated to 0°C, μ_f is the final Poisson's ratio at very low temperatures (taken to be equal to that of fresh ice 0.33)[111] and θ_0 is a characteristic temperature. The results are shown in Figure 41. The final least-squares equation is

$$\mu = 0.333 + 6.105 \times 10^{-2} \exp\left(-\frac{\theta_i}{5.48}\right). \tag{4.16}$$

A decrease in μ with decreasing average ice temperature is clearly indicated. Langleben and Pounder[87] have, on the other hand, reported no systematic variations in μ as measured by small-sample resonance methods with changes in salinity, temperature or ice type. They recommend that an average value of 0.295 be used for sea ice. Further experimentation will be necessary to eliminate the lack of agreement in these results. A relation between μ and brine volume v_b or overall porosity v should be explored.

Time-Dependent Effects

Stress rate

Tensile strength. As was pointed out earlier, in tests concerned with the elastic behavior of sea ice, if the rate of stress application $\dot{\sigma}$ is greater than 0.5 kg/cm^2 - sec, it has been assumed that the failure strength is independent of $\dot{\sigma}$. Actually most of the tests discussed in this section were performed at a constant rate of strain $\dot{\epsilon}$. The stress rate $\dot{\sigma}$ is constant only if Hooke's law holds. The assumption of the independence of σ_f and $\dot{\sigma}$ was based on the results of Jellinek[73] who showed that the strength of snow cylinders that failed in tension behaved in this manner. That this assumption was also satisfactory for sea ice in the range $0.01 \leq \dot{\sigma} \leq 0.18$ kg/cm^2 - sec was demonstrated by Peyton's data[122] which show no pronounced variation in σ_f with changes in $\dot{\sigma}$ for direct tension tests on sea ice from Point Barrow, Alaska. Peyton[122] then extended these measurements to higher values of $\dot{\sigma}$ ($\sim$2.6 kg/cm^2 - sec) and fitted by least-squares a relation

$$\sigma_f = a\dot{\sigma}^b \theta_i^c S_i^d z^e \tag{4.17}$$

in the linearized form

$$\ln \sigma_f = \ln a + b \ln \dot{\sigma} + c \ln \theta_i + d \ln S_i + e \ln z \tag{4.18}$$

to the test results. Here a, ..., e are constants, σ_f the failure strength, $\dot{\sigma}$ the rate of stress application, θ_i the test temperature, S_i the ice salinity, and z the position of the sample in the ice sheet. The average value of the coefficient b was found to be 0.05 indicating to us that σ_f is essentially independent of $\dot{\sigma}$.

Until additional evidence to the contrary becomes available, it is also probably satisfactory to assume that σ_f values determined by ring tensile tests are independent of $\dot{\sigma}$ in the $\dot{\sigma}$ range usually encountered in these tests ($1 \leq \dot{\sigma} \leq 3$ kg/cm^2 - sec). An examination of the results of Butkovich[34] supports this suggestion, which should, of course, be experimentally verified.

Flexural strength. The effect of variations in $\dot{\sigma}$ on the value of the flexural strength as determined by small beam tests has been studied in considerable detail by Tabata.[162,168] During each constant deflection-rate test a plot of applied load vs time was recorded and the failure was classified as elastic or "plastic" depending upon whether or not the plot was linear or showed a curvature. The percentage of samples that failed elastically increased from zero at low values of $\dot{\sigma}$ ($\dot{\sigma} \lesssim 0.2$ kg/cm^2 - sec) to 100% at high values of $\dot{\sigma}$ ($\dot{\sigma} \lesssim 0.6$ kg/cm^2 - sec). Between these two regions there is a mixed region in which both elastic and plastic breaks occur (Fig. 42). The

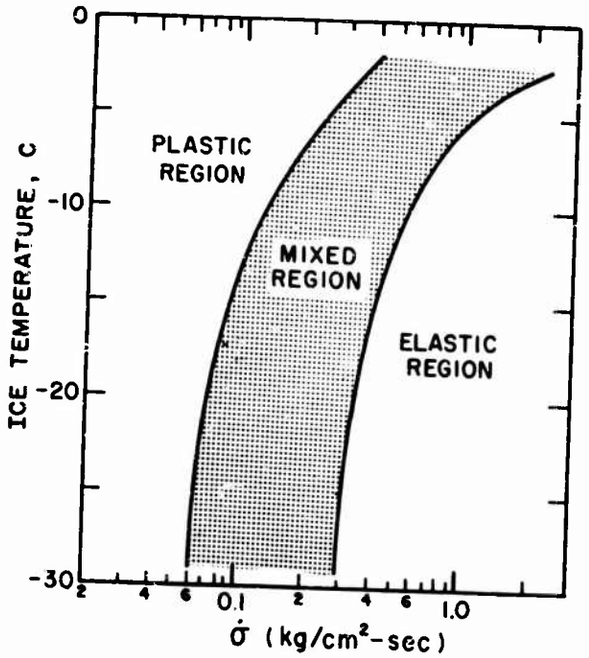

Figure 42. Approximate boundary lines between the regions of elastic, mixed, and plastic failures in relation to temperature and stress rate $\dot{\sigma}$. Ice salinities vary between 1.0 and 1.4‰ and ice densities between 0.86 and 0.87 g/cm³ (Tabata).[168]

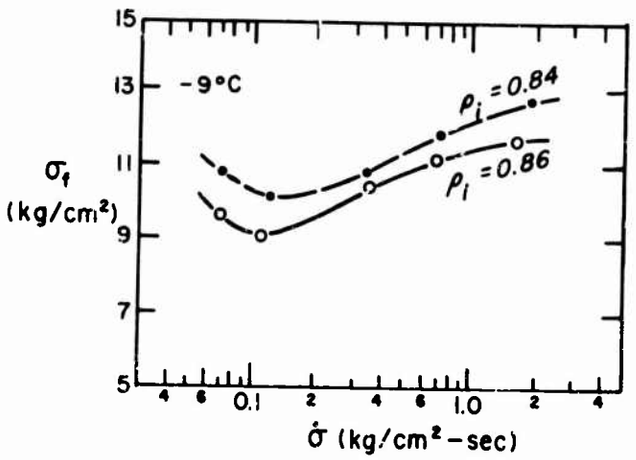

Figure 43. Relation between small-beam flexural strength σ_f and stress rate $\dot{\sigma}$ at -9C (Tabata).[168]

boundaries separating these different "failure types" are, of course, dependent on the test temperature; higher values of $\dot{\sigma}$ are required to achieve elastic failure at temperatures near the melting point. It will, in the future, be interesting to separate the effects of variations in sample temperature from effects associated with variations in the volume of brine and air in the ice.

When constant temperature plots of σ_f vs $\dot{\sigma}$ are prepared and only specimens that failed elastically are included, σ_f appears to be independent of $\dot{\sigma}$ in the range 0.3 to 8 kg/cm^2 - sec. If, however, both plastic and elastic breaks are considered (Fig. 43), as $\dot{\sigma}$ increases there first occurs a slight decrease ($\sim$1 kg/cm^2) in σ_f and then an increase. The minimum occurs in the range of the "mixed region" between plastic and elastic failures. Tabata[162] suggests that the increase in σ_f with decreasing $\dot{\sigma}$ in the low $\dot{\sigma}$ range is due to plastic deformation of the samples before breaking. The increase in σ_f with $\dot{\sigma}$ in the high stress rate range is presumed to be related to the increase in the static Young's modulus with increasing $\dot{\sigma}$ at $\dot{\sigma}$ values greater than 3 to 5 kg/cm^2 - sec. Because the samples used by Tabata in these studies were obtained from very warm, new sea ice (20 to 25 cm thick) and it was necessary to store the ice for appreciable periods of time, significant brine drainage occurred prior to testing. How the replacement of the initial brine by air affects the results is currently unknown. It would be desirable to repeat this careful series of tests on sea ice produced in the laboratory so that brine drainage prior to testing could be minimized.

Tabata and his co-workers[165, 166, 167, 169] have also studied the effect of variations in the manually applied average stress rate $\dot{\sigma}$ on the failure strength as measured by in-situ cantilever beam tests on ice less than 30 cm thick. Mean ice temperatures were quite high, varying from -0.8 to -2.5C. Ice salinities varied from 4.7 to 13.6‰. Although in-situ tests avoid the brine drainage problem, the results are difficult to analyze because of the vertical variation in the temperature and salinity of the ice sheet. The results are, however, quite interesting. Pull-ups, push-downs and pull-sideways tests gave approximately the same results. The value of $\dot{\sigma}$ varied in the range of 0.1 to 40 kg/cm^2 - sec.

The results of these tests (Fig. 44) show that the flexural strength σ_f is independent of $\dot{\sigma}$ at values of $\dot{\sigma} < 1.0$ kg/cm^2 - sec. On the other hand when $\dot{\sigma} > 1.0$ kg/cm^2 - sec, σ_f increases as a linear function of ln $\dot{\sigma}$. That the transition between these two behavorial regions coincides with the change from plastic to elastic deformation has been demonstrated by examining plots of applied force vs deflection for individual beam tests. These plots change from curved to linear at values of $\dot{\sigma} \geq 1$ kg/cm^2 - sec. It is reasonable to assume that this transition to elastic behavior will occur at lower values of $\dot{\sigma}$ for lower test temperatures. The slope also appears to increase as the ice temperature is lowered.

Compressive strength. The effect of variations in $\dot{\sigma}$ on the value of the compressive strength of sea ice from Point Barrow, Alaska, has also been studied by Peyton[122, 123] using eq 4.17 and eq 4.18. The range of stress rates used was $0.06 \leq \dot{\sigma} \leq 8.2$ kg/cm^2 - sec. The average value of b as determined by least-squares was 0.23 (Peyton, 1967). This indicates that although compressive strength is more dependent on $\dot{\sigma}$ than tensile strength, the variation is still small. The general increase in compressive strength with an increase in $\dot{\sigma}$ is comparable to, although much less pronounced than, the increase in flexural strength with increasing $\dot{\sigma}$ as demonstrated by Tabata and his co-workers.

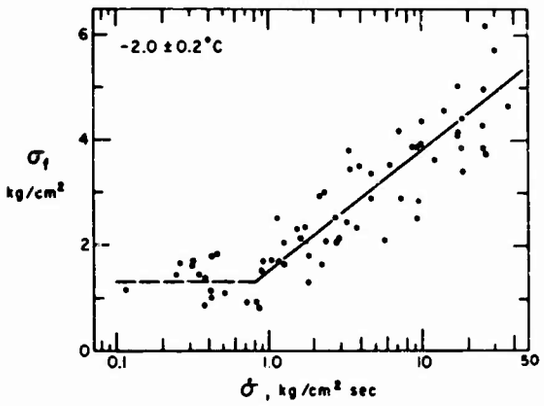

Figure 44. Relation between in-situ flexural strength σ_f and the stress rate $\dot{\sigma}$ at -2C (Tabata, Fujino and Aota).[169]

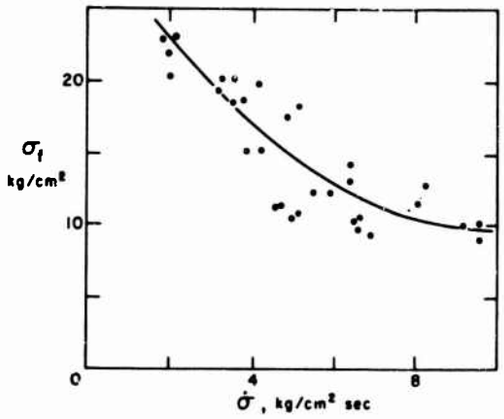

Figure 45. Relation between compressive strength σ_f and stress rate $\dot{\sigma}$ (Peyton).[123]

Peyton[123] has also presented some results of compressive strength measurements vs $\dot{\sigma}$ (Fig. 45) as determined on ice from Cook Inlet, Alaska. These tests indicate a sharp decrease in σ_f with increasing $\dot{\sigma}$. It is interesting that this decrease occurs in the same range of $\dot{\sigma}$ values (compare Fig. 43, 44 and 45) in which both Peyton's Point Barrow compressive data and Tabata's flexural data indicate an increase in σ_f with increasing $\dot{\sigma}$. Peyton has suggested that because the general structure of the ice at Point Barrow and Cook Inlet is different, the minimum $\dot{\sigma}$ values of the Cook Inlet tests can be interpreted to match the Barrow results at the maximum strength value of "comparable" ice. This would then indicate a general $\sigma_f = f(\dot{\sigma})$ relation with a maximum value of σ_f at $\dot{\sigma} \sim 1$ kg/cm² - sec. The experimental evidence is, at present, not sufficient for definite conclusions. An overall theory of the rate dependence is still required.

Elastic modulus. It has already been noted that the values of E determined by static methods are consistently lower than when determined by dynamic methods. Considerable insight into this difference has been provided by the work of Tabata and his associates on the relation between static E values and $\dot{\sigma}$ using small sample beams[162, 168] and in-situ cantilever tests.[165, 166, 167, 169] In the beam tests, although more data would be desirable, log E appears to increase with log $\dot{\sigma}$, approaching the dynamic value at large values of $\dot{\sigma}$.[162] The results of the cantilever tests are shown in Figure 46. Again a pronounced change in E with $\dot{\sigma}$ was noted. The increase in the value of E determined during the 1965 field season over that obtained in 1964 is attributed to the increase in the percentage of infiltrated snow ice present in 1965. This interpretation is supported by the results of dynamic measurements (Fig. 39).

Creep

Studies of the viscoelastic properties of sea ice have been performed mainly by Tabata[155, 158, 163] and Tabata and Ono.[160] They have utilized both small sample, and in-situ, test procedures. As Tabata has pointed out,[158] the in-situ procedures avoid brine drainage problems that would be encountered when small samples are stressed for long periods of time.

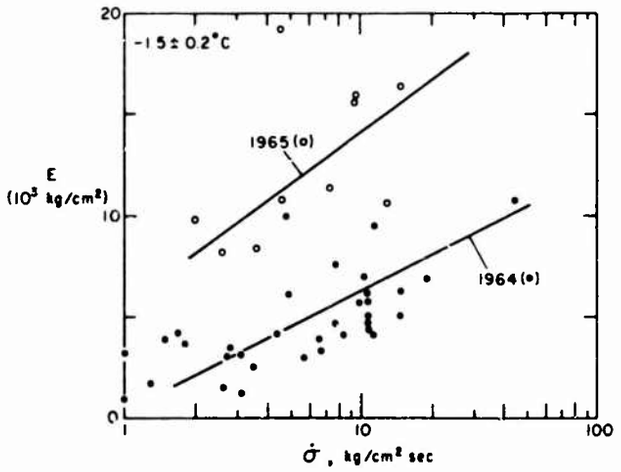

Figure 46. Relation between elastic modulus E and stress rate $\dot{\sigma}$ at -1.5C as determined by in-situ beam tests (Tabata, Fujino and Aota).[169]

However, as mentioned earlier, in-situ tests are not without their disadvantages. In particular in long-time in-situ tests the presence of warm sea water in the channel cut to produce the beam will modify the vertical temperature profile in the beam. Because of this problem and ice formation in the channels, Tabata limited his in-situ tests to time periods of less than two hours.

The in-situ tests were of two types. In one a standard cantilever was prepared and the load applied at the end of the cantilever. In the other a rectangular beam was cut which was still fixed to the ice sheet at both ends. The load was applied to the center of the beam. In both cases the deflections of the beams were measured relative to the neighboring ice. A typical deflection-time plot of the results of an in-situ test are shown in Figure 47.[155, 158] Upon application of the load we note an instantaneous elastic deformation (AB), a transient creep portion (BC) and a linear steady state creep portion (CD). When the load is removed the beam experiences an immediate elastic contraction (DE) and then with the passage of time gradually approaches the value of the permanent deformation G (note that EG ~BB'). The time-dependent portions of both the loading and unloading curves can be shown to be to a good approximation exponential functions of time.[158] Results similar to the loading portion of this curve (AD) have also been obtained by subjecting small sea ice samples to constant compressive stresses in the laboratory.[158, 160]

Such a deflection-time behavior can be analyzed by a rheological model composed of a Maxwell unit and a Voigt unit connected in series (Fig. 47). The elastic spring constants and the viscous dash-pot constants associated with these models are E_1, E_2 and η_1, η_2 respectively. In addition the relaxation time τ_1 and the retardation time τ_2 ($\tau_1 = \eta_1/E_1$, $\tau_2 = \eta_2/E_2$) can be obtained. A summary of the results of these studies is given in Table II. It should be noted that the values of η_1, η_2 and η in Table II are related to the specific tests under discussion, not to a pure shear test as is the true physical constant η.

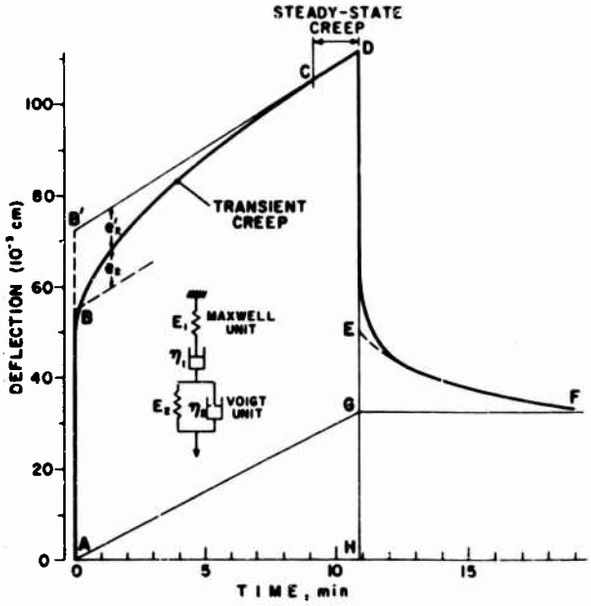

Figure 47. Deflection-time curve for sea ice.[155,158]

The in-situ results show appreciable changes depending upon whether the beam is deflected vertically or horizontally. There currently are insufficient in-situ tests to study any possible correlations between the viscoelastic parameters and the state of the ice. With the exception of the values of τ_1, the small sample results are of the same order of magnitude as the values from the in-situ tests. There also does not appear to be any pronounced variation in the small-sample elastic or viscosity constants with the state of the sea ice. However, the values of E_2, η_1 and η_2 decrease as the angle ϕ between the axis of the cylindrical test specimen and the ice sheet surface changes from 90 to 0 degrees. Tabata[158] has suggested that the low viscosity when ϕ = 0 degrees is caused by slip between the platelets that compose the crystals of sea ice. It is also possible that some of the difference between the values of the constants at ϕ = 0 and 90 degrees could be produced by differences in the volume of infiltrated snow ice present in the sample. For many practical purposes, the utilization of the four constants associated with the combined Maxwell-Voigt model is inconvenient. Therefore, Tabata has also used a simple Maxwell model to study his test results. The values of the Maxwell model constants E and τ are also given in Table II.

In a later paper,[163] Tabata has analyzed the results of time dependent deflection studies on fixed end beams by using an elastic approach and taking the tension of the neutral surface into account. He obtained values of E from the initial instantaneous deflection. E is shown to decrease as a linear function of salinity and presumably also of brine volume as indicated by dynamic tests. As was anticipated in the discussion of the relative magnitudes of static and dynamic values of E, these E values are considerably lower than the dynamic values. The creep rate was studied by replacing E in the elastic deflection equation with a time dependent viscosity term $\eta(t)$ and evaluating

Table II. Mean values of elastic moduli and viscosity constants of sea ice.[158, 160]

A. In-situ beam tests

			Maxwell-Voigt model						Maxwell model	
Deflection direction	θ_i (°C)	S_i (‰)	E_1 (10^9 dy/cm²)	E_2 (10^9 dy/cm²)	η_1 (10^{11} dy-min/cm²)	η_2 (10^{10} dy-min/cm²)	τ_1 (min)	τ_2 (min)	E (10^9 dy/cm²)	τ (min)
Vertical (down)	- 2.5	5.5	5.4	12.0	1.1	4.7	20.	6.5	3.4	32.0
Horizontal	- 1.9	4.9	45.0	97.0	8.9	35.0	23.	1.8	39.0	28.0

B. Small specimen compression tests

Angle between core axis and ice sheet surface ϕ	θ_i (°C)	S_i (‰)	E_1 (10^9 dy/cm²)	E_2 (10^9 dy/cm²)	η_1 (10^{11} dy-min/cm²)	η_2 (10^{10} dy-min/cm²)	τ_1 (min)	τ_2 (min)	E (10^9 dy/cm²)	τ (min)	Stress (kg/cm²)	Density (g/cm³)
90°	- 3.7	4.1	1.4	4.8	4.4	4.6	366.	11.0	1.3	4.8	3.5	
60°	- 3.2	3.8	2.5	4.5	1.5	3.8	78.	8.2	2.1	.9	3.4	
30°	- 2.3	4.6	.7	2.9	.4	1.0	98.	3.5	.5	1.2	2.6	
0°	- 5.0	3.5	1.1	1.8	1.2	2.7	125.	14.0	.8	1.7	3.1	
90°	- 2.8	.81	.5	5.0	3.7	6.4	885.	10.0	--	--	4.3	.85
90°	- 5.0	.99	--	7.3	2.0	7.2	--	10.0	--	--	4.4	.88
90°	-13.0	2.7	.7	3.3	6.2	2.2	689.	6.5	--	--	4.1	.86
90°	-16.8	2.3	1.1	6.3	7.2	11.2	726.	17.0	--	--	4.6	.86
90°	-23.5	1.7	2.0	9.7	12.3	19.9	713.	18.0	--	--	5.2	.83
90°	-26.3	2.6	1.8	6.9	5.4	17.2	254.	29.0	--	--	4.6	.86

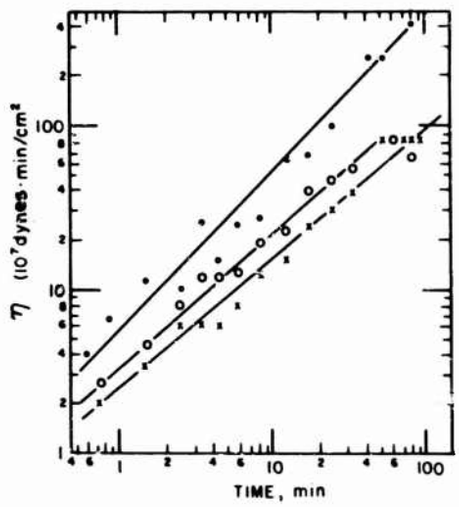

Figure 48. Typical examples of the relation between the coefficient of viscosity η (t) of sea ice and the time of loading as determined from in-situ fixed-ended beams (Tabata).[163]

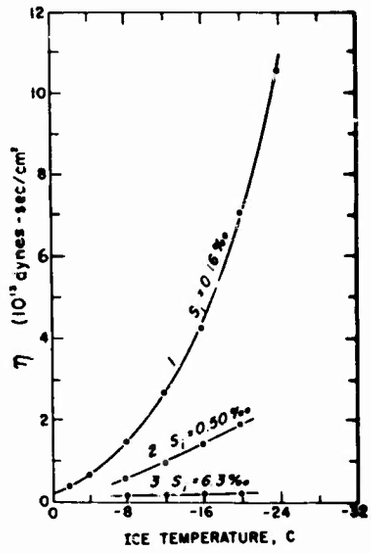

Figure 49. Coefficient of viscosity η vs ice temperature for specimens of different salinities. Curves 1 and 2 based on flexural studies, curve 3 based on torsion (Nazintsev).[103]

η(t) as a function of t. Some representative results are shown in Figure 48 and suggest a power law with an average power of 0.67. This indicates that the relation between strain ε and time t is

$$\varepsilon = k\, t^{1/3} \tag{4.19}$$

where k is a constant. Relation 4.19 is similar to the empirical Andrade creep law. Large scale tank tests[64] have also produced similar deflection vs time profiles to those observed by Tabata.

Nazintsev[103] has also used small-sample tests (rods in torsion and beams in flexure) to study the time-dependent deformation of sea ice in the temperature range -4 to -28C. At constant stress he found that only after 3 days was a consistent relation observed between strain rate $\dot{\varepsilon}$ and temperature. Figure 49 shows some of his better results. In this figure curves 1 and 2 were determined in flexure and curve 3 in torsion. A pronounced variation of viscosity with salinity and temperature is suggested. When the present authors attempted to analyze his complete results (his Table 1, p. 52) in terms of brine volume, no consistent relation was noted. Considering the fact that the majority of Nazintsev's tests were performed on young or annual sea ice, the extremely low salinities reported suggest that significant brine drainage occurred during testing. This drainage may explain the lack of correlation between η and v_b. Although there was a complete overlap of the values determined by torsion and flexure in the low viscosity range, viscosity values higher than 50 dy-sec/cm^2 were observed only in flexure. When Nazintsev attempted to analyze his results in terms of a "Glen-type" power law between strain rate and shear stress, he observed that the power n was roughly 1.6 as compared with a value of 3.5 for glacier ice. One should consider, however that the use of the power law itself is empirical. The relation of strain rate to stress should be linear at low stress levels.

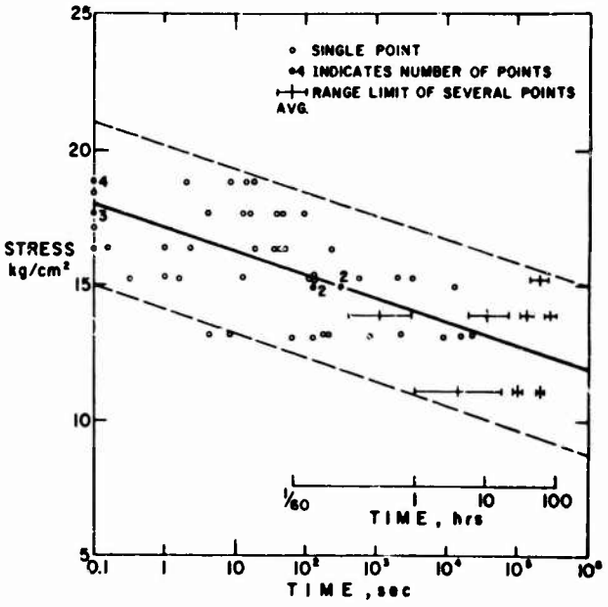

Figure 50. Stress-rupture behavior of natural sea ice at -20C (range -10C to -28C). Dashed lines indicate the 95% confidence limits (Kingery and French).[77]

The time-dependent stress-rupture behavior of sea ice has also been studied by Kingery and French[77] using small simply-supported beams. The results (Fig. 50) indicate a linear relation between stress and log (rupture time). There is an appreciable scatter in the results which is undoubtedly in large part produced by the wide range of temperatures (-10 to -29C) at which the tests were performed. It would be interesting to study changes in the creep-rupture behavior of sea ice with changes in the state of the ice at the time of testing.

5. PLATE CHARACTERISTICS

There is a wide range of applied problems, the solution of which depends upon a knowledge of the mechanical properties of sea ice. It is beyond the scope of this review to discuss these in detail. A comprehensive selection of papers dealing with these problems is, however, included in the reference list. For a representative sampling of these papers see Hertz (1884), Bernshtein (1929), Shul'man (1946), Wyman (1950), Nevel (1958, 1966) Meyerhof (1960), Assur (1961a), and Cutcliffe, Kingery and Coble (1963). All of these problems have certain features in common: it is usually necessary to be able to estimate effective values of flexural strength σ_f, elastic modulus E, and Poisson's ratio μ for the ice sheet as a whole. Using these values it is then necessary to calculate such composite properties as the flexural rigidity, the action radius, the section modulus, the moment of inertia, and the position of the neutral axis. In the past the considerable vertical variation in the physical properties of the sea ice has usually been ignored and the ice sheet has been assumed to be homogeneous. In concluding this paper we would like to show how the vertical variation in the physical properties of sea ice sheets can readily be incorporated into the treatment of problems that deal with the ice sheet as a whole.[22]

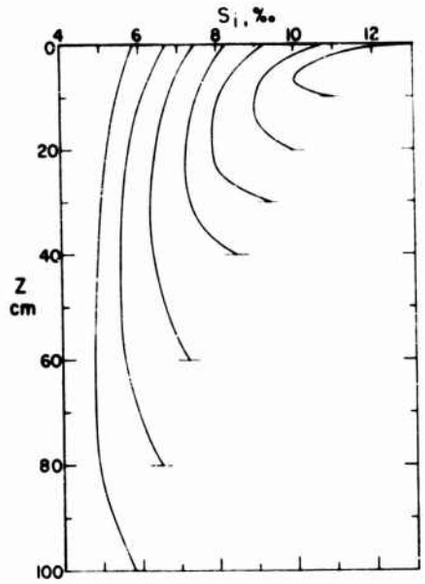

Figure 51. Series of schematic salinity profiles for sea ice of various thicknesses.

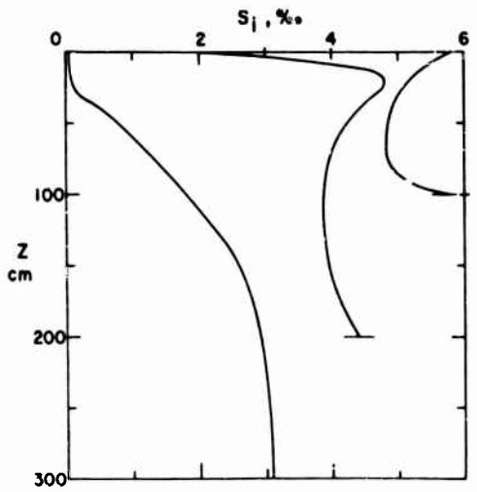

Figure 52. Series of schematic salinity profiles for sea ice 100, 200, and 300 cm thick. The low salinity values at the top of the 200 cm profile indicate that this ice has been through a period of summer melt.

As has been demonstrated, the main variable controlling the vertical variation in the physical characteristics of sea ice is the vertical variation of the volume of brine in the ice ν_b. The value of ν_b at any position in the ice sheet is, in turn, determined via the phase relations by the ice temperature θ_i and salinity S_i at that point. Fortunately ice salinity profiles go through a systematic series of changes as ice growth progresses. Representative values for salinity profiles can be obtained by examining the published literature[97, 186, 145] and are shown schematically in Figures 51 and 52. These profiles can be adjusted so that the variation in salinity is a smooth function of the ice thickness h. If the ice temperature profile is known, a brine volume profile can be calculated by using the brine volume tables published by Assur.[17] Recently Frankenstein and Garner[51] have calculated a linear expression based upon these tables

$$\nu_b = \frac{S_i}{10^3}\left[-\frac{49.185}{\theta_i} + 0.532\right] \tag{5.1}$$

where S_i is expressed in ‰, θ_i in degrees C and ν_b in absolute ratios. The approximate relation holds in the temperature range $-0.5 \geq \theta_i \geq -22.9$C with a correlation coefficient of 0.9995. One can estimate the ice temperatures from the ice surface temperature θ_0 by assuming a linear profile which in many cases is a good approximation.[93]

One must subtract the thickness of the strengthless skeleton layer ($h_{sk} \sim 2.5$ cm) from the total ice thickness. This correction becomes quite important when the properties of thin ice sheets are considered. Now express position in the ice sheet in terms of a transformed dimensionless distance $\tilde{z}$

where $\tilde{z}$ varies from a value of 0 at the bridging layer at the top of the skeleton layer to a value of 1 at the upper surface of the ice sheet

$$\tilde{z} = \frac{h - h_{sk} - z}{h - h_{sk}} . \tag{5.2}$$

Here h is the total ice thickness including the skeleton layer and z is the vertical distance to any position in the ice sheet measured from the upper surface of the sheet. If a linear approximation is used for the temperature profile, the value of θ_i at any $\tilde{z}$ is

$$\theta_i = \theta_b - \Delta\theta\,\tilde{z} \tag{5.3}$$

where

$$\Delta\theta = \theta_0 - \theta_b \tag{5.4}$$

and

$$\theta_b = \theta_w - (\theta_w - \theta_0)\left(\frac{h_{sk}}{h}\right) \tag{5.5}$$

where θ_b is the temperature at the bridging layer and θ_w the water temperature. If a linear temperature profile and a constant ice salinity are assumed, it is possible over a limited temperature range to express the brine-volume profile analytically in terms of the salinity and density of the brine and ice. Because of these restrictions, Assur[22] has also suggested the expression of ν_b and $\sqrt{\nu_b}$ as polynomials in $\tilde{z}$ and utilize the relations

$$\frac{E}{E_0} = 1 - \frac{\nu_b}{\nu_0} \tag{5.6}$$

and

$$\frac{\sigma_f}{\sigma_0} = 1 - \left(\frac{\nu_b}{\nu_0}\right)^{1/2} \tag{5.7}$$

to express the variation of E and σ_f with ν_b. We expand here these ideas considering that at high brine volumes σ_f does not approach the value of ~ 0.25 suggested by the linear extrapolation of σ_f determinations performed on cold ($\sqrt{\nu_b} < 0.40$) sea ice (see p. 36). Instead σ_f remains roughly constant at $\sqrt{\nu_b} > 0.40$ (see Fig. 26, 31, 32). As discussed earlier, these are still just indications inasmuch as the problem of plastic stress relief for ring tensile samples at high temperatures has not been resolved. Although the data available on the behavior of E at large brine volumes are very limited, it is reasonable that E must behave in a similar manner: if sea ice possesses strength at values of $\nu_b > 0.25$, it also must have resistance to strain and therefore a value of E. On p. 22 and 23 a method was suggested for handling the observed variation in σ_f by using eq 3.40 and setting $\nu_0 = 1$ in that equation. This gives

$$\frac{\sigma_f}{\sigma_0} = 1 - \sqrt{\nu_b}\,(2 - \sqrt{\nu_b}) \tag{5.8}$$

where - 2 represents the limiting slope as $\sqrt{\nu_b}$ approaches zero. A similar relation can be constructed for E in such a way that it satisfies the available data in the low brine volume range

$$\frac{E}{E_0} = 1 - \nu_b (4 - 3\nu_b). \tag{5.9}$$

Note that eq 5.8 and eq 5.9 are both zero when $\nu_b = 1$ and approach eq 5.7 and eq 5.6 respectively with $\nu_0 = 0.25$ at small values of ν_b. This can be verified by approximating eq 5.8 and eq 5.9 with their first derivatives at $\nu_b \to 0$.

It is convenient to express eq 5.8 and eq 5.9 in terms of polynomials in $\tilde{z}$

$$\frac{E}{E_0} = a_0 + a_1 \tilde{z} + a_2 \tilde{z}^2 + a_3 \tilde{z}^3 + \ldots \tag{5.10}$$

and

$$\frac{\sigma_f}{\sigma_0} = b_0 + b_1 \tilde{z} + b_2 \tilde{z}^2 + b_3 \tilde{z}^3 + \ldots \tag{5.11}$$

Assur[22] shows how to calculate the coefficients simply upon the basis of values at selected levels. The average values of E and σ_f for the whole ice sheet excluding the skeleton layer now becomes

$$\frac{\overline{E}}{E_0} = \mathfrak{M}_0 = \int_0^1 \frac{E}{E_0}\, d\tilde{z} = a_0 + \frac{a_1}{2} + \frac{a_2}{3} + \frac{a_3}{4} + \ldots \tag{5.12}$$

and

$$\frac{\overline{\sigma}_f}{\sigma_0} = \int_0^1 \frac{\sigma_f}{\sigma_0}\, d\tilde{z} = b_0 + \frac{b_1}{2} + \frac{b_2}{3} + \frac{b_3}{4} + \ldots \tag{5.13}$$

Note that in this approach it is always possible to integrate over the complete thickness ($\tilde{z} = 0$ to $\tilde{z} = 1$) of the ice sheet i.e. the problem of the possible occurrence of a zero strength or E layer ($\nu_b \geq \nu_0$ in eq 5.6 or eq 5.7) in the ice sheet is avoided.

The average strength of the profile according to eq 5.13 becomes important in some engineering problems, such as forces exerted on vertical piles. Normally, however, one deals with bending for which more sophisticated calculations are required.

As a result of the vertical variation in E, the neutral axis is no longer in the center of the ice sheet. Finding its location is similar to finding the center of gravity of a cross section with a width in each layer reduced according to the ratio E/E_0. Defining the $n^{\underline{th}}$ moment as

$$\mathfrak{M}_n = \int_0^1 \tilde{z}^n \frac{E(\tilde{z})}{E_0}\, d\tilde{z} \tag{5.14}$$

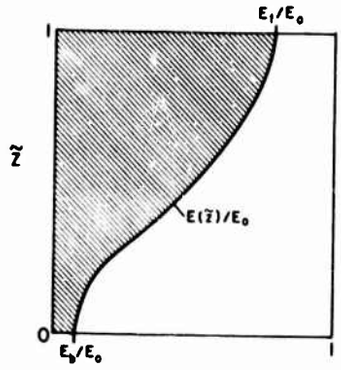

Figure 53. Relative width of effective cross-section (E/E_0) vs dimensionless ice thickness $\tilde{z}$.

where the superscript ~ indicates that the parameter is calculated using the reduced cross section (see Fig. 53), $\tilde{z}_n$ the non-dimensional distance to the neutral axis measured from the bridging layer at the bottom of the ice sheet is

$$\tilde{z}_n = \frac{\tilde{M}_1}{\tilde{M}_0} \tag{5.15}$$

with

$$\tilde{M}_1 = \frac{a_0}{2} + \frac{a_1}{3} + \frac{a_2}{4} + \frac{a_3}{5} + \dots \tag{5.16}$$

and $\tilde{M}_0$ from eq 5.12. As eq 5.15 clearly shows, the position of the neutral axis will shift with the coefficients a_1, a_2, ... which in turn are determined by the salinity and temperature profiles.

To obtain D, the flexural rigidity of the ice sheet, we calculate the moment of inertia $\tilde{I}$ of our reduced cross section using the general relation

$$\tilde{I} = \tilde{M}_2 - \tilde{M}_0 \tilde{z}_n^2 = \tilde{M}_2 - \frac{\tilde{M}_1^2}{\tilde{M}_0} . \tag{5.17}$$

Then

$$D = \frac{E_0 \tilde{I} h_b^3}{1-\mu^2} = \frac{E_0 h_b^3}{1-\mu^2}\left[\tilde{M}_2 - \frac{\tilde{M}_1^2}{\tilde{M}_0}\right] \tag{5.18}$$

with

$$\tilde{M}_2 = \frac{a_0}{3} + \frac{a_1}{4} + \frac{a_2}{5} + \frac{a_3}{6} + \dots \tag{5.19}$$

The term

$$h_b = h - h_{sk} \tag{5.20}$$

appears when the transformation is made back to dimensional units from the non-dimensional $\tilde{z}$ scale. The action radius ℓ can easily be obtained from eq 5.18 by using eq 1.5. Thus the deflections and moments for all previously solved classical plate problems may be utilized provided ℓ for sea ice is defined using eq 5.18.

It now remains to define the flexural strength σ_f for use in plate equations. The stress in the bottom fiber σ_b is

$$\sigma_b = -\frac{M}{S_b} \tag{5.21}$$

where M is a bending moment and S_b is the section modulus (see eq 1.1) while σ_f is defined as

$$\sigma_f = -\frac{6M}{h_b^2} = \frac{6\sigma_b S_b}{h_b^2}. \tag{5.22}$$

Referring to Figure 53 we see that

$$\sigma_b S_b = \sigma_b \frac{E_0}{E_b} \tilde{S}_b h_b^2 \tag{5.23}$$

with

$$\tilde{S}_b = \frac{\tilde{I}}{\tilde{z}_n} = \frac{\tilde{M}_0\tilde{M}_2 - \tilde{M}_1^2}{\tilde{M}_1}. \tag{5.24}$$

Here E_b refers to the modulus of elasticity in the bottom fiber. Therefore

$$\sigma_f = 6\sigma_b \frac{E_0}{E_b} \tilde{S}_b. \tag{5.25}$$

Similarly the flexural strength with the top fiber in tension becomes

$$\sigma_f = 6\sigma_t \frac{E_0}{E_t} \tilde{S}_t \tag{5.26}$$

where the subscript t refers to the top fiber and

$$\tilde{S}_t = \frac{\tilde{I}}{1 - \tilde{z}_n} = \frac{\tilde{M}_0\tilde{M}_2 - \tilde{M}_1^2}{\tilde{M}_0 - \tilde{M}_1}. \tag{5.27}$$

Now σ_b and E_b or σ_t and E_t can be calculated from eq 5.8 and eq 5.9 by introducing ν_b for the bottom or the top, respectively. Note that the product $\sigma_b E_0 / E_b$ in eq 5.25 is defined by the state of the bottom fiber which is relatively constant. $\tilde{S}_b$ on the other hand, is highly weather dependent. In the top fiber (eq 5.26) both $\sigma_t E_0 / E_t$ and $\tilde{S}_t$ are weather dependent.

We started this review with practical problems, discussed the chemical, crystallographic, mechanical and physical aspects involved and in conclusion showed how to utilize this knowledge to solve practical problems.

LITERATURE CITED

1. Abele, G. and Frankenstein, G. (1967) Snow and ice properties as related to roads and runways in Antarctica, U.S. Army Cold Regions Research and Engineering Laboratory Technical Report 176.
2. Anderson, D. L. (1958) "A model for determining sea ice properties" in Arctic sea ice, U.S. National Academy of Sciences, National Research Council, Pub. 598, p. 148-152.
3. _____ (1958) Preliminary results and review of sea ice elasticity and related studies, Transactions, Engineering Institute of Canada, 2, p. 116-122.
4. _____ and Weeks, W. F. (1958) A theoretical analysis of sea ice strength, Transactions American Geophysical Union, vol. 39, p. 632-640.
5. Anderson, D. L. (1960) The physical constants of sea ice, Research, vol. 13, p. 310-318.
6. Anderson, D. L. (1961) Elastic wave propagation in layered anisotropic media, Journal of Geophysical Research, vol. 66, p. 2953-2963.
7. Anderson, D. L. (1962) "Elastic properties of sea ice from dynamic measurements" in Summary report - Project Ice Way (W. D. Kingery, Ed.), Air Force Cambridge Research Laboratory, Surveys in Geophysics, no. 145 (AFCRL - 62 - 498), p. 153-172.
8. Anderson, D. L. (1963) "Use of long-period surface waves for determination of elastic and petrological properties of ice masses" in Ice and snow - Properties, processes and applications (W. D. Kingery, Ed.). Cambridge, Mass: MIT Press, p. 63-68.
9. Arnol'd - Aliab'ev, V. I. (1924) Sostoianie i rasprostranenie ledianogo pokrova Finskogo zaliva ... (Ice cover in the Gulf of Finland...), Morskoi Sbornik, vol. 77, p. 139-150.
10. _____ (1925) O metodakh issledovaniia l'dov Finskogo zaliva s ledokolov (Methodology of ice study from ice-breakers in the Gulf of Finland), Zhurnal Geofiziki i Meteorologii, vol. 2, p. 79-88.
11. _____ (1929) Issledovanniia prochnosti l'da Finskogo zaliva v 1923, 1927 i 1928 gg. (Investigation of ice strength of the Finnish Gulf in 1923, 1927, and 1928), Izvestiia Glavnoi Geofizicheskoi Observatorii, Leningrad, vol. 2, p. 15-28.
12. _____ (1930) Opredelenie polostei vo l'du i pribory dlia etoi tseli (The determination of air bubbles in ice and instruments for measuring the same). Izvestiia Glavnoi Geofizicheskoi Observatorii, Leningrad 4, p. 34-36.
13. _____ (1933) K voprosu o khimizme l'da Finskogo zaliva, v sviazi s izucheniem ego prochnosti (The strength of ice in the Gulf of Finland and its chemical composition). Izvestiia Sektora Fiziko-Khimicheskogo Analiza Instituta Obshchei i Neorganicheskoi Khimii 6, p. 229-233.

LITERATURE CITED (Cont'd)

14. Arnol'd - Aliab'ev, V.I. (1934) Metody opredelenia plotnosti i rykhlosti l'da v ekspeditsionnoi obstanovke (Determination of density and porosity of ice under field conditions). Trudy Komissii po izucheniu vechnoi merzloty. Akademy of Sciences USSR 3, p. 127-150,

15. _____ (1938) Moshchnost', stroenie i plostnost' l'da Karskogo moria po dannym ekspeditsii na l/p, "Malygin", v 1934 godu (The thickness, structure and density of Kara sea ice according to the data obtained by the Malygin expedition of 1934). Trudy Arkticheskogo Instituta 110, p. 57-81. Translation, CRREL Microfilm 100 (SIP U5277).

16. _____ (1939) O prochnosti l'da Barentsova i Karskogo morei (Strength of the ice in the Barents and Kara Seas). Problemy Arktiki, 6, p. 21-30.

17. Assur, A. (1958) "Composition of sea ice and its tensile strength" in Arctic sea ice, U.S. National Academy Sciences - National Research Council Pub. 598, p. 106-138.

18. _____ (1961) Traffic over frozen or crusted surfaces. Proc. 1st Intern. Conf. Mechanics of Soil - Vehicle Systems (Torino - St. Vincent). p. 913-923.

19. _____ (1961) Bearing capacity of floating ice sheets. Proc. Am. Soc. Civil Engineers, J. Eng. Mechanics Div. 87, p. 63-66.

20. _____ and Weeks, W.F. (1963) Growth, structure, and strength of sea ice. Internat. Un. Geodes. Geophys. (Comm. Snow and Ice, Berkeley) Pub. 61, p. 95-108.

21. _____ (1964) Growth, structure, and strength of sea ice. USA CRREL Research Rept. 135, 19 p.

22. Assur, A. (1966) "Flexural and other properties of sea ice sheets" in Proceedings of conference, Institute of Low Temperature Science, Hokkaido University, Aug 1966.

23. Bader, H. (1964) Density of ice as a function of temperature and stress, USA CRREL Special Report 64, 6 p.

24. Baranov, G.I. (1965) Physico-mechanical properties of Antarctic sea ice, Soviet Antarctic Expedition, Information Bulletin 5 (6), p. 430-432.

25. Bennington, K.O. (1963) Some crystal growth features of sea ice, Journal of Glaciology, vol. 4, p. 669-688.

26. _____ (1963) "Some chemical composition studies of arctic sea ice" in Ice and snow - processes, properties, and applications (W.D. Kingery, Ed.). Cambridge, Mass: MIT Press, p. 248-257.

27. Bernshtein, S.A. (1929) Ledianaia zheleznodorozhnaia pereprava (A railroad ice crossing), Nauchno - Tekhnicheskii Komitet Narodnogo Komisariata Putei Soobshecheniia, Trudy, 84, p. 36-82.

LITERATURE CITED (Cont'd)

28. Blinov, L. K. (1965) Solevoi sostav morskoi vody i l'da (Salt composition of sea water and ice), Gosudarstvennyi Okeanograficheskii Institut (Leningrad), Trudy 83, p. 5-55.

29. Bogorodskii, V. V. (1958) Ul'trazvukovoi metod opredeleniia tolshchiny l'dov (Ultrasonic method of determining ice thickness). Problemy Arktiki 4, p. 65-77. Translation DRB Canada, T325R.

30. _____ (1958) Uprugie kharakteristiki l'da (Elastic properties of ice). Akusticheskii Zhurnal 4, p. 19-23.

31. Brown, J. H. and Howick, E. E. (1958) Physical measurements of sea ice, U. S. Navy Electronics Laboratory, Research and Development Report 825, 23 p.

32. Brown, J. H. (1963) "Elasticity and strength of sea ice" in Ice and snow - Processes, properties and applications (W. D. Kingery, Ed.) Cambridge, Mass: MIT Press, p. 79-106.

33. Butkovich, T. R. (1954) Ultimate strength of ice, USA SIPRE Research Report 11, 12 p.

34. _____ (1956) Strength studies of sea ice. USA SIPRE Research Report 20, 15 p.

35. _____ (1958) Recommended standards for small-scale ice strength tests, Transactions, Engineering Institute of Canada, 2, p. 112-115.

36. _____ (1959) On the mechanical properties of sea ice, Thule, Greenland, 1957, USA SIPRE Research Report 54, 11 p.

37. _____ (1959) Some physical properties of ice from the TUTO tunnel and ramp, Thule, Greenland, USA SIPRE Research Report 47, 17 p.

38. Butiagin, T. P. (1961) Prochnost' ledyanogo pokrova v ledovykh nagruzkakh gidrosooruzheniia (The strength of the ice cover under ice loading at hydrotechnic installations). Trudy Transportno-Energeticheskogo Instituta 11, p. 25-48.

39. Cherepanov, N. V. (1957) Opredelenie vozrasta dreifuiushchikh l'dov metodom kristallooptricheskogo issledovaniia (Determination of the age of drifting ice by optical study of the crystals). Problemy Arktiki 2, p. 179-184.

40. Chernigovskii, N. T.; Somov, M. M.; Petrova, A. N.; Antonov, V. S.; and Zotin, M. I. (1943) "L'dy arkticheskikh morei (The ice of the arctic seas)", Izdatel' stvo Glavsevmorputi, Moscow.

41. Chikovskii, S. S. (1961) O vliianii temperatury morskogo l'da na ego prochnost' (Influence of temperature of sea ice on its strength). Problemy Arktiki i Antarktiki 8, p. 93-96.

42. Cutcliffe, J. L.; Kingery, W. D.; and Coble, R. L. (1963) "Elastic and time dependent deformation of ice sheets" in Ice and snow - Processes, properties, and applications (W. D. Kingery, Ed.), Cambridge, Mass: MIT Press, p. 305-310.

LITERATURE CITED (Cont'd)

43. Demiianov, N.I. (1957) Ledovye nabliudeniia na dreifuiushchei stantsii "Severnyi Polius - 4" (Ice observations on the drifting station "North Pole - 4"), Materialy nabliudenii nauchno - issledovatel'skikh dreifuiushchikh stantsii "Severnyi Polius - 3" i "Severnyi Polius - 4" Vol. I. Izdatel'stvo Arkticheskogo Instituta.

44. Dykins, J.E. (1963) "Construction of sea ice platforms" in Ice and snow - Processes, properties and applications (W.D. Kingery, Ed.), Cambridge, Mass: MIT Press, p. 289-301.

45. _____ (1966) "Tensile properties of sea ice grown in a confined system" in Proceedings of conference, Institute of Low Temperature Science, Hokkaido University, Aug. 1966.

46. Elbaum, C. (1959) Substructures in crystals grown from the melt. Progress in Metal Physics 8, p. 203-253.

47. Filippova, L.I. and Shul'man, A.R. (1949) O relaksatsii napriazhenii vo l'du (Elastic deformation in ice). Trudy Gosudarstvennogo Gidrologicheskogo Instituta 16, p. 96-100.

48. Frankenstein, G. (1959) Strength data on lake ice, USA SIPRE Technical Report 59, 6p.

49. _____ (1961) Strength data on lake ice, Part II, USA CRREL Technical Report 80, 18 p.

50. _____ (1967) Ring tensile strength studies of ice, USA CRREL Technical Report 172.

51. _____ and Garner, R. (1967) Linear relationship of brine volume and temperature from -0.5 to -22.9C for sea ice, Journal of Glaciology 6.

52. Fujino, K. (1966) Electrical properties of sea ice, Proceedings of Conference, Institute of Low Temperature Science, Hokkaido University, August 1966.

53. Goetze, C.G. (1965) A study of brittle fracture as applied to ice, USA CRREL Technical Note (unpublished).

54. Gold, L.W. (1963) "Deformation mechanisms in ice" in Ice and snow - Processes, properties, and applications (W.D. Kingery, Ed.), Cambridge, Mass: MIT Press, p. 8-27.

55. _____ (1963) Crack formation in ice plates by thermal shock, Canadian Journal of Physics, vol. 41 (10), p. 1712-1728. National Research Council Report 7548.

56. _____; Black, L.D.; Trofimenkof, F.; and Matz, D. (1958) Deflections of plates on elastic foundations, Transactions, Engineering Institute of Canada 2, p. 123-128.

57. Graystone, P. and Langleben, M.P. (1962) "Ring tensile strength of sea ice" in Ice and snow - Processes, properties, and applications (W.D. Kingery, Ed.), Cambridge, Mass: MIT Press, p. 114-123.

58. Hallett, J. (1960) Crystal growth and the formation of spikes in the surface of supercooled water, Journal of Glaciology, vol. 3, p. 698-702.

LITERATURE CITED (Cont'd)

59. Harrison, J.D. and Tiller, W.A. (1963) "Controlled freezing of water" in Ice and snow - Processes, properties and applications (W.D. Kingery, Ed.). Cambridge, Mass: MIT Press, p. 215-225.

60. _____ (1963) Ice interface morphology and texture developed during freezing, Journal of Applied Physics, vol. 34, p. 3349-3355.

61. Hertz, H. (1884) Uber das Gleichgewicht schwimmender elastischer Platten, Wiedmann's Ann. d. Phys. Chem. 22, p. 449-455.

62. Hendrickson, G. and Rowland, R. (1965) Strength studies on antarctic sea ice. USA CRREL Technical Report 157, 20 p.

63. Hillig, W.B. (1958) "The kinetics of freezing of ice in the direction perpendicular to the basal plane" in Growth and perfection of crystals (R.H. Doremus, Ed.), New York: Wiley and Sons, p. 350-359.

64. Hobbs, H.A. and Kingery, W.D. (1962) "Long-time tests of sea ice sheet deformation" in Summary report - Project Ice Way, (W.D. Kingery, Ed.), AF Cambridge Research Laboratory Surveys in Geophysics no. 145 (AFCRL - 62 - 498), p. 130-152.

65. Hobbs, H.A.; Cutcliffe, J. L. and Kingery, W.D. (1963) "Effect of creep and temperature gradients on long-time deformation of ice sheets" in Ice and snow - Processes, properties, and applications (W.D. Kingery, Ed.), p. 311-321.

66. Hunkins, K. (1960) Seismic studies of sea ice, J. Geophys. Res. 65, p. 3459-3472.

67. Ishida, T. (1958) Velocity of elastic waves in ice (in Japanese), Low Temperature Science, A 17, p. 99-107.

68. _____ (1959) Propagation of elastic waves in sea ice (in Japanese), Low Temperature Science, A 18, p. 157-169.

69. _____ (1963) Propagation of elastic waves in sea ice (in Japanese), Low Temperature Science, A 21, p. 141-149.

70. Istoshin, Iu. V. (1960) Ob amerikanskikh issledovaniiakh fizicheskikh svoistv morskogo l'da (American investigations of the physical properties of sea ice). Meteorologiia i Gidrologiia 11, Translation, Amer. Meteorol. Soc. T - R - 388, p. 46-48.

71. Ivanov, K.E.; Kobeko, P.P.; and Shul'man, A.P. (1946) Deformatsiia ledianogo pokrova pri dvizhenii gruzov (Deformation of ice cover under moving loads). Zhurnal Tekhnicheskoi Fiziki 16, Translation, CRREL Files S-438, p. 257-262.

72. James, D.W. (1966) On the nature of the solid/liquid interface transition at the onset of constitutional supercooling. Trans. Metal Soc. AIME, p. 936.

73. Jellinek, H.H.G. (1958) The influence of imperfections on the strength of ice. Proc. Phys. Soc. (London) 71, p. 797-814.

LITERATURE CITED (Cont'd)

74. Kashtelian, V.I. (1960) Priblizhennoe opredeienie usilii, razrushaiushchikh ledianoi pokrov (Approximate determination of forces destroying the ice cover). Problemy Arktiki i Antarktiki 5, p. 31-38.

75. Khanina, S.K. and Shul'man, A.R. (1949) Izuchenie techeniia estestvennykh l'dov (Investigation of natural ice deformation), Trudy Gosudarstvennogo Gidrologicheskogo Instituta 16, p. 89-95.

76. Kingery, W.D. and French, D.N. (1962) "Comparison of different methods for measuring sea ice strength" in Summary report - Project ice way, Air Force Cambridge Research Laboratory Surveys in Geophysics no. 145 (AFCRL - 62 - 498), p. 124-129.

77. Kingery, W.D. and French, D.N. (1963) "Stress-rupture behavior of sea ice" in Ice and snow - Processes, properties, and applications" (W.D. Kingery, Ed.). Cambridge, Mass: MIT Press, p. 124-129.

78. Köhler, R. (1929) Beobachtungen an Profilen auf See - Eis (Observations of profiles on sea ice), Z. Geophysik 5, p. 314-316.

79. Korunov, M. (1940) Raschet ledianykh pereprav (Calculation of ice crossings), Avtobronetankovyi Zhurnal 10, p. 62-67.

80. Krylov, A.N. (1901) "Nabliudeniia nad krepost'iu l'da"... ("Observations of ice strength...") in Ermak vo l'dakh (S. Makarov, Ed.), St. Petersburg, p. 418-435.

81. Kubo, Y. (1958) Load-bearing capacity of an ice cover, Part 2, (in Japanese) Seppyo 20, p. 97-104.

82. Kudriavtsev, V.A. (1957) Izuchenie mekhanicheskikh i fizicheskikh svoistv l'da (Study of the mechanical and physical properties of ice), Izdatel'stvo Akademii Nauk SSSR, Moscow, 63 p. Translation, American Meteorological Society T - R - 260.

83. Kusunoki, K. (1958) Measurement of gas bubble content in sea ice, I. (in Japanese) Low Temperature Science 17, p. 123-134.

84. Laktionov, A.F. (1931) O svoistvakh morskogo l'da (The properties of sea ice), Trudy Instituta po Izucheniiu Severa 49, p. 71-96.

85. Langleben, M.P. (1959) Some physical properties of sea ice, II, Canadian Journal of Physics 37, p. 1438-1454.

86. _____ (1962) Young's modulus for sea ice, Canadian Journal of Physics 40(1), p. 1-8.

87. _____ and Pounder, E.R. (1963) "Elastic parameters of sea ice" in Ice and snow - Processes, properties, and applications (W.E. Kingery, Ed.). Cambridge, Mass: MIT Press, p. 69-78.

88. _____ (1964) Arctic sea ice of various ages. I. Ultimate strength. J. Glaciology, 5(37), p. 93-98.

89. Lavrov, V.V. (1957) Modelirovanie l'da (Ice models). Problemy Arktiki 2, p. 185-191.

90. _____ (1958) Priroda masshtabnogo effekta u l'da i prochnost' ledianogo pokrova (The nature of the scale effect in ice and the strength of an ice cover). Doklady Akad. Nauk SSSR 122, p. 570-573.

LITERATURE CITED (Cont'd)

91. Lavrov, V.V. (1962) Voprosy fiziki i mekhaniki l'da (Questions of the physics and mechanics of ice). Trudy Arkticheskogo i Antarkticheskogo Nauchno - Issledovatel' skogo Instituta 247, 118 p.

92. _____ (1962) O kharaktere raboty l'da pod nagruzkoi (The behavior of ice under a load). Zhurnal Tekh. Fiziki 32 (1), p. 101-105. Translation, Soviet Physics - Technical 7(1), p. 66-69.

93. Lewis, E.L. (1966) "Heat flow through winter ice" in Proceedings of conference, Institute of Low Temperature Science, Hokkaido University, Aug 1966.

94. Lin'kov, E.M. (1958) Izuchenie uprugikh svoistv ledianogo pokrova v arktike (Study of the elastic properties of an ice cover in the arctic). Vestnik, Leningradskogo Univ. 13, p. 17-22.

95. Makarov, S.O. (1901) "Zametki po ledovedeniiu (Notes on ice science)" in Ermak vo L'dakh, St. Petersburg, p. 388-417.

96. Maksimovich, G.A. (1955) "Morskie l'dy (Sea ice)" in Khimicheskaia geografiia vod sushi, Gosudarstvennoe Izdatel' stvo Geograficheskoi Literatury, Moscow, p. 259-261.

97. Malmgren, F. (1927) On the properties of sea ice. Sci. Res. Norwegian North Pole Exped. with the "Maud", 1918-1925, vol. 1, no. 5, 67 p.

98. Mariutin, T.P. (1936) O kreposti morskogo l'da (The strength of sea ice). Meteorologiia i Gidrologiia 2, p. 70-73.

99. Meyerhof, G.G. (1960) Bearing capacity of floating ice sheets. Proc. Am. Soc. Civil Engineers, J. Eng. Mechanics Div. 86, p. 113-145.

100. Mullins, W.W. and Sekerka, R.F. (1964) Stability of a planar interface during solidification of a dilute binary alloy. J. Appl. Phys. 35. p. 444-451.

101. Naghdi, P.M. and Rowley, J.C. (1953) On the bending of axially symmetric plates on elastic foundations. Midwestern Conference on Solid Mechanics, 1st Proceedings, p. 119-123.

102. Nazarov, V.S. (1938) K izucheniiu svoistv morskogo l'da (An investigation of the properties of sea ice), Trudy Arkticheskogo Instituta, Leningrad 110, p. 101-108.

103. Nazintsev, Iu. L. (1961) Nekotoryye rezul'taty nablyudenii nad plasticheskimi svoistvami morskogo l'da (Some results of observations on the plastic properties of sea ice), Trudy Arkticheskogo i Antarkticheskogo Nauchno - Issledovatel' skogo Instituta 256, p. 47-60.

104. Nelson, K.H. (1953) A study of the freezing of sea water, University of Washington, Dept. of Oceanography, Ph. D. Thesis, 129 p.

105. _____ and Thompson, Th.G. (1954) Deposition of salt from sea water by frigid concentration, University of Washington, Dept. of Oceanography, Technical Report 29.

LITERATURE CITED (Cont'd)

106. Neronov, I.N. (1946) K voprosu o velichine vremennogo soprotivleniia na izgib vesennego taiushchego l'da (The problem of the value of temporary resistance to bending of thawing spring ice), Trudy Nauchno - Issledovatel'skikh Uchrezhdenii Ser. V, no. 20, p. 50-57. U.S. Army Corps of Engineers, Arctic Construction and Frost Effects Laboratory Translation 25.

107. Nevel, D.E. (1958) The theory of a narrow infinite wedge on an elastic foundation, Transactions, Engineering Institute of Canada 2, p. 132-140.

108. _____ (1961) The narrow free infinite wedge on an elastic foundation, USA CRREL Research Report 79, 11 p.

109. _____ (1963) Circular plates on elastic, sealed foundations, USA CRREL Research Report 118, 14 p.

110. _____ (1966) Time dependent deflection of a floating ice sheet, USA CRREL Research Report 196, 9 p.

111. Northwood, T.D. (1947) Sonic determination of the elastic properties of ice, Canadian Journal of Research A25, p. 88-95.

112. Oliver, J.; Crary, A.P.; and Cotell, R.D. (1954) Elastic waves in arctic pack ice, Transactions American Geophysical Union 35, p. 282-293.

113. Owston, P.G. (1958) The structure of ice I, as determined by X-ray and neutron diffraction analysis, Advances in Physics 7, p. 171-188.

114. Paige, R.A. and Lee, C.W. (1966) Sea ice strength studies on McMurdo Sound during the austral summer 1964-65, U.S. Naval Civil Engineering Laboratory, Technical Report R-437, 23 p.

115. Pedder, A. Iu. (1929) Nabliudeniia nad krepost'iu l'da reki Angary (Strength of Angara river ice). Zhurnal Geofiziki i Meteorologii 6, p. 69-76.

116. Perey, F.G.J. and Pounder, E.R. (1958) Crystal orientation in ice sheets. Canadian J. Phys. 36, p. 494-502.

117. Peschanskii, I.S. (1958) "Physical and mechanical properties of arctic ice and methods of research" in Arctic sea ice, U.S. National Academy of Sciences - National Research Council Pub. 598, p. 100-104.

118. _____ (1960) Morskie arkticheskie i antarkticheskie l'dy (Arctic and Antarctic sea ice). Problemy Arktiki i Antarktiki 4, p. 111-129.

119. _____ (1963) Ledovedenie i ledotekhnika (Ice science and ice technique). Leningrad, Izd-vo "Morskoi Transport". 345 p.

120. _____ et al. (1964) Mekhanicheskie svoistva uprochnennogo l'da (Mechanical properties of strengthened ice). Problemy Arktiki i Antarktiki 16, p. 45-53.

LITERATURE CITED (Cont'd)

121. Petrov, I.G. (1954-55) "Fiziko - mekhanicheskie svoistva i tolshchina ledianogo pokrova (Physical and mechanical properties and thickness of ice cover)" in Materialy nabliudenii nauchno - issledovatel'skoi dreifuiushchei stantsii 1950-51 goda (Observations of the drifting research station of 1950-51). (M.M. Somov, Ed.), p. 103-165. Arkticheskii Nauchno - Issledovatel'skii Institut 2, Leningrad. Translation, Amer. Meteorol. Soc., ASTIA Document No. AD 117137.

122. Peyton, H.R. (1963) "Some mechanical properties of sea ice" in Ice and snow - Processes, properties, and applications (W.D. Kingery, Ed.), Cambridge, Mass: MIT Press, p. 107-113.

123. _____ (1966) Sea ice in Cook Inlet. University of Alaska, Arctic Envir. Eng. Lab. Rept. 25 p.

124. Pounder, E.R. (1958) Mechanical strength of ice frozen from an impure melt. Canadian J. Phys. 36, p. 363-370.

125. _____ and Little, E.M. (1959) Some physical properties of sea ice, I. Canadian J. Phys. 37, p. 443-473.

126. Pounder, E.R. (1961) Heat flow in ice sheets and ice cylinders. Un. Geodes. Geophys. Internat. (Commission des Neiges et Glaces, Helsinki), Pub. 54, p. 56-62.

127. _____ and Stalinsky, P. (1961) Elastic properties of Arctic sea ice, International Union of Geodesy and Geophysics, Helsinki, Pub. 54, p. 35-39.

128. _____ (1962) "The physics of sea ice" in The sea, Vol. I, Physical Oceanography (M.N. Hill, Ed.). New York: Interscience, p. 826-838.

129. _____ and Langleben, M.P. (1964) Arctic sea ice of various ages. II. Elastic properties, Journal of Glaciology 5(37), p. 99-105.

130. Pounder, E.R. (1965) The physics of ice. Oxford: Pergamon Press, 151 p.

131. Richardson, C. and Keller, E.E. (1966) The brine content of sea ice measured with a nuclear magnetic resonance spectrometer, Journal of Glaciology 6(43), p. 89-101.

132. Ringer, W.E. (1906) De Veranderingen in Samenstelling van Zeewater bij bet Bevri zen (Changes in the composition of sea water upon freezing), Chem. Weekblad 3, p. 223-249.

133. Ripperger, E.A. and Davids, N. (1947) Critical stresses in a circular ring, Proceedings, American Society of Civil Engineers 12, p. 619-635.

134. Rutter, J.W. and Chalmers, B. (1953) A prismatic substructure formed during solidification of metals, Canadian Journal of Phys. 31, p. 15-39.

135. Sala, I. (1957) Einige Messungen der Eisfestigkeit, Geophysica 5, p. 150-152.

LITERATURE CITED (Cont'd)

136. Sala, I. (1959) On the strength characteristics of sea ice, Teknillinen Aikakauslehti 49, p. 503-504, 507-508, 511-512, 536.

137. _____ (1961) Experimental studies on the stress concentration index of sea ice, International Union of Geodesy and Geophysics, (Commission on Snow and Ice, Helsinki), Pub. 54, p. 15-19.

138. Sarapkin, P.S. (1928) K kharakteristike fizicheskikh svoistv vody, snega i l'da solianogo ozera Karachi i presnogo ozera Uzul-Kulia (The physical properties of water, snow and ice in the salt lake Karacha and Lake Uzul-Kul), Omskii Meditsinskii Zhurnal 3, no. 3, p. 41-58.

139. Savel'ev, B.A. (1954) Instruktivnye ukazaniia po opredeleniiu soderzhaniia tverdoi, zhidkoi i gazoobraznoi fazy v zasolennykh l'dakh (Procedural notes on determination of content of solid, liquid and gaseous phases in saline ice), Materialy po Laboratornym Issledovaniiam Merzlykh Gruntov, Sbornik no. 2, p. 176-192. Izdatel' stvo Akademii Nauk. Translation, Defense Research Board, Canada, T344R.

140. _____ (1957) "Izuchenie mekhanicheskikh i fizicheskikh svoistv l'da (Study of the mechanical and physical properties of ice)". 63 p. Izdatel'stvo Akademii Nauk SSSR, Moscow.

141. _____ (1958) Izuchenie l'dov v rayone dreifa stantsii SP-4 v period taianiia i razrusheniia ikh v 1955 g. (Study of ice in the region of the drift of station NP-4 during melting and break-up in 1955). Problemy Severa 2, p. 47-79. Translation, Problems of the North, 2, p. 45-75, Nat. Res. Council, Canada (1961).

142. _____ (1963) Stroenie, sostav i svoistva ledianogo pokrova morskikh i presnykh vodoemov (Structure, composition and properties of the ice cover of sea and fresh waters). Moscow, Izd-vo Moskovskogo Universiteta, 541 p.

143. _____ (1963) Uprugo-viazko-plasticheskie svoistva l'da (Properties of elasticity, viscosity and plasticity of ice). Doklady na Mezhdunarodnoi konferentsii po merzlotovedeniiu, Moscow, Izd-vo Akad. Nauk SSSR, p. 229-235.

144. _____ (1963) Rukovodstvo po izucheniiu svoistv l'da (Manual on the study of ice properties). Moscow, Izd-vo Moskovskogo Universiteta, 198 p.

145. Schwarzacher, W. (1959) Pack-ice studies in the Arctic Ocean. J. Geophys. Res. 64, p. 2357-2367.

146. Serikov, M.I. (1961) Mekhanicheskie svoistva morskogo antarkticheskogo l'da (Mechanical properties of Antarctic sea ice). Inform. Biull. Sovetskoi Antarkticheskoi Ekspeditsii 25, p. 23-27. Translation, Sov. Antarctic Exp. Info. Bull. 3, p. 181-185.

147. _____ (1962) Prochnost' morskogo antarkticheskogo l'da pri izgibe (Flexural strength of Antarctic sea ice). Informatsionnyi Biulleten Antarkticheskoi Ekspeditsii 36, p. 30-35. Translation, Sov. Antarctic Exp. Info. Bull. 4, p. 188-191.

LITERATURE CITED (Cont'd)

148. Serikov, M.I. (1962) Izuchenie fiziko-mekhanicheskikh svoistv morskikh l'dov (Study of the physical and mechanical properties of sea ice). Sovet. Antarkticheskaia Eksped., Trudy 20, p. 155-164.

149. Shuleikin, V.V. (1953) "Fizika Moria (Physics of the sea)." 989 p. Izdatel'stvo Akademii Nauk SSSR, Moscow.

150. Shul'man, A.R. (1946) K raschetu gruzopod"emnosti ledianykh pereprav po teorii tsentral'nogo izgiba uprugoi plity na uprugom osnovanii (The calculation of the load capacity of ice crossing based on the theory of central bending of an elastic plate on an elastic foundation). Trudy Nauchno-Issledovatel'skogo Uchrezhdeniia, Ser. 5(20), p. 30-38. Translation, Arctic Const. Frost Effects Lab. TL-25.

151. _____ and Kazanskii, M.M. (1946). Teoreticheskie i opytnye osnovaniia tablits gruzopod"emnosti ledianogo pokrova (Theoretical and experimental basis for the tables of load capacity of the ice cover), Trudy Nauchno - Issledovatel'skogo Uchrezhdeniia, Ser. 5 (20), p. 58-87. U.S. Army Corps of Engineers, Arctic Construction Frost Effects Laboratory Translation 25.

152. Shumskii, P.A. (1955) K izucheniiu l'dov severnogo Ledovitogo okeana (A study of ice in the Arctic Ocean), Vestnik Akademii Nauk SSSR 25, no. 2, p. 33-38. Translation, CRREL files, S-4456.

153. Smirnov, V.I. (1961) O kolichestvennykh kharakteristikakh l'da kak material (Quantitative characteristics of ice as a material), Trudy Arkticheskogo i Antarkticheskogo Nauchno - Issledovatel'skogo Instituta 256, p. 40-46.

154. Smith, D.D. (1964) Ice lithologies and structure of ice island Arlis II, Journal of Glaciology 5, p. 17-38.

155. Tabata, T. (1955) A measurement of the visco-elastic constants of sea ice, (in Japanese) Low Temperature Science A 14, p. 25-32.

156. _____ (1956) Studies on the visco-elastic properties of sea ice, (in Japanese) Low Temperature Science A 15, p. 101-115.

157. _____ and Ono, N. (1957) On the structure of sea ice, (in Japanese) Low Temperature Science A 16, p. 197-210.

158. Tabata, T. (1958) "Studies on visco-elastic properties of sea ice" in Arctic sea ice, U.S. National Academy of Sciences, National Research Council, Pub. 598, p. 139-147.

159. _____ (1958) Studies on mechanical properties of sea ice II. Measurement of elastic modulus by lateral vibration method, Low Temperature Science A 17, p. 147-166. Translation, American Meteorological Society T - J - 10.

160. _____ and Ono, N. (1958) Studies on mechanical properties of sea ice I. On the static visco-elasticity of sea ice, (in Japanese) Low Temperature Science A 17, p. 135-145.

LITERATURE CITED (Cont'd)

161. Tabata, T. (1959) Studies on mechanical properties of sea ice III. Measurement of elastic modulus by the lateral vibration method, Low Temperature Science A 18, p. 116-129. Translation, American Meterorological Society T - J - 12.

162. _____ (1960) Studies on mechanical properties of sea ice V. Measurement of flexural strength, Low Temperature Science A 19, p. 187-201. Translation, American Meteorological Society T - J - 17.

163. _____ (1962) Studies on mechanical properties of sea ice VI. Bending tests of sea ice beams (in Japanese). Low Temperature Science, Ser. A 20, p. 187-198.

164. _____ and Ono, N. (1962) On the crystallographic study of several kinds of ices (in Japanese). Low Temperature Science, Ser. A 20, p. 199-214.

165. Tabata, T. and Fujino, K. (1964) Studies on mechanical properties of sea ice VII. Measurement of flexural strength in situ (in Japanese). Low Temperature Science, Ser. A 22, p. 147-154.

166. _____ (1965) Studies of the mechanical properties of sea ice VIII. Measurement of flexural strength in-situ (in Japanese). Low Temperature Science A 23, p. 157-166.

167. Tabata, T. (1966) Studies of the mechanical properties of sea ice IX. Measurement of the flexural strength in-situ (in Japanese). Low Temperature Science, A 24, p. 259-268.

168. _____ (1966) "The flexural strength of small sea ice beams" in Proceedings of conference, Institute of Low Temperature Science, Hokkaido University, Aug 1966.

169. _____; Fujino, K.; and Aota, M. (1966) "The flexural strength of sea ice in-situ" in Proceedings of conference, Institute of Low Temperature Sciences, Hokkaido University, Aug 1966.

170. Tiller, W.A.; Jackson, K.A.; Rutter, J.W.; and Chalmers, B. (1953) The redistribution of solute atoms during the solidification of metals. Acta Met. 1, p. 428-437.

171. Tiller, W.A. (1963) "Principles of solidification" in The art and science of growing crystals, Wiley and Sons, p. 276-312.

172. Treshnikov, A.F. (1963) Osobennosti ledovogo rezhima Yuzhnogo Ledovitogo Okeana (Features of the ice regime of the southern ocean). Trudy Sovetskoi Antarkticheskoi Ekspeditsii 21, 237 p.

173. Tsurikov, V.L. (1939) Nekotorye dannye o l'de Aral'skogo moria (Some data on Aral Sea ice). Izvestiia Gosudarstvennogo Geograficheskogo Obshchestva 71, p. 1200-1219.

174. _____ (1940) Problema prochnosti morskogo l'da (The problem of ice strength). Severnyi Morskoi Put' 16, p. 45-74.

LITERATURE CITED (Cont'd)

175. Tsurikov, V.L. (1947) K voprosu o vliianii polostnosti l'da na ego prochnost' (The problem of the influence of the ice porosity on its strength), Gosudarstvennyi Okeanograficheskii Institut (Leningrad), Trudy 2(14), p. 66-88.

176. _____ (1947) O vliianii solenosti morskogo l'da na ego prochnost (The influence of the salinity of sea ice on its strength), Gosudarstvennyi Okeanograficheskii Institut, Trudy 2(14), p. 89-108.

177. _____ and Tserenina, M.I. (1964) Obzor inostrannykh issledovanii morskogo l'da (Survey of foreign research on sea ice), Trudy Gosudarstvennogo Okeanograficheskogo Institut, Vyp. 76, p. 127-207.

178. Tsurikov, V.L. (1965) Formation of the ionic composition and salinity of sea ice, Oceanology 5, p. 59-66.

179. Untersteiner, N. (1966) Natural desalination and equilibrium salinity profile in old sea ice, Proceedings of Conference, Institute of Low Temperature Science, Hokkaido University, August 1966.

180. Voitkovskii, K.F. (1957) Eksperimental'nye issledovaniia plasticheskikh svoistv l'da (Experimental investigations of the plastic properties of ice), Sezonnoe promerzanie gruntov i primenenie l'da dlia stroitel'nykh tselei, p. 101-130.

181. _____ (1960) Mekhanicheskie svoistva l'da (The mechanical properties of ice), Izdatel'stvo Akademii Nauk SSSR, Moscow, 100 p. Translation, Air Force Cambridge Research Laboratory - 62-838.

182. Volkov, N.A.; Spichkin, V.A.; and Shil'nikov, V.I. (1961) Ledoissledovatel' skiye raboty (Ice investigations), USSR Arkticheskii i Antarkticheskii Nauchno-Issledovatel'skii Institut. Rezul'taty nauchno-issledovatel' skikh rabot dreifuiushchikh stantsii "Severnyi Polius-4" i "Severnyi Polius-5" 1955-56 goda. Leningrad 6, p. 7-26.

183. Walton, D. and Chalmers, B. (1959) The origin of the preferred orientation in the columnar zone of ingots, Transactions, Metallurgical Society of America, Institute of Mining and Metallurgical Engineers 215, p. 447-457.

184. Weeks, W.F. (1958) "The structure of sea ice: a progress report" in Arctic sea ice, U.S. National Academy of Sciences, National Research Council Pub. 598, p. 96-98.

185. _____ and Anderson, D.L. (1958) An experimental study of the strength of young sea ice. Transact. Am. Geophys. Un. 39, p. 641-647.

186. Weeks, W.F. and Lee, O.S. (1958) Observations on the physical properties of sea ice at Hopedale, Labrador. Arctic 11, p. 134-155.

187. Weeks, W.F. (1962) Tensile strength of NaCl ice. J. Glaciology 4, p. 25-52.

188. _____ and Hamilton, W.L. (1962) Petrographic characteristics of young sea ice, Point Barrow, Alaska. Am. Mineral. 47, p. 945-961.

LITERATURE CITED (Cont'd)

189. Weeks, W.F. and Assur, A. (1963) "Structural control of the vertical variation of the strength of sea and salt ice" in Ice and snow - Processes, properties, and applications (W.D. Kingery, Ed.). Cambridge, Mass: MIT Press, p. 258-276.

190. Weeks, W.F. and Lofgren, G. (1966) "The effective solute distribution coefficient during the freezing of NaCl solutions" in Proceedings of conference, Institute of Low Temperature Science, Hokkaido University, August 1966.

191. Weeks, W.F. (1967) Understanding the variations of the physical properties of sea ice, SCAR Bulletin (Symposium on Antarctic Oceanography, Santiago, Chile).

192. Weinberg, B.P. (1936) Izuchenie svoistv l'da v svete osvoeniia trassy severnogo morskogo puti (Ice properties in relation to the Northern Sea Route), Biulleten'Arkticheskogo Instituta 6, p. 369-375.

193. _____; Al'tberg, V. Ia.; Arnol'd-Aliab'ev, V.I.; and Golovkov, M.P. (1940) Led, svoistva, vozniknovenie i ischeznovenie l'da (Ice, its properties, appearance and disappearance), Gosudarstvennoe Izdatel'stvo Tekhniko-Teoreticheskoi Literatury, Moscow, 524 p.

194. Wilson, J.T. (1955) Coupling between moving loads and flexural waves in floating ice sheets, USA SIPRE Research Report 34, 27 p.

195. Wyman, M. (1950) Deflections of an infinite plate, Canadian J. Res. 28 A, p. 293-302.

196. Yakovlev, G.N. (1962) Ledoissledovatel'skie raboty v Tsentral'noi Arktike (Research on sea ice in the central Arctic), Problemy Arktiki i Antarktiki, no. 11, p. 47-57, Translation, Arctic Inst. North Amer. (1966).

197. Yamachi, K. and Kuroiwa, D. (1956) Visco-elasticity of ice in the temperature range 0° to -100°C, Low Temperature Science A 15, p. 171-183, Translation, Defence Research Board, Canada, T63J.

198. Zubov, N.N. (1945) L'dy Arktiki (Arctic ice), Izdatel' stvo Glavsevmorputi, Moscow, 360 p, Translation, U.S. Naval Electronics Laboratory (1963).

199. Zvolinskii, N.V. (1946) K voprosu o deformatsii plavaiushchego ledianogo sloia (On the problem of the deformation of a floating ice layer), Trudy Nauchno-Issledovatel'skogo Uchrezhdeniia, Ser. 5(20), p. 16-29, U.S. Army Corps of Engineers, Arctic Construction and Frost Effects Laboratory Translation 25.

Unclassified

Security Classification

DOCUMENT CONTROL DATA - R & D

(Security classification of title, body of abstract and indexing annotation must be entered when the overall report is classified)

1. ORIGINATING ACTIVITY (Corporate author)	2a. REPORT SECURITY CLASSIFICATION
U.S. Army Cold Regions Research and Engineering Laboratory, Hanover, N.H.	Unclassified
	2b. GROUP

3. REPORT TITLE

THE MECHANICAL PROPERTIES OF SEA ICE

4. DESCRIPTIVE NOTES (Type of report and inclusive dates)

Monograph

5. AUTHOR(S) (First name, middle initial, last name)

Wilford F. Weeks and Andrew Assur

6. REPORT DATE	7a. TOTAL NO. OF PAGES	7b. NO. OF REFS
September 1967	94	199

8a. CONTRACT OR GRANT NO.	9a. ORIGINATOR'S REPORT NUMBER(S)
b. PROJECT NO.	Cold Regions Science and Engineering Part II, Sect. C3
c. DA Project 1VO25001A130	9b. OTHER REPORT NO(S) (Any other numbers that may be assigned this report)
d.	

10. DISTRIBUTION STATEMENT

This document has been approved for public release and sale; its distribution is unlimited.

11. SUPPLEMENTARY NOTES	12. SPONSORING MILITARY ACTIVITY
	U.S. Army Cold Regions Research and Engineering Laboratory

13. ABSTRACT

This review discusses the state of thinking of each of the main national groups investigating sea ice and gives an overall appraisal of the field as a whole. Emphasis is placed on (1) the physical basis for interpreting sea ice strength (phase relations, air volume, and structural considerations), (2) theoretical considerations (strength models, air bubbles and salt reinforcement, and interrelations between growth conditions and strength), (3) experimental results (tensile, flexural, shear, and compressive strength, elastic modulus, shear modulus and Poisson's ratio, time dependent effects, and creep), and (4) plate characteristics. The paper includes a review of problems in sea ice investigations, relates the chemical, crystallographic, mechanical, and physical aspects involved, and concludes by showing how to utilize this knowledge to solve practical problems.

DD FORM 1 NOV 68 1473 REPLACES DD FORM 1473, 1 JAN 64, WHICH IS OBSOLETE FOR ARMY USE.

Unclassified

Security Classification

14. KEY WORDS	LINK A		LINK B		LINK C	
	ROLE	WT	ROLE	WT	ROLE	WT
Sea ice--Chemical analysis						
Sea ice--Crystal structure						
Sea ice--Mechanical properties						
Sea ice--Physical properties						
Sea ice--Strength						
Models (Sea ice)						